

Microtubule-based positioning mechanisms

Juliane Teapal

Thesis committee

Promotors

Prof. Dr M.E. Janson
Professor of Cell Biology, with special attention to the physics of the cell
Wageningen University

Prof. Dr B.M. Mulder
Professor of Theoretical Cell Physics
Wageningen University

Other members

Prof. Dr A. Akhmanova, Utrecht University
Prof. Dr J. van der Gucht, Wageningen University
Prof. Dr P.T. Tran, CNRS, Paris, France / University of Pennsylvania, USA
Dr C. Fleck, Wageningen University

This research was conducted under the auspices of the Graduate School: Experimental Plant Sciences (EPS)

Microtubule-based positioning mechanisms

Juliane Teapal

Thesis

submitted in fulfillment of the requirements for the degree of doctor
at Wageningen University

by the authority of the Rector Magnificus

Prof. Dr M.J. Kropff,

in the presence of the

Thesis Committee appointed by the Academic Board

to be defended in public

on Friday 5 September 2014

at 11 a.m. in the Aula.

Juliane Teapal
Microtubule-based positioning mechanisms
142 pages.

PhD thesis, Wageningen University , Wageningen , NL (2014)
With references, with summaries in English, German and Dutch

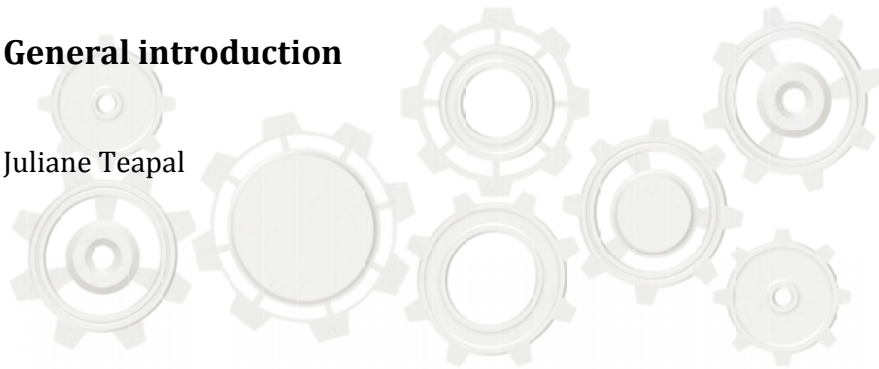
ISBN: 978-94-6257-047-4

CONTENTS

CHAPTER 1: GENERAL INTRODUCTION	1
1.1. PATTERNING OF CELLS	2
1.2. THE CYTOSKELETON AND ITS DYNAMICS	4
1.3. MICROTUBULE-FACILITATED POSITIONING OF CELLULAR COMPONENTS	8
1.4. PATTERNING OF MICROTUBULES IN MITOTIC SPINDLES	11
1.5. THE MODEL ORGANISM FISSION YEAST	13
1.6. THESIS OUTLINE	17
CHAPTER 2: A MICROTUBULE BASED MECHANISM FOR EQUIDISTANT POSITIONING OF MULTIPLE NUCLEI	23
2.1. INTRODUCTION	24
2.2. RESULTS	25
2.3. DISCUSSION	32
2.4. MATERIALS AND METHODS	34
CHAPTER 3: A MODEL FOR EQUIDISTANT POSITIONING OF MULTIPLE NUCLEI	43
3.1 INTRODUCTION	44
3.2. FORMULATION OF A MODEL	45
3.3. RESULTS	54
3.4. DISCUSSION	62
3.5. MATERIAL AND METHODS	64
CHAPTER 4: MICROTUBULE GROWTH AND SLIDING ARE COUPLED PROCESSES THAT REGULATE SPINDLE ASSEMBLY	71
4.1. INTRODUCTION	72
4.2. RESULTS	74
4.3. DISCUSSION	82
4.4. MATERIAL AND METHODS	85
CHAPTER 5: GENERAL DISCUSSION AND FUTURE RESEARCH DIRECTIONS	93
5.1. ORGANELLE PATTERNS IN EUKARYOTES	94
5.2. ORGANELLE DISPERSION BASED ON REPULSIVE FORCES	95
5.3. REGULATION OF THE SPINDLE MIDZONE	98
SUMMARY	113
ZUSAMMENFASSUNG	117
SAMENVATTING	121
ACKNOWLEDGEMENT	125
CURRICULUM VITAE	129
LIST OF PUBLICATIONS	130
EDUCATION STATEMENT	131

General introduction

Juliane Teapal



Chapter

1

Abstract

Living cells contain structures of well-regulated size and periodicity that require molecular mechanisms to set a length scale. Mechanisms involving the reaction and diffusion of interacting compounds have long been known to define length scales in cells. The generation of long cytoskeletal filaments with a well-regulated length distribution is another important scale-providing mechanism. In many cases, reaction diffusion and filament systems work side-by-side. In this thesis I will describe the positioning of two important cellular structures: the nucleus and the so-called spindle midzone of the cells division apparatus. Both mechanisms are based on microtubule filaments, which are an important component of the cytoskeleton. In particular I will describe how multiple nuclei may attain a constant internuclear distance as often is observed in multinucleated cells. Further, I will discuss how a confined zone of microtubule overlap can be positioned within the mitotic spindle that orchestrates cell division. In this introduction, I will introduce the concept of dynamic instability, that regulates the length of microtubule filaments and I will summarize our current knowledge on microtubule-based positioning mechanisms.

1.1. Patterning of cells

A brief look at the animal and plant kingdom shows a large variety of spatial patterns like the periodic stripes of zebras and seashells or radial patterns in plant flowers. The patterns are generated because differentiated cells form well-ordered structures within tissues. Not only tissues are patterned, but also the cells that make up the tissues. Cells are not sacks filled with a homogenous solution of various molecules; rather they contain complex cellular structures like nuclei and chloroplasts that are essential for their function. Some of these structures are periodic in nature including the lobes of so-called pavement cells on the surface of plant leaves (Figure 1.1 A) or the periodic arrangement of cytoskeletal filaments in myotubes that enable muscles to contract. To build such complex structures, cells must have mechanisms to set a length scale.

Despite important developments in technologies like microscopy and tools to study single molecules and their interactions, knowledge is still limited on how sets of molecules interact to give structure to cells. The sequencing of whole genomes gave us lists of parts with which to build a cell but not the instruction manual how to put these parts together to form a cell. Biochemical experiments and large-scale proteomic approaches have shown which cellular components interact or fit into each other [2]. However, to learn how multiple components assemble into structures also requires an understanding of the physical forces and physical mechanism involved in molecular interactions. This is certainly true for the mechanisms that are described in this thesis.

Mechanisms based on the reaction and diffusion of interacting compounds are a prime example of a physical mechanism that can pattern cells. Turing proposed that a solution of initially homogeneously distributed reaction-components can form patterns, in which the concentration of the components varies periodically. In a Turing scheme there are two opposing reactions: one that forms a product and one that breaks it down (reviewed in [3]). The reaction can for example be the phosphorylation and dephosphorylation of a protein or the cycling between a monomer and a multimer. The reactions are fueled for example by the hydrolysis of ATP and patterning is thus an energy-consuming process. One of the reaction products may act as a morphogen, i.e. a compound that drives the formation of a cellular structure. A good example of a reaction-diffusion scheme is the patterning of the early *Drosophila* embryo by the transcription factor bicoid [4]. This protein is locally produced by a pool of mRNA at the anterior side of the embryo. Bicoid will diffuse away from its production site but is degraded. The production is local but degradation occurs homogeneously throughout the cell. The result is an exponentially decaying concentration of bicoid away from the anterior. The embryo contains many nuclei, which will ultimately form cells with different cell fates dependent on bicoid concentration. Importantly, the length scale of the bicoid concentration gradient, and thus of the cellular pattern that it forms, is set by the diffusion coefficient of bicoid and its rate of degradation. While mechanisms based on reaction-diffusion (Figure 1.1 B) can

polarize cells and form patterns, it is becoming clear that mechanical processes like the growth of cytoskeletal filaments and the directed motion of motor proteins along them can also define length scales in cells [3].

In the remainder of this introduction I will first introduce the cytoskeleton, focusing on microtubules, and I will show that their dynamic properties are key to their ability to set a length scale in a cell. I will then discuss how microtubules can aid the positioning of cellular objects and will summarize our current understanding of the patterning of microtubules in the cells division apparatus, the mitotic spindle. Lastly I will introduce the fission yeast *Schizosaccharomyces pombe* as a suitable model organism for studying microtubule-based positioning mechanisms.

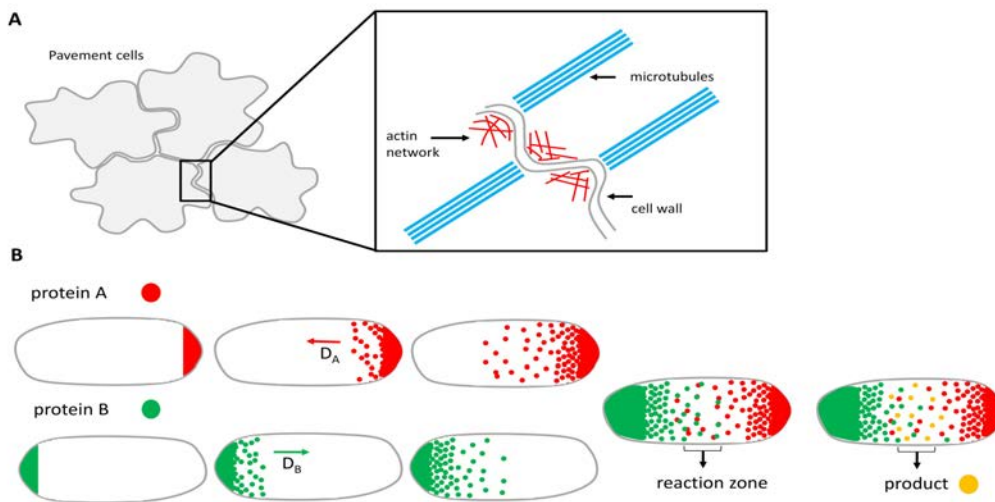


Figure 1.1 Pattern formation in nature

(A) Cartoon of the puzzle-piece-pattern of pavement cells, which are part of the plant epidermis. Zoom in: The form is regulated by the spatial localisation of actin (red) and microtubule networks (blue), the localisation of which is limited by reaction-diffusion mechanism and thus determines the size of pavement curves. **(B)** Spatial localisation of proteins can generate spatially controlled reactions required for pattern establishment. Example of a reaction of two proteins with each other to form a product. Protein A and B are expressed at the opposite ends of the cell and form a gradient, the size of which is determined by their diffusion constants. These gradients dictate spatially and temporally the reaction zone and therefore the spatial generation of the product (yellow).

1.2. The cytoskeleton and its dynamics

Cytoskeleton

The cytoskeleton can generate forces that change cellular architecture and perform a variety of functions in cells. It mechanically supports the cell membrane of animal cells and helps to shape and remodel cells during cell motility. Moreover, the filaments form diverse patterns within cells that direct processes like intercellular transport of organelles and the motion of chromosomes during cell division. Unlike the bone structure of the human body, the cell's cytoskeleton is very dynamic and filaments continuously exchange protein subunits with the cytosol leading to filament growth and shrinkage [5]. It was long believed that only eukaryotic cells have cytoskeletal filaments, but over the last decade many homologues of cytoskeletal proteins have been found in prokaryotic cells, which also assemble into filaments [6].

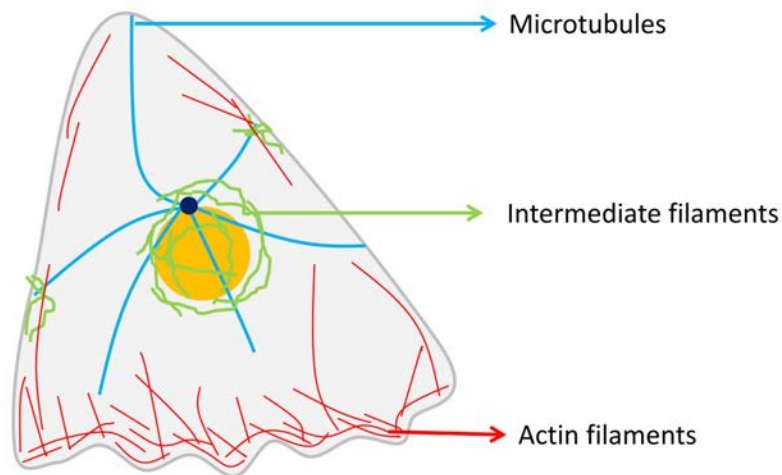


Figure 1.2: The localisation of the three cytoskeletal filaments within endothelia cell

Actin filaments (red) localize mainly along the membrane and to support among others the cell shape. Microtubules (blue) form an astral network spanning through the complete cell, nucleating from the microtubule organization centre (dark blue) and are required for example for intercellular transport. Intermediate filaments (green) support the nuclear envelope [10].

The multiple functions of the eukaryotic cytoskeleton are based on the contribution of three filament systems: microtubules, actin filaments and intermediate filaments (IMs). Microtubules are 25 nm in diameter and are very rigid. Individual microtubules can span the length of a typical cell. Actin filaments are 7 nm in diameter and are more floppy. Their function heavily depends on their ability to form bundles and other crosslinked networks with the aid of various crosslinking proteins [2, 7-9]. Intermediate

filaments have a diameter of about 10 nm (Figure 1.2). They have a variety of functions including supporting the nuclear envelope and other membranes in animal cells [8]. Actin and microtubules are most dynamic and their length is determined by various proteins that regulate monomer turnover at their ends or sever the filaments into multiple parts. These processes enable control over the length distribution. Microtubules in interphase cells are for example long, whereas microtubules during cell division are shorter and more dynamic [5]. The ability to control length enables microtubules and actin filaments to set cellular length scales. Microtubules in eukaryotic cells play a leading role in the cellular processes discussed in this thesis: cell division and the positioning of nuclei. We will discuss the regulation of microtubule length in more detail below.

Microtubules

Microtubules are the most rigid of the cytoskeletal filaments. They are composed of tubulin subunits, which themselves are heterodimers of alpha and beta tubulin. The dimers arrange longitudinally into protofilaments with the beta tubulin subunit pointing towards the so-called plus-end of the microtubule and the alpha subunits towards the minus-end (Figure 1.4). Thirteen protofilaments are arranged sideways into a hollow cylinder with a diameter of 25 nm. The polar arrangement of tubulin dimers in the microtubule lattice gives the microtubule an overall polarity and different properties to both ends [11]. Polarity is used by motor enzymes that bind to microtubules and translocate towards a specific end. These motor enzymes orchestrate for example directed transport of cell material along neuronal axons that contain networks of microtubules that all point into the same direction. Microtubules are universally involved in aspects of cell polarity (Figure 1.3).

Microtubules have the ability to switch between states of net growth and net shrinkage, a property known as dynamic instability. Shrinkage involves the hydrolysis of tubulin-bound GTP at the inter-dimer interface. Hydrolysis is triggered when GTP-bound subunits are incorporated at a growing microtubule end. GTP-hydrolysis promotes a conformational change on the tubulin dimer that makes the microtubule prone to disassembly, shedding subunits from its end. Structural and molecular features at microtubule ends, involving GTP-tubulin that is not yet hydrolyzed, can however delay the onset of disassembly. A switch from assembly to disassembly is called a catastrophe and the reverse is called a rescue. Microtubules in cells grow at rates between 2 and 20 $\mu\text{m}/\text{min}$ and the stochastic event of a catastrophe occurs typically on the time scale of a minute [5]. Pauses in microtubule dynamics have also been observed but are little understood. Microtubule plus-ends are generally more dynamic compared to

minus-ends [15]. The parameters of dynamic instability are highly regulated in cells [2]. Amongst others, proteins have been characterized that speed up assembly (XMAP215, [16]), induce catastrophes (MCAK, [17]) or generate rescues (CLASP, [18]). Regulation of the activities of these proteins enables cells to control the average length of microtubules (Figure 1.4 C).

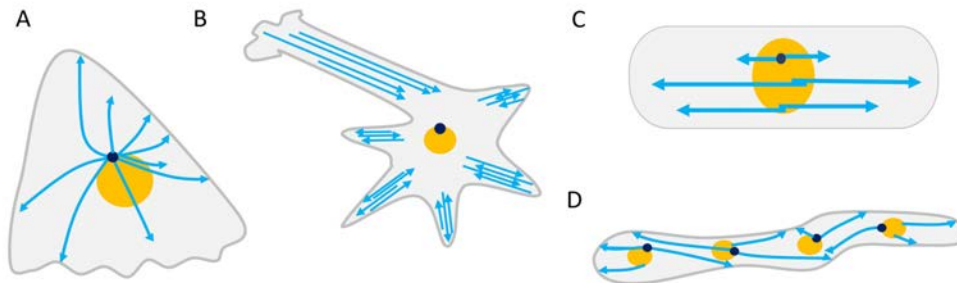


Figure 1.3: Polarized microtubule networks in different organisms

(A) Cartoon of an animal cell during interphase, where a radial array of microtubules nucleates from the centrosome and spans throughout the cell. The microtubule plus-ends face the cell periphery and minus-ends are focused at the centrosome [10]. **(B)** Differentiated neuronal cells arrange microtubules into linear parallel structures at the axon with the plus-ends pointing to the cell periphery and antiparallel at the dendrites. The parallel microtubule network as well as the antiparallel network allows transport of vesicles in both directions with the support of plus-end and minus-end directed motors [12]. **(C)** The microtubule network in *S. pombe* cells consist of antiparallel microtubule bundles connected to the nuclear envelope, with the plus-ends facing the cell tips. They deliver polarity and growth factors [13]. **(D)** Filamentous fungi contain multiple nuclei that are dispersed throughout the cell. Microtubules are connected with the minus-ends to the SPB at the nuclear envelope and the plus-ends growing towards the cell membrane. (light blue: microtubules, arrow head represents the plus-end, yellow: nuclei, dark blue: centrosomes (spindle pole body in *S. pombe*)) [14]. Cartoons are not scaled.

The life of a microtubule starts with its nucleation. Microtubules nucleate spontaneously in purified tubulin solutions of sufficient concentration. In cells it is believed that nucleation is always templated to regulate the number of microtubules [5]. The prime protein involved in nucleation is gamma tubulin, which forms ring-like templates that are either localized at microtubule organizing centers (MTOCs), like the centrosome in animal cells, or have a more dispersed cellular localization. The spatial and temporal regulation of nucleation sites is an important cellular instrument to control the shape and extend of microtubule networks. Microtubule plus-ends grow away from the nucleation sites, whereas the minus-ends can stay connected to these sites. For growth after nucleation two growth regimes can be distinguished: bounded and unbounded growth. We consider for the case of non-dynamic minus-ends bounded growth occurs

when the average length lost during a shrinkage event at a plus-end exceeds the length lost during a growth event: $v_{\text{growth}}^+ / r_{\text{catastrophe}}^+ > v_{\text{shrinkage}}^+ / r_{\text{rescue}}^+$ (v for velocity, r indicates a rate of occurrence and the plus sign indicates a property of the plus end). Unbounded growth occurs for the opposite scenario. In this case the average length of microtubules will increase without bounds. In absence of rescues, growth is always bounded for non-zero catastrophe rate and the length of microtubules follows an exponential distribution with an average length of $L_{MT} = \frac{v_{\text{growth}}}{r_{\text{catastrophe}}^+}$. This assumes that the catastrophe rate is independent of length, a concept challenged by recent work [19, 20]. Nonetheless, this simple case demonstrates a mechanism for length control (Figure 1.4 D). A special case of dynamic instability is filament treadmilling. Treadmilling filaments grow at plus-ends and shrink at the minus-end while maintaining a constant length. Microtubule treadmilling occurs in animal spindles where it is involved in regulating spindle size [21].

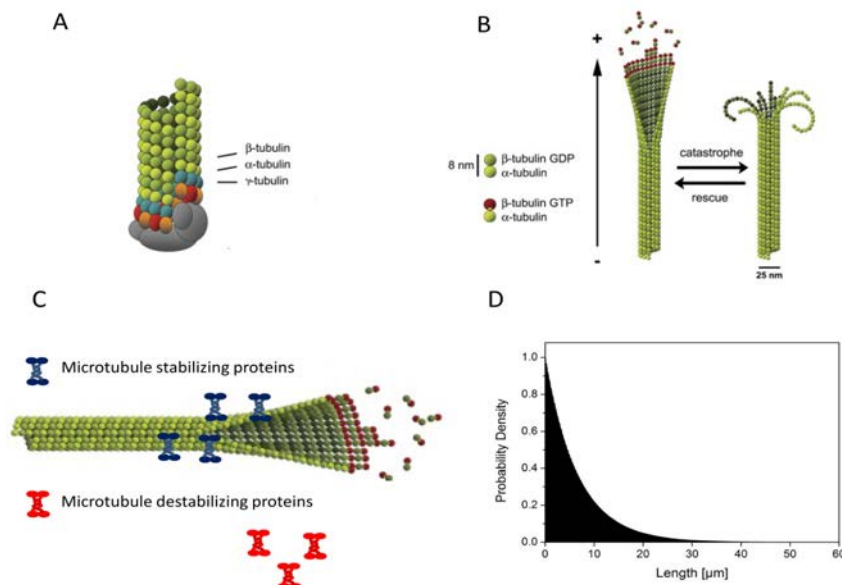


Figure 1.4: Lifecycle of a microtubule

(A) Microtubules nucleate from γ -tubulin and grow by adding heterodimers of α - and β -tubulin. **(B)** Ends of growing microtubules have sheet-like extensions. GTP bound to beta tubulin is hydrolysed upon assembly ultimately leading to microtubule shrinkage characterized by protofilaments peeling off from microtubules. **(C)** Transitions between assembly states are regulated by stabilizing or destabilizing proteins that may modulate structural properties of the microtubule ends (A, B and C adapted from Pastuglia, M. and D. Bouchez [22], use permitted by Elsevier). **(D)** Simulated length distribution of dynamic microtubules for free growth based on parameters measured in *S. pombe* cells (growth velocity = 2 $\mu\text{m}/\text{min}$, shrinkage = 9 $\mu\text{m}/\text{min}$, simulation duration = 500 min, average distribution of 10 simulations is depicted). No microtubule rescues are generated and microtubules shrink back to their nucleation point and start a new growth phase.

Summarizing, dynamic instability facilitates rich dynamic phenomena in microtubule networks at the expense of GTP hydrolysis. Tubulin subunits shed from shrinking ends exchange GDP (the hydrolyzed form of GTP) for GTP for new rounds of assembly and disassembly. Likewise, actin filaments also have growing and shrinking ends, which in this case is facilitated by ATP hydrolysis. Intermediate filaments do not consume nucleotide energy packages and therefore cannot exhibit highly dynamic states. Their assembly is most likely regulated by phosphorylation [8].

1.3. Microtubule-facilitated positioning of cellular components

Multiple ways have been proposed in which microtubules can aid the positioning of cellular components. First of all, motor enzymes may translocate components in a directed manner along microtubules. Dynein motors run towards microtubule minus-ends and kinesins either walk to the plus- or minus-end depending on their intermolecular domain organization [23, 24]. Moreover, objects can be coupled to the ends of both growing and shrinking microtubules for transport. The interface between growing microtubule ends and extending membrane tubules of the endoplasmic reticulum (ER) is for example formed by EB1 proteins that bind to growing microtubule plus-ends and STIM1 proteins that interact both with EB1 and the ER [25]. The interface between shrinking microtubules and kinetochores on chromosomes is on the other hand formed by dam1 proteins that diffuse along microtubules. Microtubule ends constitute a barrier to dam1 diffusion and diffusion away from the shrinking end allows dam1 to maintain its binding energy to microtubules while exerting pulling forces on chromosomes [26, 27]. Also motor proteins can serve as an interface between dynamic microtubules and objects [28, 29]. Lastly, microtubules can position objects by growing against them. If a microtubule encounters a physical barrier in the cell like organelles or a membrane, the addition of GTP-tubulin is restricted due to the spatial constraints. Yet thermal fluctuations between the object and the microtubule end allow for the occasional addition of GTP-tubulin albeit at a decreased rate [30, 31], thus generating forces by the so-called Brownian ratchet mechanism [31, 32]. Microtubules that generate pushing forces also more frequently experience catastrophes due to the decreased concentration of GTP-tubulin [33].

Microtubule based mechanisms are used to position spindles and nuclei for cell division. The spindle position in animal cells and the position of the nucleus in fission yeast cells [13] have been shown to regulate the position of cell cleavage during cytokinesis, generating daughter cells of controlled sizes. Inspired by aster-like microtubule networks attached to nuclei in animal cells it was proposed that microtubules pushing forces against the cell cortex may aid the positioning of nuclei in the centre of cells. In animal cells, microtubule plus-ends grow away from the nuclear-attached centrosome, which is the dominant Microtubule Organizing Centre (MTOC) during interphase. Microtubules impinge on the cell cortex, generate a brief push on the centrosome and

then retract through disassembly. The feasibility of pushing based centring was elegantly demonstrated using an *in vitro* model system in which artificial microtubule asters centred themselves inside micro-fabricated chambers [34, 35]. Microtubule dynamic instability is the key to understanding the centring mechanism in this case. The time required to grow from the MTOC towards the boundary depends on the distance between boundary and MTOC. Microtubules on the MTOC side that is closest to the boundary will therefore more frequently interact with the boundary. Each interaction constitutes a pushing event and MTOCs will thus move away from the closest boundary. The numbers of pushes on all sides of the MTOC are in equilibrium when the MTOC is in the centre of the confinement. A theoretical analysis of the mechanism shows that amplitudes of oscillations away from the centre are decreased if the number of interacting microtubules is increased [36]. The speed at which the MTOC returns to the centre after a perturbation, however, becomes slow when too many microtubules are involved. Fastest positioning is achieved when on average one microtubule interacts with the boundary. The dynamics of centring also depends on the parameters of dynamic instability [36].

An investigation of nuclear positioning in rod-shape fission yeast cells showed that pushing-based centring mechanisms are indeed relevant for cells. Interphase fission yeast cells have about four bundles of microtubules. Each bundle has one to a few microtubules that point with their plus-end to the left cell tip and a similar number of microtubules that point to the right. These microtubules overlap with their minus ends in the centre of the bundle and here the bundle is connected to the nucleus of the cell. Life cell imaging showed that individual microtubule pushing events at the tips of cells correlate to deformations of the nuclear envelope suggesting that the nucleus is pushed back and forth in the cell. Moreover, the repositioning of nuclei that are offset from the centre by centrifugation forces was microtubule dependent and modelling showed that the dynamics of centring is in agreement with 1.) the dynamics of microtubules, and 2.) the several pico-newtons of force that they are known to generate ([13], Figure 1.5 A). Microtubule pushing forces more generally contribute to nuclear migration as demonstrated recently in the *Drosophila* oocyte where microtubule growth is required to move the nuclei from the posterior to the anterior margin to polarize the cell [37].

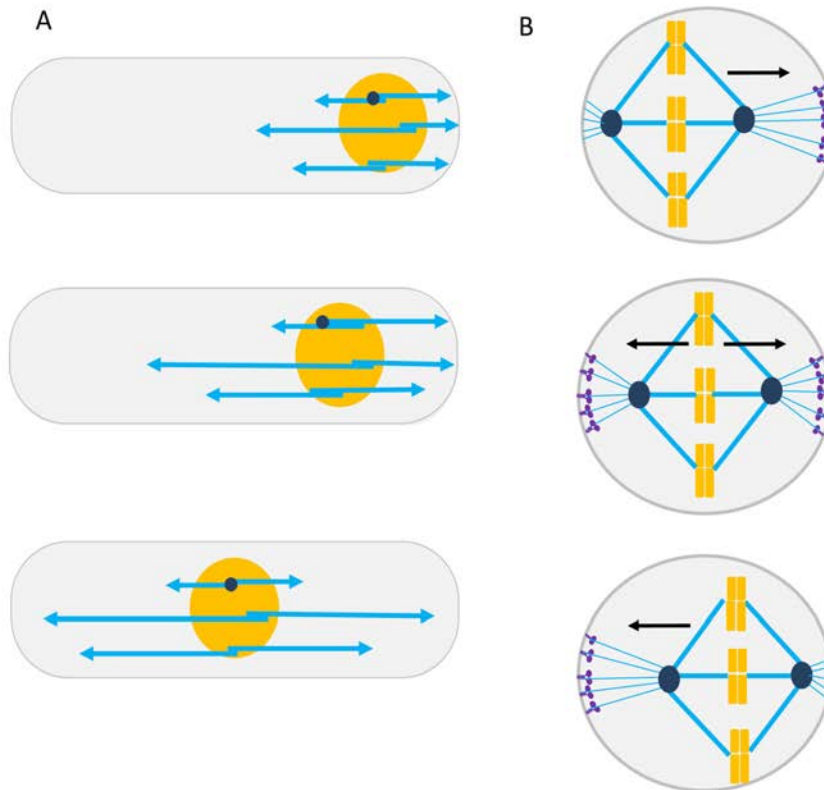


Figure 1.5 Positioning mechanisms based on pushing and pulling forces

(A) Cartoon of nuclear positioning in *S. pombe*. Microtubules (light blue) attached to the nucleus (yellow) grow with their plus-end (arrow head) towards the cell tip and generate pushing forces to position the nucleus. Nuclear displacement to one side of the cell generates a higher frequency of pushing events at this side compared to the opposite side. The frequency of pushing forces is balanced, when the nucleus is positioned in the cell middle. **(B)** Cartoon of the positioning of the mitotic spindle in *C. elegans*. Kinetochore microtubules (light blue) are attached to chromosomes (yellow). The spatial localisation of cortical dynein (purple) controls the spindle position. Aster microtubules attached to the centrosome (dark blue) grow towards the cell cortex and cortical dynein generates pulling forces, inducing spindle movement.

The situation in meiotic fission yeast cells contrasts sharply from the interphase situation outlined above. Now instead of having a stable central position, the nucleus moves back and forth between the cells ends. The movement, which is believed to facilitate pairing of chromosomes, is driven by dynein motors at the cell wall that pull on microtubules growing from the nucleus[38]. Cortical pulling forces also play an important role in positioning mitotic spindles in animal cells [39]. Astral microtubules radiate outwards from the spindle towards the cortex where dynein is localized (Figure 1.5 B). Using again an *in vitro* model system it was shown that under certain conditions pulling forces can position an aster of microtubules in the center of a bounding

geometry [29]. It is therefore likely that positioning of spindles is mediated by a combination of pushing and pulling forces at the cortex.

The positioning mechanisms for nuclei and spindles elegantly demonstrate that dynamic instability, which governs microtubule length, facilitates precise positioning of objects. Microtubules that remain overly short will be inefficient in pushing or pulling and those that grow too long will curve around the boundaries, obstructing positioning. The recent work on nuclear and spindle positioning has given insight into how a single object can be positioned within a bounding geometry. Many cells however, have the ability to position multiple objects on a regular lattice. Examples are nuclei in multinucleated cells or bacterial micro-compartments. The cytoskeleton is often implicated in positioning in these cases but how these arrays are organized is very much an open question.

1.4. Patterning of microtubules in mitotic spindles

Cell division allows organism to proliferate and enables the formation of complex multicellular tissue morphologies; it is essential to life. Microtubules in eukaryotic cells play a leading role in the events during cell division. They form the mitotic spindle, which segregates chromosomes into two sister chromatids at different sides of the cell. Moreover, the mitotic spindle and remnants thereof, including the midbody in animal cells and the phragmoplasts in plants, regulate cytokinesis during which two daughter cells are formed. The spindle is reconfigured as the cell proceeds through the cell cycle stages but one important feature is conserved: spindle bipolarity. Microtubules on the two spindle sides have an opposing polarity: plus-ends point inwards and minus-ends congress near the spindle poles (Figure 1.6). A subset of microtubules, termed inter-polar microtubules, overlap their plus-ends in an antiparallel manner at the spindle centre. Another subset of microtubules, called kinetochore microtubules, establish connections with a kinetochore complex at one of the sister chromatids during prometaphase (Figure 1.6). Each kinetochore ultimately gets connected to microtubules from only one of the two spindle sides. Dramatic changes occur at the transition from metaphase to anaphase. Now connections between the two sister chromatids are severed and kinetochore-bound microtubules disassemble at their plus ends to pull sister chromatids to opposite spindle poles (anaphase-A). The inter-polar microtubules persist and not only keep the poles separated during chromosome movement but also enable spindles to further elongate during anaphase-B thereby increasing the distance between the two sister chromatids ([8], Figure 1.6).

During anaphase the inter-polar microtubules form antiparallel overlapping regions that are remarkably constant in length [40]. A multiple of these overlapping regions aligns in the centre of the spindle, a region that is referred to as both central spindle and midzone in literature. The latter refers by definition to all microtubules in between the two

spindle poles, but the term is used ubiquitously to indicate the interdigitating part only [41]. In animal cells, the midzone regulates cleavage furrow initiation, i.e. the inward motion of the plasma membrane, and the completion of cytokinesis. In plant cells, the anaphase spindle is transformed into the phragmoplast in which the midzone is proposed to recruit cell wall material to form a new cell wall section in the cell centre [42]. The central position of the midzone is thus essential to regulate the position of cytokinesis. Many proteins are known to localize to the short regions of microtubule overlap that form the midzone but the mechanism by which these regions are patterned throughout the spindle remains unknown.

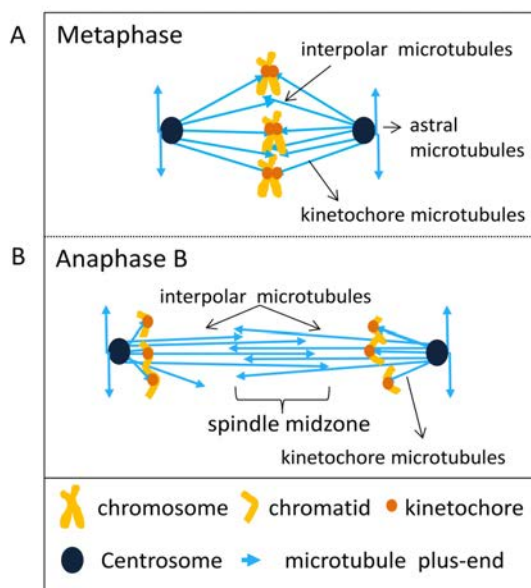


Figure 1.6 The spindle apparatus during metaphase and anaphase B

(A) Cartoon of a metaphase spindle. Kinetochore microtubules are attached to one of the sister chromatids, interpolar microtubules generate antiparallel overlaps in the spindle middle. Astral microtubules grow with their plus-ends to the cell periphery for spindle positioning. **(B)** In anaphase B sister chromatids are already segregated by the kinetochore microtubules and sliding interpolar microtubules increases their distance further.

Amongst the proteins that localize to the midzone are motors of the Kinesin 5 and 6 families that slide antiparallel microtubules apart whilst microtubules grow at their plus ends [43, 44]. These combined activities drive spindle elongation during anaphase-B. A key player in midzone assembly is the ase1p/MAP65/PRC1 (yeast/plant/mammal) family of microtubule crosslinking proteins [45, 46]. Most homologues have been shown to form dimers that selectively bind with high affinity to regions of antiparallel overlap *in vitro* and *in vivo* [45-47]. Apart from forming the overlap these crosslinking proteins have physical interactions with many other midzone proteins, including the aforementioned motors. Crosslinks may thus recruit many regulatory functions to the midzone. PRC1 in mammalian cells binds to KIF4 [40, 48], a protein that slows down microtubule growth and prevents microtubule catastrophes. Moreover, ase1p and PRC1 were shown to bind to clasp homologues [18], proteins that are known to cause rescues. The interaction with crosslinkers allows both KIF4p and clasp to prevent the dissociation of microtubules in overlap. These activities are in agreement with the long-

lifetime of overlapping microtubules as visualized using fluorescent-tags [49, 50]. They do not undergo catastrophe. The fact that crosslinkers, motors and regulators of microtubule dynamic instability interact with each other makes the midzone a fascinating structure. How do microtubule sliding, crosslinking and dynamics affect each other to pattern overlaps in the spindle?

1.5. The model organism fission yeast

Many key discoveries on microtubule organization have been made using the fission yeast *Schizosaccharomyces pombe* as a model system as evidenced from the above overview on microtubule systems. It was first isolated in 1893 from east African beer explaining the name pombe, the Swahili word for beer. The nickname fission yeast originates from its reproduction mechanism in which two daughter cells are created through medial fission of the mother cell. This is in contrast to budding yeast in which new cells grow as a bud on top of the mother cell. Fission yeast was first used as a model system for genetic research in the 1950s. Because of the ease of cell culturing it was soon used as a model system to study basic principles of eukaryotic cells. It has a short generation time of about two hours, making these cells very suitable for studies on mitosis and cell cycle regulation. Starting in the 1970s, Paul Nurse combined the previously developed tools to study cell cycle checkpoints, i.e. control mechanisms that regulate whether cells can proceed to the next stage of a cell cycle [51]. For the characterization of the cyclin-dependent protein kinases, the main player in driving the cell cycle during mitosis he, together with T. Hunt and L. Hartwell, was awarded with the Nobel Prize in Physiology/Medicine in 2001. The following important landmark for *S. pombe* as a model system was the publication of the complete sequenced genome in 2002 [52]. Fission yeast contains an estimated number of 4979 genes, which is one of the smallest genomes of a eukaryotic cell. Many genes that were shown to regulate aspects of the cell division and cellular organization in fission yeast are also present in the human genome.

Fission yeast has a high efficiency of homologous recombination making its genome very amendable. The use of PCR-derived constructs for homologue recombination [53] allow targeted insertion and deletion of genes and gene fragments into the genome for (partial) gene deletion and gene tagging. The ability to directly tag a gene with a gene coding for a fluorescent protein is a very strong asset for microscopy studies on cellular organization since fusion proteins can be expressed under the control of the endogenous promoter. Moreover, the construction of temperature sensitive mutants allows for the conditional functional inhibition of essential proteins. *S. pombe* cells have a dominant haploid proliferation state. Cells of two mating types (h⁺ and h⁻) readily conjugate and form haploid spores under nutritional limiting conditions. In this way modifications of multiple genes can easily be combined to form a new cell line that for example expresses two gene products tagged with green and red fluorescent proteins respectively.

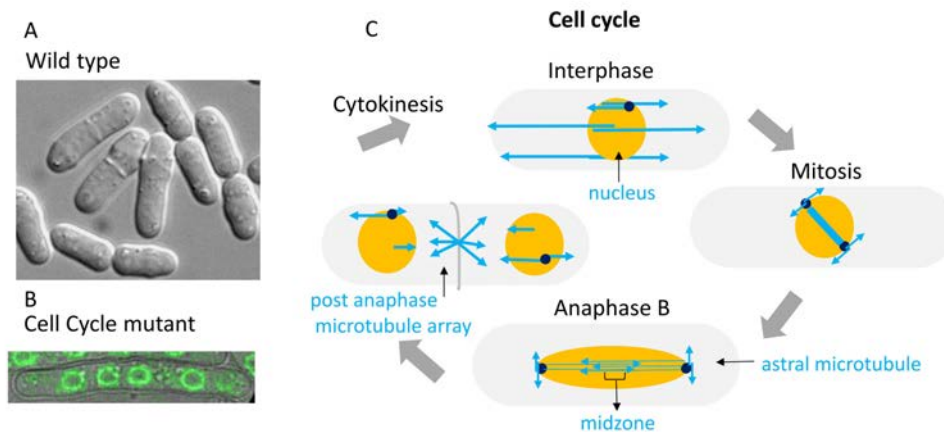


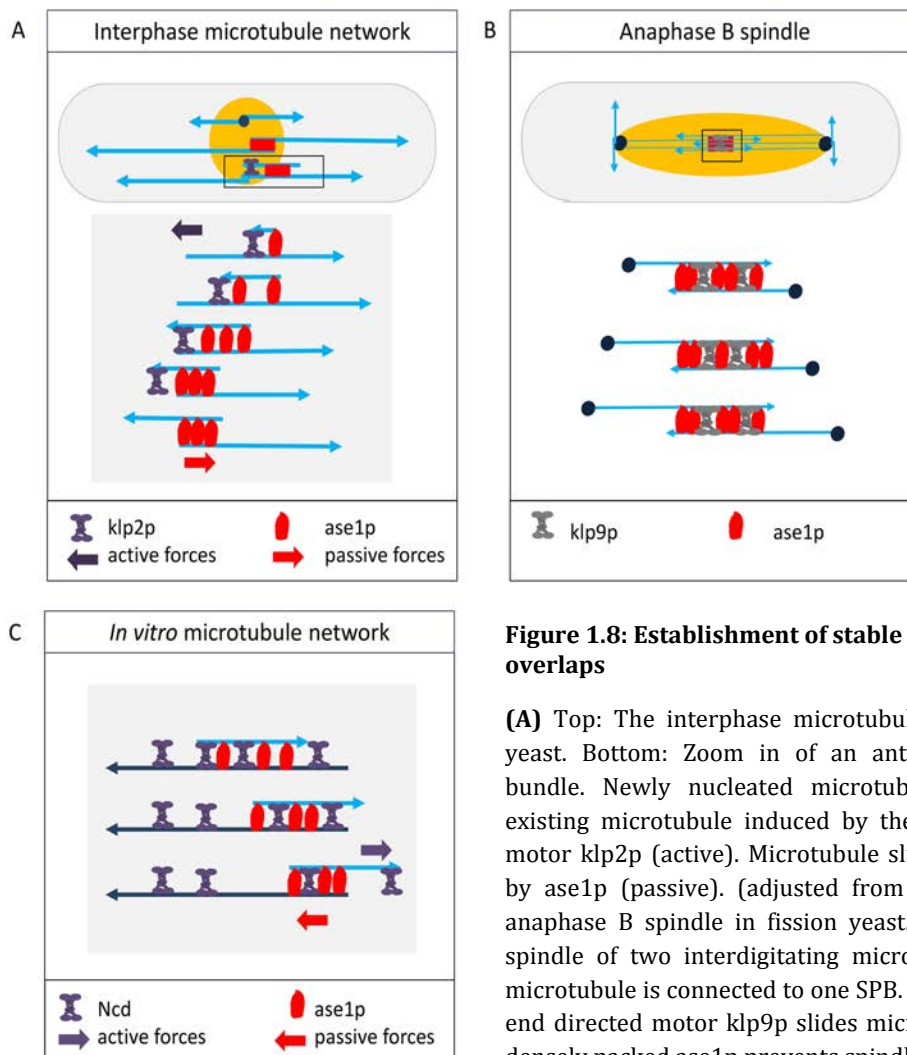
Figure 1.7: The fission yeast *S. pombe*

(A) *S. pombe* cells are rod-shaped with a length of approximately 12 μm [54]. Picture taken by J.Teapal. (B) Temperature-sensitive mutations in cell cycle genes create for example cells that duplicate their genomes without undergoing cytokinesis, forming single cells with four nuclei in this case [51]. Image taken by J. Teapal. (C) Summary of the microtubule network of fission yeast throughout the cell cycle [55]. The direction of growth of microtubule plus-ends is indicated with an arrow. Spindle pole bodies (red) are the main microtubule-organizing centres (MTOCs) but function along with more dispersed MTOCs. *S. pombe* cells undergo a closed mitosis and form a compact linear bipolar spindle, where kinetochore microtubules connected to the chromosomes and interpolar microtubules interdigitate at the spindle middle and form the midzone. Astral microtubules nucleate from the SPB to align the spindle along the length axis of the cell [56]. During anaphase B the spindle elongates and a midzone of overlapping microtubule plus-ends is formed. Just before cytokinesis, post anaphase microtubules nucleate at the cytokinetic ring.

Fission yeast cells are rod-shaped and elongate by tip-growth during interphase up to a length of about 14 μm . The cell diameter is only 3-4 μm , which makes it relatively easy to visualize intercellular patterns of fluorescent proteins with confocal microscopy. Microtubules typically run along the long axis of the cells and can be imaged particularly well. The varying layout of microtubules throughout the cell cycle has been well characterized ([6] and Figure 1.7).

Interphase cells have microtubules whose plus ends grow away from gamma-tubulin complexes near the cell nucleus forming a bipolar microtubule bundle that functions in nuclear positioning and the establishment of cell polarity. Minus-ends in general remain connected to the MTOC and are not dynamic. Fission yeast undergoes a closed mitosis, implying that the mitotic spindle is organized within the nucleus without the breakdown of the nuclear envelope. Spindle microtubules grow from gamma-tubulin complexes at the spindle pole bodies (SPBs) and form a near 1-dimensional array. Astral microtubules grow away from SPBs on the cytoplasmic side of the nuclear envelope and are believed

to align the spindle longitudinally by generating pushing forces against the cell cortex. Lastly, microtubules grow away from cortical gamma-tubulin complexes located at the cell centre during the last stages of anaphase. The function of this post anaphase array of microtubules is not well described but may involve the formation of a barrier that prevents the separated nuclei from congressing as long as the two daughter cells are not yet divided. Many of the genes involved in microtubule regulation are conserved in higher eukaryotes. The study of microtubule systems in *S. pombe* will therefore yield mechanistic insight into the regulatory mechanism that are likely present as well in the more complex networks of higher eukaryotic cells, including mammalian cells [57, 58].



(C) In vitro microtubule network consisting out of a template microtubule (dark blue) fixed to the surface and a transport microtubule (light blue). The minus-end directed motor Ncd slides the microtubules apart, but ase1p remains in the shortened overlap and slows down microtubule sliding (adjusted from [1]). SPB= dark blue circle, microtubule plus-end = arrow head. Large arrows indicate the direction of the force generation.

Fission yeast appears to be a suitable system to study regulation of the midzone because of the relative simple spindle layout. In contrast to higher eukaryotes, only a single region of overlap of about 15 interdigitating microtubules regulates anaphase-B elongation [59]. Moreover, in contrast to higher eukaryotes in which microtubule minus-ends undergo disassembly, minus-ends of microtubules in fission yeast are stably attached to the spindle pole bodies at the spindle poles [60]. There is also no microtubule severing and moreover, there are no dynein motors bound at the cortex that apply additional forces on the spindle [61]. Importantly however, *ase1p* crosslinkers were shown to interact with both clasp (*cls1p*) [18] and kinesin-6 (*klp9p*) [43] suggesting that similar crosstalk between microtubule based activities occurs as in high eukaryotes. The interpolar microtubules in fission yeast are known to form a central midzone to enable anaphase-A and anaphase-B motions but there is no known role for the midzone in regulating the location of cytokinesis. Instead the location of the interphase nucleus is regulating the site of cellular fission [1]. Perhaps for this reason the protein *ase1p* is not essential in yeast allowing for extensive genetic perturbation of the system for in depth mechanistic studies.

Already work on the fission yeast system has given insight into physical mechanisms that may be important for midzone organization. Fission yeast harbours another bipolar microtubule structure during interphase in which the polarity is inverted in comparison to the spindle [62]. In this network, microtubule plus-ends grow away from the nucleus towards the cell tips to deliver cell polarity factors and to push the nucleus towards the cell centre ([13], Figure 1.3). New microtubules are nucleated off the sides of existing microtubules whereas other microtubules are removed by depolymerisation. Moreover, the new microtubules slide towards the minus ends of the exiting microtubules. It was shown that the minus-end directed motor *klp2p*, which drives this motion, is slowed down by *ase1p* crosslinkers that assemble in between the overlapping microtubules ([63],

Figure 1.8 A). Inspired by this findings, *in vitro* experiments with purified components were conducted to investigate the interaction between active motors and passive crosslinkers in detail. *Ase1p* was shown to diffuse along microtubules while being bound to them and the ends of microtubules constituted a barrier for *ase1p* diffusion. This allows *ase1p* to stay associated with overlaps even when the overlap between two microtubules is shortened by the action of molecular motors. The resulting compaction of *ase1p* crosslinkers was shown to be persistent because *ase1p* has a residence time of several minutes within overlaps ([47], Figure 1.8 B). This persistent build-up of *ase1p* in between overlaps cause a slow-down of motorized sliding as the two microtubules move further apart. The physical properties of *ase1p* therefore prevent microtubules from sliding apart, a property that may be utilized by cells within the midzone of the spindle.

1.6. Thesis Outline

The architecture of the cell is well organized but organizing mechanisms are often not understood. In many organisms it has been shown that networks of cytoskeletal filaments, of which microtubules are a prominent component, are essential for pattern formation. The initial goal of my thesis work was to modulate the interactions between overlapping microtubules that govern the organization of a bipolar array of microtubules in interphase fission yeast cells. At the time it was shown that passive microtubule crosslinkers (*ase1p*) and molecular motors are involved in a tug of war that determines the relative sliding velocity of overlapping microtubules. I set out to modulate the proteins involved by perturbing the yeast genome and to visualize the resulting dynamics of microtubules in networks. A similar tug of war between motors and other microtubule crosslinkers takes however place in mitotic spindles and new *in vitro* work in the laboratory with purified microtubule components suggested how this could aid the spatial organization of the mitotic spindle. Moreover, reports on fission yeast cells with multiple nuclei suggested that the bipolar microtubule arrays I investigated may not only position single nuclei in cells but may also regulate the spacing between neighbouring nuclei in multinucleated cells. These two developments have set the stage for this thesis on microtubule-based positioning mechanisms.

In chapter **two** of this thesis, I used *S. pombe* mutant cells with a defect in cell cycle regulation to generate yeast cells with multiple nuclei. I demonstrate using live cell imaging that microtubule growth from one nucleus toward a neighbour may generate a repulsive force between nuclei. The force is expected to depend on the internuclear distance and therefore enables cells to set up a pattern of regularly spaced nuclei. Moreover, the work shows that motor proteins may generate additional repulsive or attractive forces between nuclei, which may allow cells to switch between different patterns. The obtained mechanistic understanding in this simple model system will aid investigations on more complex multi nuclear systems such as myotubes.

In chapter **three**, we developed a 1D-stochastic model to demonstrate that force generation by growing microtubules is indeed sufficient to organize nuclei in an equidistant pattern. Modelling of microtubule interactions with nuclei and the cell wall explained the equilibrium inter-nuclear distance attained and the magnitude of oscillations around the equilibrium position. The mechanism was further investigated in terms of robustness to variations in parameters of dynamic instability and cell length.

In chapter **four**, we analysed the regulation of the spindle midzone during anaphase spindle elongation in various fission yeast mutants with defects in the regulation of microtubule sliding, microtubule crosslinking and microtubule dynamic instability. This

integral approach shows that spindle elongation velocity is strongly coupled to the dynamics of microtubule growth. The findings suggest that forces generated by microtubule crosslinkers may play a role in regulating spindle elongation similar to what was earlier observed in *in vitro* work. These show that crosslinkers more strongly restrain sliding because the ends of microtubules constitute a barrier to the diffusion of crosslinkers.

In chapter **five**, our findings are summarized and an outline is given for follow-up studies in yeast and other cells that can provide further insights into microtubule-based patterning in the spindle. Results on the binding of crosslinkers to microtubule bundles *in vitro* assays are shown that suggest how crosslinkers may become immobilized in the spindle centre.

References

1. Rincon, S.A. and A. Paoletti, *Mid1/anillin and the spatial regulation of cytokinesis in fission yeast*. Cytoskeleton, 2012. **69**(10): p. 764-777.
2. Fletcher, D.A. and R.D. Mullins, *Cell mechanics and the cytoskeleton*. 2010. **463**(7280): p. 485-492.
3. Howard, J., S.W. Grill, and J.S. Bois, *Turing's next steps: the mechanochemical basis of morphogenesis*. 2011. **12**(6): p. 392-398.
4. Grimm, O., M. Coppey, and E. Wieschaus, *Modelling the Bicoid gradient*. Development, 2010. **137**(14): p. 2253-2264.
5. Mitchison, T. and M. Kirschner, *Dynamic instability of microtubule growth*. 1984. **312**(5991): p. 237-242.
6. Gitai, Z., *The New Bacterial Cell Biology: Moving Parts and Subcellular Architecture*. Cell, 2005. **120**(5): p. 577-586.
7. Bornens, M., *The Centrosome in Cells and Organisms*. Science, 2012. **335**(6067): p. 422-426.
8. Bruce Alberts, A.J., Julian Lewis, Martin Raff, Keith Roberts, and Peter Walter., *Molecular Biology of the Cell*. 2002.
9. Ketelaar, T., et al., *Positioning of Nuclei in Arabidopsis Root Hairs: An Actin-Regulated Process of Tip Growth*. The Plant Cell Online, 2002. **14**(11): p. 2941-2955.
10. Malek, A.M. and S. Izumo, *Mechanism of endothelial cell shape change and cytoskeletal remodeling in response to fluid shear stress*. Journal of Cell Science, 1996. **109**(4): p. 713-726.
11. Desai, A. and T.J. Mitchison, *MICROTUBULE POLYMERIZATION DYNAMICS*. Annual Review of Cell and Developmental Biology, 1997. **13**(1): p. 83-117.
12. Stepanova, T., et al., *Visualization of Microtubule Growth in Cultured Neurons via the Use of EB3-GFP (End-Binding Protein 3-Green Fluorescent Protein)*. The Journal of Neuroscience, 2003. **23**(7): p. 2655-2664.
13. Tran, P.T., et al., *A Mechanism for Nuclear Positioning in Fission Yeast Based on Microtubule Pushing*. The Journal of Cell Biology, 2001. **153**(2): p. 397-412.
14. Gladfelter, A. and J. Berman, *Dancing genomes: fungal nuclear positioning*. 2009. **7**(12): p. 875-886.
15. Walker, R.A., et al., *Dynamic instability of individual microtubules analyzed by video light microscopy: rate constants and transition frequencies*. The Journal of Cell Biology, 1988. **107**(4): p. 1437-1448.
16. Zanic, M., et al., *Synergy between XMAP215 and EB1 increases microtubule growth rates to physiological levels*. 2013. **15**(6): p. 688-693.
17. Hunter, A.W., et al., *The Kinesin-Related Protein MCAK Is a Microtubule Depolymerase that Forms an ATP-Hydrolyzing Complex at Microtubule Ends*. Molecular Cell, 2003. **11**(2): p. 445-457.

18. Bratman, S.V. and F. Chang, *Stabilization of Overlapping Microtubules by Fission Yeast CLASP*. *Developmental Cell*, 2007. **13**(6): p. 812-827.
19. Gardner, M.K., et al., *Chromosome Congression by Kinesin-5 Motor-Mediated Disassembly of Longer Kinetochore Microtubules*. *Cell*, 2008. **135**(5): p. 894-906.
20. Tischer, C., D. Brunner, and M. Dogterom, *Force- and kinesin-8-dependent effects in the spatial regulation of fission yeast microtubule dynamics*. 2009. **5**.
21. Rogers, G.C., S.L. Rogers, and D.J. Sharp, *Spindle microtubules in flux*. *Journal of Cell Science*, 2005. **118**(6): p. 1105-1116.
22. Pastuglia, M. and D. Bouchez, *Molecular encounters at microtubule ends in the plant cell cortex*. *Current Opinion in Plant Biology*, 2007. **10**(6): p. 557-563.
23. Mallik, R. and S.P. Gross, *Molecular Motors: Strategies to Get Along*. *Current Biology*, 2004. **14**(22): p. R971-R982.
24. Sharp, D.J., G.C. Rogers, and J.M. Scholey, *Microtubule motors in mitosis*. 2000. **407**(6800): p. 41-47.
25. Grigoriev, I., et al., *STIM1 Is a MT-Plus-End-Tracking Protein Involved in Remodeling of the ER*. *Current Biology*, 2008. **18**(3): p. 177-182.
26. Gardner, M.K. and D.J. Odde, *Dam1 complexes go it alone on disassembling microtubules*. 2008. **10**(4): p. 379-381.
27. Ramey, V.H., et al., *The Dam1 ring binds to the E-hook of tubulin and diffuses along the microtubule*. *Molecular Biology of the Cell*, 2011. **22**(4): p. 457-466.
28. Gibeaux, R., et al., *Spindle pole body-anchored Kar3 drives the nucleus along microtubules from another nucleus in preparation for nuclear fusion during yeast karyogamy*. *Genes & Development*, 2013. **27**(3): p. 335-349.
29. Laan, L., et al., *Cortical Dynein Controls Microtubule Dynamics to Generate Pulling Forces that Position Microtubule Asters*. *Cell*, 2012. **148**(3): p. 502-514.
30. Hill, T.L. and M. Kirschner, *Bioenergetics and kinetics of microtubule and actin filament assembly-disassembly*. *Int. Rev. Cytol*, 1982.
31. Mogilner, A. and G. Oster, *The Polymerization Ratchet Model Explains the Force-Velocity Relation for Growing Microtubules*. *European Biophysics Journal*, 1999. **11/1998**.
32. van Doorn, G.S., et al., *On the stall force for growing microtubules*. 2000. **29**(1): p. 2-6.
33. Janson, M.E., M.E. de Dood, and M. Dogterom, *Dynamic instability of microtubules is regulated by force*. *The Journal of Cell Biology*, 2003. **161**(6): p. 1029-1034.
34. Faivre-Moskalenko, C. and M. Dogterom, *Dynamics of microtubule asters in microfabricated chambers: The role of catastrophes*. *Proceedings of the National Academy of Sciences*, 2002. **99**(26): p. 16788-16793.
35. Holy, T.E., et al., *Assembly and positioning of microtubule asters in microfabricated chambers*. *Proceedings of the National Academy of Sciences*, 1997. **94**(12): p. 6228-6231.

36. Dogterom, M. and B. Yurke, *Microtubule dynamics and the positioning of microtubule organizing centers*. Physical Review Letters, 1998. **81**(2): p. 485-488.
37. Zhao, T., et al., *Growing Microtubules Push the Oocyte Nucleus to Polarize the Drosophila Dorsal-Ventral Axis*. Science, 2012. **336**(6084): p. 999-1003.
38. Tolić-Nørrelykke, I., *Push-me-pull-you: how microtubules organize the cell interior*. 2008. **37**(7): p. 1271-1278.
39. Grill, S.W., et al., *The Distribution of Active Force Generators Controls Mitotic Spindle Position*. Science, 2003. **301**(5632): p. 518-521.
40. Hu, C.-K., et al., *KIF4 Regulates Midzone Length during Cytokinesis*. Current Biology, 2011. **21**(10): p. 815-824.
41. Glotzer, M., *The 3Ms of central spindle assembly: microtubules, motors and MAPs*. 2009. **10**(1): p. 9-20.
42. Kosetsu, K., et al., *MICROTUBULE-ASSOCIATED PROTEIN65 Is Essential for Maintenance of Phragmoplast Bipolarity and Formation of the Cell Plate in Physcomitrella patens*. The Plant Cell Online, 2013.
43. Fu, C., et al., *Phospho-Regulated Interaction between Kinesin-6 Klp9p and Microtubule Bundler Ase1p Promotes Spindle Elongation*. Developmental Cell, 2009. **17**(2): p. 257-267.
44. Sharp, D.J., et al., *Antagonistic microtubule-sliding motors position mitotic centrosomes\par in Drosophila early embryos*. 1999. **1**(1): p. 51-54.
45. Loïodice, I., et al., *Ase1p Organizes Antiparallel Microtubule Arrays during Interphase and Mitosis in Fission Yeast*. Molecular Biology of the Cell, 2005. **16**(4): p. 1756-1768.
46. Yamashita, A., et al., *The Roles of Fission Yeast Ase1 in Mitotic Cell Division, Meiotic Nuclear Oscillation, and Cytokinesis Checkpoint Signaling*. Molecular Biology of the Cell, 2005. **16**(3): p. 1378-1395.
47. Braun, M., et al., *Adaptive braking by Ase1 prevents overlapping microtubules from sliding completely apart*. 2011. **13**(10): p. 1259-1264.
48. Bieling, P., I.A. Telley, and T. Surrey, *A Minimal Midzone Protein Module Controls Formation and Length of Antiparallel Microtubule Overlaps*. Cell, 2010. **142**(3): p. 420-432.
49. Fridman, V., et al., *Midzone organization restricts interpolar microtubule plus-end dynamics during spindle elongation*. EMBO reports, 2009. **10**(4): p. 387-393.
50. Mallavarapu, A., K. Sawin, and T. Mitchison, *A switch in microtubule dynamics at the onset of anaphase B in the mitotic spindle of Schizosaccharomyces pombe*. Current Biology, 1999. **9**(23): p. 1423-1428.
51. Nurse, P., *A Long Twentieth Century of the Cell Cycle and Beyond*. Cell, 2000. **100**(1): p. 71-78.
52. Wood, V., et al., *The genome sequence of Schizosaccharomyces pombe*. 2002. **415**(6874): p. 871-880.

53. Bähler, J., et al., *Heterologous modules for efficient and versatile PCR-based gene targeting in Schizosaccharomyces pombe*. *Yeast*, 1998. **14**(10): p. 943-951.
54. Sveiczer, A., B. Novak, and J.M. Mitchison, *The size control of fission yeast revisited*. *Journal of Cell Science*, 1996. **109**(12): p. 2947-2957.
55. Neumann, F.R. and P. Nurse, *Nuclear size control in fission yeast*. *The Journal of Cell Biology*, 2007. **179**(4): p. 593-600.
56. Tolić-Nørrelykke, I.M., et al., *Positioning and Elongation of the Fission Yeast Spindle by Microtubule-Based Pushing*. *Current Biology*, 2004. **14**(13): p. 1181-1186.
57. Wixon, J., *Featured Organism: Schizosaccharomyces pombe, The Fission Yeast*. *Comparative and Functional Genomics*, 2002. **3**(2): p. 194-204.
58. Forsburg, S.L., *The yeasts Saccharomyces cerevisiae and Schizosaccharomyces pombe: models for cell biology research*.
59. McIntosh, J.R., et al., *Conserved and divergent features of kinetochores and spindle microtubule ends from five species*. *The Journal of Cell Biology*, 2013. **200**(4): p. 459-474.
60. Khodjakov, A., S. La Terra, and F. Chang, *Laser Microsurgery in Fission Yeast: Role of the Mitotic Spindle Midzone in Anaphase B*. *Current Biology*, 2004. **14**(15): p. 1330-1340.
61. Yamamoto, A., et al., *A Cytoplasmic Dynein Heavy Chain Is Required for Oscillatory Nuclear Movement of Meiotic Prophase and Efficient Meiotic Recombination in Fission Yeast*. *The Journal of Cell Biology*, 1999. **145**(6): p. 1233-1250.
62. Carazo-Salas, R.E., C. Antony, and P. Nurse, *The Kinesin Klp2 Mediates Polarization of Interphase Microtubules in Fission Yeast*. *Science*, 2005. **309**(5732): p. 297-300.
63. Janson, M.E., et al., *Crosslinkers and Motors Organize Dynamic Microtubules to Form Stable Bipolar Arrays in Fission Yeast*. *Cell*, 2007. **128**(2): p. 357-368.



A microtubule based mechanism for equidistant positioning of multiple nuclei

Juliane Teapal, Bela M. Mulder and Marcel E. Janson

Chapter

2

Abstract

Many cells harbor regularly spaced arrays of organelles like carboxysomes, nucleoids and notably multiple nuclei. Such equidistant positioning can ensure even partitioning of organelles during cell division or, in the case of nuclei, control cell size during cellularization. The positioning mechanisms involved are as yet poorly understood. We used multinucleated fission yeast cells as a model system to mechanistically dissect spacing by dynamically unstable cytoskeletal filaments. Cytokinesis-defected *cdc11* cells accumulated multiple nuclei over time, which were found to be clustered near the cell center. Cells that lacked the kinesin *klp2p*, however, had equidistant patterns of nuclei. This regular pattern reappeared after nuclear positions were perturbed by centrifugation forces. Based on live cell imaging we propose that neighboring nuclei are pushed apart by microtubules growing in the internuclear space. Our results demonstrate how cells may exploit dynamic instability to generate distance dependent forces required for equidistant spacing of organelles.

2.1. Introduction

Cells are highly compartmentalized and positioning of organelles and other cellular components is crucial for many aspects of cellular functioning. Organelles can be localized to specific sites or be dispersed to make their function available throughout the cell. In many cases cytoskeletal networks are involved in positioning. Tubules of the ER, for example, are dispersed along polarized microtubules that radiate out from centrosomes in interphase [1]. Other organelles are dispersed in the absence of a single radially organized cytoskeletal network. Examples are nuclei in multinucleated cells, prokaryotic organelles and chloroplasts in plants [2-7]. In some of these systems organelles can be found at well-regulated equidistant positions from each other, demonstrating that there are active mechanisms involved that control distance [2, 3, 8, 9].

During cellularization of multinucleate embryonic syncytia, the positioning of nuclei is important, as it determines the size of cells that forms around them [10]. Additionally, functions of nuclear spacing are underscored by muscle diseases and malfunctions that correlate with aberrant dispersion of nuclei in multinucleate myotubes [5, 11]. Regular spacing of organelles and chromosomes in prokaryotes ensures that daughter cells inherit an equal number of items during cell division [2, 3]. Although many molecules have been identified with a role in positioning, there is as of yet no model organism for which the mechanism of equidistant organelle positioning has been mechanistically dissected.

To gain mechanistic insight into the patterning of organelles, we studied nuclear positioning in multinucleated fission yeast cells (*S. pombe*). Interphase fission yeast cells have a single nucleus, but cells temporarily harbor two or more nuclei during cytokinesis, karyogamy (mating) and sporulation. Two nuclei congress during karyogamy to allow chromosome pairing but nuclei must remain separated during cytokinesis and sporulation. Congression of nuclei was shown to involve the molecular motor klp2p. Nuclei organize a polarized microtubule network around them with microtubule plus-ends pointing outwards. Minus-end directed klp2p motors are thought to generate contractile forces between the interdigitating networks of two nuclei, drawing the nuclei together. The activity of klp2p is down regulated to prevent nuclear congression during cytokinesis [12-14]. Moreover, down regulation of klp2p was shown to space nuclei apart in cell cycle mutants with multiple nuclei [19]. The nature of the forces that separates nuclei is however unknown.

We quantified nuclear positioning in interphase *cdc11* mutants with four nuclei and find that nuclei can form equidistant patterns in the absence of klp2p. Imaging of microtubules suggested that repulsive interactions between nuclei involve microtubule-pushing forces generated when a microtubule originating from one nucleus impinges onto a neighbor. The frequency of such events is expected to decrease with increasing

internuclear distance. Thus, the net force generated between nuclei is distance-dependent allowing for control over internuclear spacing.

2.2. Results

Equidistant patterning is *klp2* dependent

The protein *cdc11p* is a component of the septin ring that is required for cytokinesis. A temperature sensitive *cdc11* mutant duplicates nuclei but fails to undergo cytokinesis. Nonetheless, cells continue to grow and will undergo multiple rounds of nuclear replication. To quantify the organization of nuclei in *cdc11* fission yeast we grew cells expressing a nuclear envelope marker at the repressive temperature [15, 16]. After two rounds of nuclear division without subsequent cytokinesis, cells contained four nuclei that clustered together, in agreement with earlier work [17]. Clusters of nuclei were positioned near the cell center (Figure 2.1 (left)). In contrast, nuclei in *cdc11* cells lacking *klp2p* were regularly distributed along the cell axis (Figure 2.1 (right)). Some degree of patterning is a priori expected because the nuclei cannot overlap, which in effect generates a repulsive force between them [18]. The distributions of nuclear positions and internuclear distances were however much narrower than expected for random nuclear positioning in the presence of overlap constraints, demonstrating that distances are regulated (Figure 2.1 B, C).

In conclusion, we confirm that *klp2p* interferes negatively with nuclear dispersion and show that its inactivation can induce a switch from a central cluster of nuclei to a well-dispersed pattern in which distances are controlled.

Interphase microtubules are required for a robust equidistant pattern

Which process controls nuclear spacing in *cdc11 klp2Δ* cells? Both spindle elongation during mitosis and microtubule growth in interphase may change the position of nuclei. Oscillations in nuclear position observed in *cdc11 klp2Δ* cells suggested the presence of an active positioning mechanism during interphase (Figure 2.1 A, kymographs). To test whether nuclear position is controlled in interphase we applied centrifugation forces to move nuclei to one side of the cell (Figure 2.2 A). Nuclear patterns were reestablished on a timescale of several hours. Nuclei in *cdc11* cells moved as a cluster towards the cell center and nuclei in *cdc11 klp2Δ* cells regained 77% of their steady state internuclear distance during the first 2.5 hours after centrifugation (Figure 2.2 B, D). Besides, in presence of the microtubule-depolymerizing drug MBC reestablishment of the nuclear pattern was not observed, confirming the role of interphase microtubules (Figure 2.2 C D).

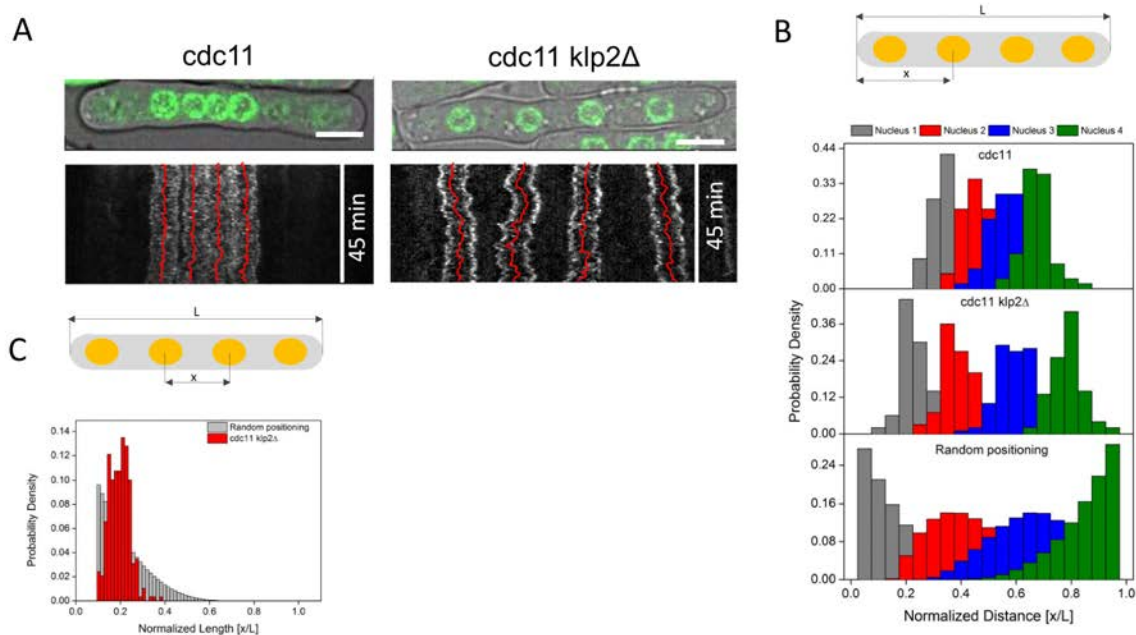


Figure 2.1: Equidistant patterning of nuclei in absence of *klp2p*

(A) Confocal projection and kymograph of tetranucleated *cdc11* and *cdc11 klp2Δ* cells expressing the nuclear envelope marker *nup107-GFP*. **(B)** Distribution of nuclear midpoint positions in tetranucleated *cdc11* (N = 126 cells) and *cdc11 klp2Δ* cells (N = 109 cells). Positions are normalized to the cell length. Bottom panel shows the distribution for random positioning of non-overlapping nuclei. **(C)** Distribution of internuclear distances, measured between midpoints of neighboring nuclei, in *cdc11 klp2Δ* cells and for random positioning of non-overlapping nuclei. Scale bar: 5 μm .

To further characterize the underlying ordering mechanism tetranucleated cells of various cell lengths were created. For this we prevented cells from going into mitosis by decreasing DNA synthesis through addition of hydroxyurea (Figure 2.3. A). Internuclear spacing increased with cell length for cells between 30 and 50 μm in length (Figure 2.3 B). We conclude that an active process involving interphase microtubules positions nuclei at equidistant positions in cells that lack *klp2p*. The distance is not controlled in an absolute sense but scales with cell length.

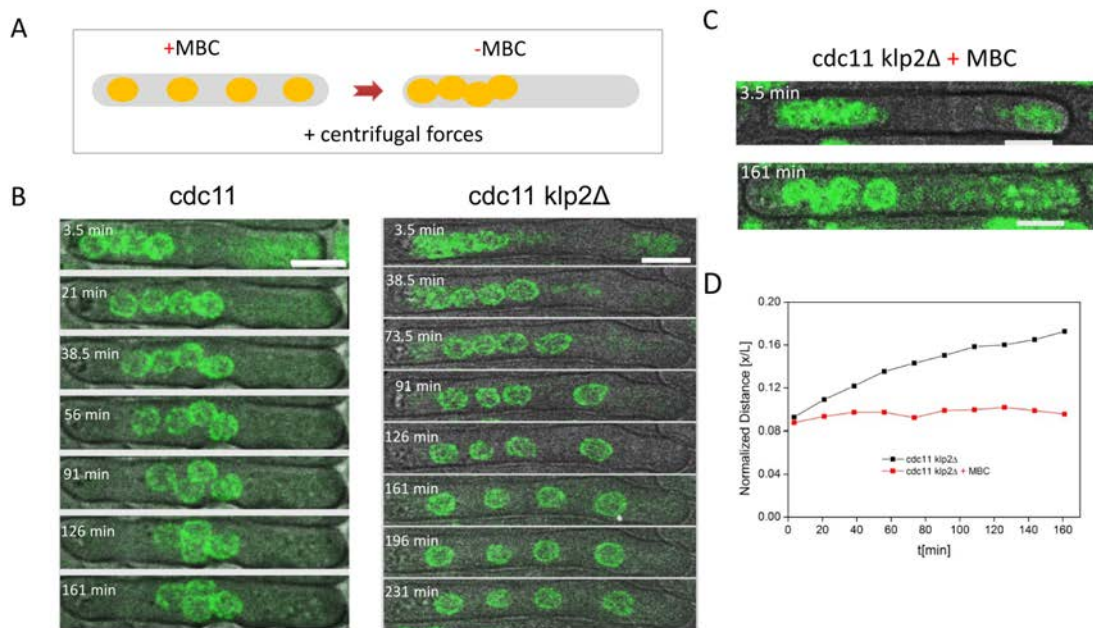


Figure 2.2: Pattern re-establishment of tetranucleated cells

(A) Cartoon of the centrifugation assay. *Cdc11* cells are treated with MBC and nuclei are displaced by centrifugation, followed by a wash out of MBC. **(B)** Nuclear motion after cell centrifugation in tetranucleated *cdc11* and *cdc11-klp2Δ* cells. Imaging commenced approximately 3.5 minutes after centrifugation. **(C)** Same as B, but not followed by MBC washout. **(D)** Internuclear distances of tetranucleated *cdc11-klp2Δ* cells over time after centrifugation (red: MBC washout, N=23 cells, black: no washout, N=12 cells). Scale bars: 5 μ m.

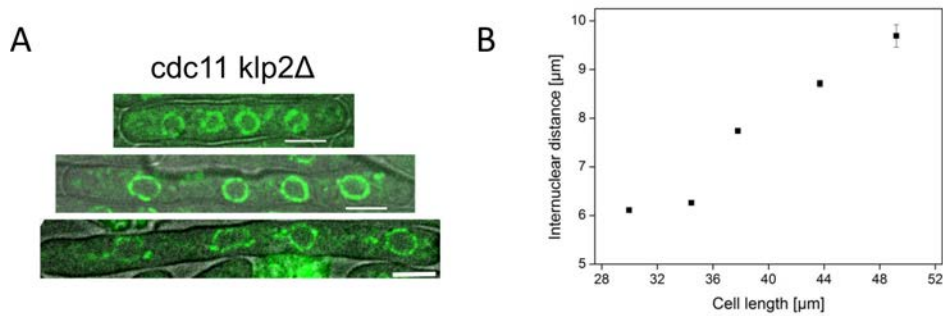


Figure 2.3: Ordering mechanism in large cells

(A) Confocal images of HU-treated tetranucleated *cdc11-klp2Δ* cells for different cell length (28.2, 42.6 and 45.8 μ m) **(B)** Internuclear distances (N=112) in HU-treated cells of various length with SE.

The Kinesin klp2p generates attractive forces between nuclei

Interphase microtubules in mononucleated *S. pombe* cells are organized in about four antiparallel assemblies that are bound to the nuclear envelope [16]. Within each assembly, a few non-dynamic microtubule minus-ends form overlaps near the nucleus and plus-ends grow towards cell ends. This high degree of polarization is slightly decreased in absence of klp2p, but the overall organization remains intact [19, 20]. To further investigate the role of microtubules in internuclear spacing we expressed GFP-tubulin in *cdc11 klp2Δ* cells. Microtubules were localized close to the nuclear envelopes suggesting that they are bound to it as observed in wild type cells (Figure 2.4 A). Growth within the space between the cell ends and the outer nuclei was primarily unidirectional towards the cell ends. In contrast, growth between nuclei was bidirectional. The growth of microtubules is thus in agreement with each nucleus having an associated bipolar microtubule network.

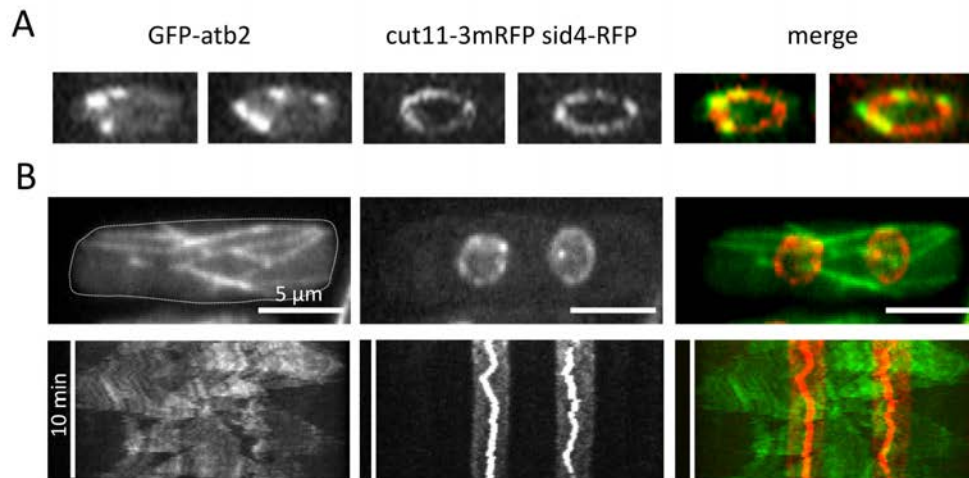


Figure 2.4: Interdigitating microtubule network in *cdc11 klp2Δ* cells

(A) Full cell projection of the nuclei in binucleated *cdc11 klp2Δ* cell expressing GFP-tubulin (GFP-atb2), the spindle pole body marker sid4-RFP and the nuclear envelope marker cut11-3mRFP. **(B)** Same as above but full cell projection and kymograph of a binucleated *cdc11 klp2Δ* cell. Scale bar: 5 μm

Interdigitating microtubules in between nuclei were proposed to facilitate congression of nuclei during karyogamy through the action of the minus-end directed motor klp2p that slide antiparallel microtubules relative to each other [19, 20]. To observe whether klp2p may have a similar role in multinucleated cells we observed binucleated *cdc11* cells just after the mitotic spindle separated the nuclei. At this stage microtubules that

adhere to the SPB form the most prominent bundles and we expressed the spindle pole marker *sid4*-mRFP to visualize the attachment point of the microtubule to the nuclear envelope. Microtubules growing from sister nuclei were observed to form internuclear bundles. In *cdc11* cells these bundles contracted in the presence of *klp2p* resulting in congression of SPBs and nuclei. This very much reminiscent the nuclear pairing during karyogamy ([21], Figure 2.5 B,C). In absence of *klp2p* the formation of internuclear bundles was observed but no contraction followed and the nuclei remained apart.

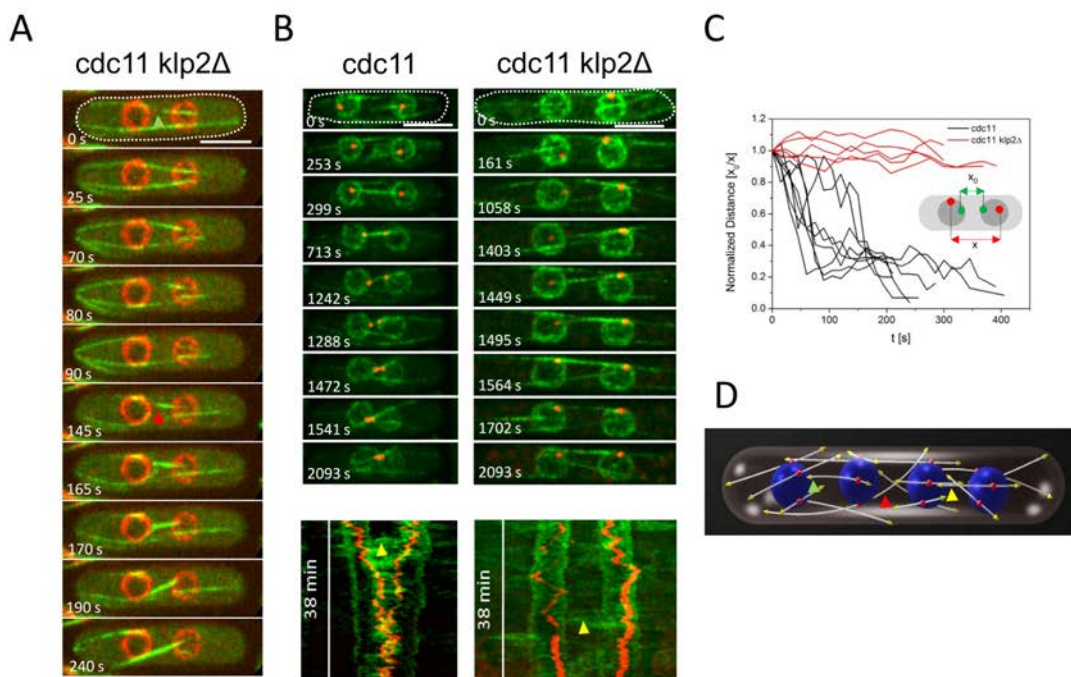


Figure 2.5: Attractive and repulsive generated forces by microtubules

(A) Impingement of growing microtubules on nuclear envelopes (NE) visualized in *cdc11 klp2Δ* cells expressing GFP-*atb2* and *cut11*-3mRFP – projection of 3 confocal planes. The first microtubule (green arrowhead) undergoes a catastrophe while in contact with the NE. The second microtubule (red arrowhead) slides along the NE and passes the nucleus. **(B)** Time series and kymographs of binucleated *cdc11* and *cdc11-klp2Δ* cells expressing GFP-*atb2*, *nup107*-GFP (NE) and *Sid4*-mRFP (SPB). Displayed images were captured directly after spindle breakdown following mitotic-spindle-mediated nuclear dispersion. Arrowheads mark bundling events of antiparallel microtubules attached to two different SPBs. **(C)** Quantification of the spindle pole body distances in *cdc11* and *cdc11 klp2Δ* cells after antiparallel microtubule bundle formation ($t=0$). **(D)** Impression of the organization of nuclei and microtubules in *cdc11 klp2Δ* cells. Multiple microtubules, of which 2 are displayed, form bipolar assemblies that are locally coupled (red) to nuclei (blue). Forces are generated by microtubule plus-ends (yellow) interacting with cell walls and nuclei. Head-on and lateral interactions of microtubules with nuclei (red arrowhead) may convey forces for nuclear motion. Bundles are established between antiparallel microtubules (yellow arrowhead). Scale bars: $5\mu\text{m}$

Interdigitating microtubules generate repulsive forces in between nuclei

Occasionally a microtubule originating from one nucleus was observed to impinge onto a neighbor nucleus. These microtubules either went under a catastrophe and retracted or grew further and eventually passed by the nucleus (Figure 2.5 A). We hypothesized that these events generate repulsive forces between nuclei in analogy to microtubules pushing in between cell walls and nuclei [16, 22]. Correlating single microtubule growth events with nuclear displacements proved to be experimentally challenging because multiple events occur simultaneously. To confirm a role for internuclear microtubules in nuclear dispersion, we therefore imaged nuclear envelope embedded SPBs to deduce information on microtubule forces. One of the interphase microtubule assemblies associates with the SPB in wild type cells and pushing forces generated by microtubules in contact with the wall cause SPB oscillations [16]. SPBs on the two outer nuclei of *cdc11 klp2Δ* cells were on average displaced away from the center of their nuclei in the direction of the cell center (Figure 2.6 A). This offset suggests that the force generated by microtubules on nuclear attachment sites is directed towards the cell center. We hypothesized that the total force on the outer nuclei is equilibrated by impacts of microtubules originating from the inner nuclei. The offset in SPB position therefore reflects an asymmetry in the microtubule network around the two outer nuclei: growth is unidirectional on one side and bidirectional on the other side. In agreement, there was no significant offset in SPB position for the inner nuclei reflecting bidirectional growth on both sides. SPBs on all four nuclei were offset in the direction of nuclear migration after centrifugation demonstrating that forces on microtubule attachment sites are adjusted when nuclei are displaced from their equilibrium positions (Figure 2.6 B).

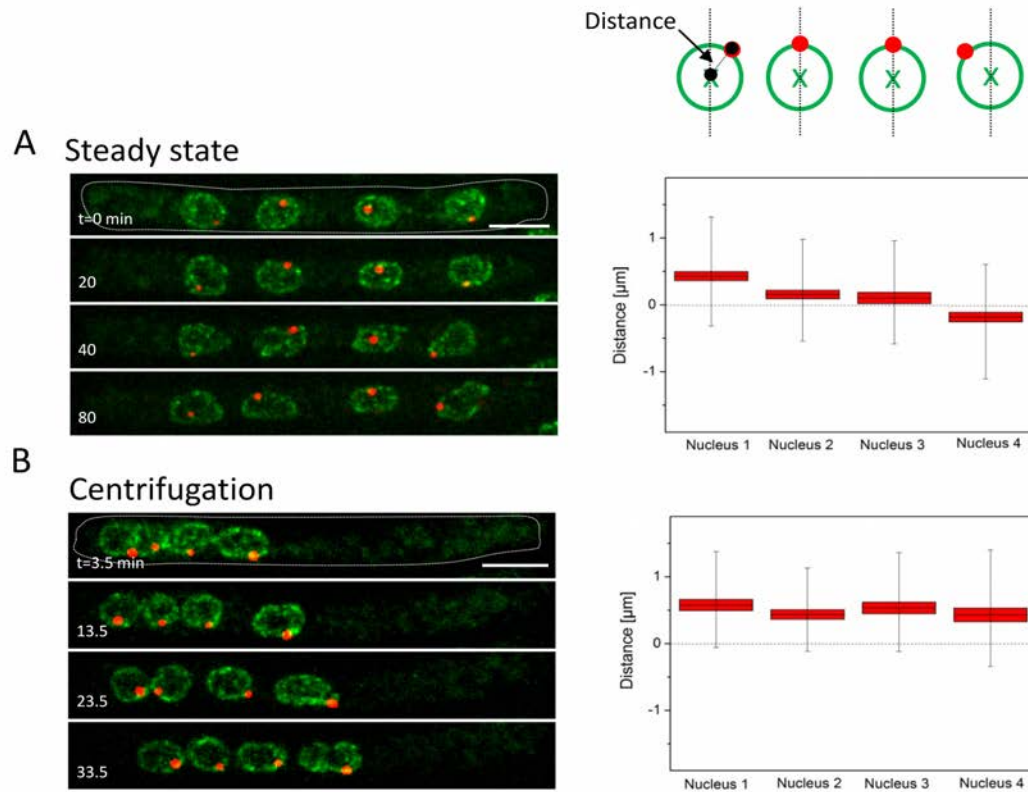


Figure 2.6: Nuclear offset of spindle pole body correlates with asymmetry in perinuclear microtubule network

(A) Quantification of the distance between SPBs and nuclear midpoints measured along the cell's long axis in *cdc11 klp2 Δ* cells expressing *nup107*-GFP (NE) and *sid4*-mRFP (SPB). Left panel shows confocal projection of 3 planes. Right panel shows average distance, standard deviation and standard error for 4 nuclei in a box plot. Data are obtained from 11 cells and eight cumulated time points at 10 minute intervals. **(B)** Same as in (A) but during the first 30 minutes after cell centrifugation. $n = 10$ cells. Scale bar: 5 μm . Cartoon: Visualisation of the movement of the SPB in response to microtubule force generation (green = nucleus, red= SPB).

2.3. Discussion

Nuclear positioning in multinucleated cells including myotubes, oocytes and plant sporocytes [23-25] is as yet not understood at a mechanistic level partly due to the complexity of cytoskeletal networks involved. Here, we were able to exploit the relatively simple architecture of the fission yeast cytoskeleton to investigate the mechanistic requirements for equidistant positioning of nuclei within single cells. We studied the interdigitating microtubule network between neighboring cells and demonstrated that dynamically unstable microtubules nucleated from the nuclear envelope can generate repulsive pushing forces on neighboring nuclei. These forces can separate nuclei in the absence of the motor *klp2p*, which generates dominant attractive forces by pulling overlapping microtubules together. Inhibition of motor function therefore induces a switch between a pattern of condensed nuclei to a pattern of equidistant spaced nuclei.

How is the distance between nuclei controlled? The average magnitude of the repulsion force is expected to decay with internuclear distance because microtubule catastrophes will more often prevent microtubules from reaching neighbouring nuclei at larger internuclear distances. In addition, microtubule buckling decreases the forces that can be generated over larger distances. The resulting distance dependent repulsive force can explain the observed establishment of an equidistant pattern. The repulsive force between nuclei that are too close to each other will be larger than the force in between other nuclei. Such a mechanism will equilibrate inter nuclear distances and the average nuclear distance will increase with the size of the confinement as is observed in cells treated with hydroxyurea.

The geometry of microtubules and nuclei in *cdc11 klp2Δ* cells shows striking similarities with multinucleated myotubes, plant cells, algae and embryos in which microtubules asters originating from nuclei interdigitate in the internuclear space [8, 25-27]. Microtubule pushing forces may therefore more generally contribute to nuclear spacing. Work in myotubes however demonstrates that additional forces by motor proteins may be required in larger systems. In myotubes both plus- and minus-end directed motors localize to the nuclear envelopes and yet other plus-end motors may bind to antiparallel microtubules in between nuclei [5, 23]. Plus-end motors may push overlapping microtubules apart to generate repulsive forces. In addition, plus-end directed motors on nuclear envelopes may interact with microtubules from neighboring nuclei to generate additional repulsive forces or to prolong the interaction between nuclei and microtubule ends. Dynamic instability will ensure that the number of microtubules that generate force decreases with internuclear spacing to facilitate equidistant positioning. The natural ruler provided by dynamic instability may thus be used by different force generating mechanisms. Minus-end directed motors on nuclear envelopes, in

combination with plus-end directed motors, were proposed to facilitate back and forth motions and nuclear rotations to navigate the crowded cytoplasm [23, 28]. These motions may speed up positioning. Our results on the *k1p2p* motor suggest that regulation of minus-end motors may additionally allow systems to switch between dispersed and clustered nuclear patterns.

Perinuclear microtubules are more generally involved in demarcating a compartment around nuclei in multinucleated cells [9, 29]. Compartments in *Ashbya gossypii* were proposed to isolate nuclei such that they can divide asynchronously [30]. Neighboring compartments are thought to repel each other in filamentous fungi and embryos to control internuclear distances. In contrast to our fission yeast system, the internuclear spacing that is established between nuclei after nuclear division in fly embryos is fixed and does not scale with the size of the confinement to fill up the complete cell. Possibly the size of the nuclear compartments is well confined through a precise control over microtubule length, preventing nuclei to move further apart. Alternatively, nuclear divisions may succeed each other too fast, which does not allow for time to move nuclei further apart. In *Ashbya*, interactions between perinuclear microtubules and cortical dynein motors were proposed to be important for a non-random spacing of nuclear compartments [31]. It is difficult to depict how cortical interactions, as opposed to internuclear interaction, can achieve equidistant patterns. Possibly, cortical interactions speed up the dispersion of nuclei through the cell and ancillary mechanisms are needed to generate equidistant patterns.

Organelles other than nuclei were also shown to set up equidistant patterns. Bacterial microdomains have been well studied. Bacterial filaments were proposed to play a role, but a mechanism based on chemophoresis forces, i.e. directed movement along a gradient of binding sites, is also a likely candidate. It becomes increasingly clear that pattern formation at the cellular level often involves the coupling of mechanical processes involving the cytoskeleton and chemical reactions [32]. With our current knowledge at hand it will therefore be interesting to learn whether and how dynamic instability is exploited for the regulation of inter organelle distances in other cellular systems.

2.4. Materials and Methods

Generation of strains

Standard fission yeast techniques were used for gene deletion and gene tagging. The cell lines used for all experiments are listed in Table 2. 1. Additional strains were crossed with strains purchased by Riken (Japan) or kindly provided by F.Chang (Columbia University, US), K. Gould (Vanderbilt University, US), M. Sato (Cancer Research, UK) and P. Tran (University of Pennsylvania, US & Institute Curie, France). All strains were confirmed by PCR. Recipes for media and culturing the yeast cells are described in [33]

Cell Culture

Before imaging, the fission yeast cells were grown in YE5S media at 25°C over night. The temperature was shifted to 36°C for two hours to generate binucleated cells and for five hours to generate tetranucleated cells. Non-temperature sensitive cells were culture at 30°C.

Table 2. 1: Fission yeast cell lines used in the experiments.

Nr.	Strain		note
	Cdc11-123-nup107-GFP::kanMx ade6-M210	h+/ts	This study,[16, 34]
JT.44			
JT.69	Cdc11-123-nup107-GFP::kanMx-klp2Δ25::ura	h-/ts	This study [16, 34]
JT.140	Cdc11-123-nup107-GFP::kanMX-sid4-RFP::kanMX-ade6-M216 Leu1-32 ura4-d18	h+/ts	This study [16, 34, 35]
JT.141	Cdc11-123-nup107-GFP::kanMX-sid4-RFP::kanMX-ade6-M216 Leu1-32 ura4-d18 klp2Δ::ura	h-/ts	This study [16, 34, 35]
JT.162	Cdc11-123-cut11-3mRFP::hygroMx leu1-32::psV-40-GFP-atb2(leu+)ade6-leu1-32 klp2Δ::ura- sid4-RFP::kanMx	h+/ts	This study [34-36]
JT.175	Cdc11-123-nup107-GFP::kanMx- klp2Δ25::ura -sid4-RFP::kanMx	h+/ts	This study [16, 34, 35]
PT.54	Nup107-GFP::kanMx	h-	[16]

Centrifugation assay

Displacement of the nuclei was done as described [37]. Before centrifugation, to one ml of cell culture 25 µg/ml MBC (dissolved in DMSO) was added to depolymerize microtubules. Cells were centrifuged for 10 min at 14000 g using an Eppendorf table centrifuge. To regrow microtubules, the cell pellet was washed twice with growth media lacking MBC.

Microscopy

Fission yeast cells were imaged on thin EMM agar pads as described [38]. For experiments that require microtubule depolymerisation, 25 mg/ml MBC was added to the cell culture and agar pad (Figure 2.2 C). All imaging was done at 25°C, at which most cells went under mitosis after three hours of imaging. When longer observation times were necessary to observe nuclear repositioning 12 mM hydroxyurea (HU) were added to the cell culture and agar pads. The onset of mitosis was postponed by blocking DNA synthesis (Figure 2.2 B,C and Figure 2.3 A).

Imaging was performed using a Spinning Disc Confocal Microscope (Nikon Ti microscope body, Yokogawa CSUX1 scanner, Photometrics Evolve camera, Metamorph software, 491nm and 561nm laser lines; 100x oil 1.45NA objective). Z-stacks were acquired with an internal spacing of 0,5 µm and the maximum intensity projections are shown. For fast simultaneous acquisition of green and red spectral bands (503nm-552nm and 584nm-900nm) a DV2 Dual View was used (Figure 2.4 A).

Imaging analyses

Position of nuclei and SPBs were either tracked by hand (Figure 2.1, Figure 2.5 C) or using automated tracking (Figure 2.5 C, Figure 2.6). For the latter, custom and existing MATLAB [39] procedures were combined. For nuclear and SPB tracking was done separately from each other. Therefore we convolved each image with a modeled image of a circle, i.e. a ring with a radius of 16 pixels (SPB= 8) and a Gaussian radial intensity profile. Afterwards, the function *imextendedmax* was used to find all regional maxima that are greater than a specific threshold. It is based on the h-maxima transform with an 8-connected neighbourhood, which connect all pixels above the threshold of the regional maximum to one component. Any pixel that has a lower intensity than the threshold will be discarded and in this way faint and small objects are automatically removed. The produced output is a binary image, where the regional maxima have the

value one and all other pixel the value zero. To find the centre of mass of these maxima we applied the function *regionprops-centroid*. The x, y positions and the frame number were written into a matrix. This matrix was used as an input for the second part of the script written by J.C. Crocker [40]. It combines the positions of each frame into trajectories depending on several parameters. The outputs are (i) an excel file with the x, y positions and frame numbers of all trajectories and (ii) the original movie with the encircled tracked nuclei or SPBs.

Random positioning of nuclei

We consider the random positioning of nuclei with diameter D into a cell of length L . This is equivalent to a well known statistical mechanical model of 1D liquids called the Tonks gas. Following [41] the single particle distribution function of a gas of N particles interacting through a pairwise potential $V(r)$, between "walls" represented by particles fixed at $r = 0$ and $r = l$ is given by

$$\rho(r) = \frac{\sum_{k=1}^N L^{-1}[\Omega^{N-k+1}](l-r)L^{-1}[\Omega^k](r)}{L^{-1}[\Omega^{N+1}](l)}$$

Equation 2.1

where L^{-1} is the inverse Laplace transform, and

$$\Omega(s) = L[e^{-\beta V}](s)$$

Equation 2.2

For non-overlapping particles, the Boltzmann factor is simply

$$e^{-\beta V(r)} = \theta(r - D)$$

Equation 2.3

with $\theta(x)$ the Heaviside function. In this case we find

$$\Omega(s) = \int_D^\infty dr e^{-sr} = \frac{e^{-sD}}{s}$$

Equation 2.4

whence

$$L^{-1}[\Omega^n](x) = \frac{(x - nD)^{n-1}}{\Gamma(n)} \theta(x - nD)$$

Equation 2.5

For our case, we placed the fixed particle at the left boundary at $r = -\frac{1}{2}D$ and the fixed particle at the right boundary at $r = l + \frac{1}{2}D$. In this way, the edges of the flanking particles act as cell ends at $r = 0$ and $r = l$, leaving the intended interval $[0, l]$ as the interior space. For $N = 4$ nuclei we thus find

$$\rho(r) = \frac{\sum_{k=1}^4 L^{-1}[\Omega^{4-k+1}](l-r)L^{-1}[\Omega^k](r + \frac{1}{2}D)}{L^{-1}[\Omega^5](l + \frac{1}{2}D)}$$

Equation 2.6

$$= 4 \frac{(l - \frac{7}{2}D - r)^3}{(l - 4D)^4} \theta\left(r - \frac{1}{2}D\right) + 12 \frac{(r - \frac{3}{2}D)(l - \frac{5}{2}D - r)^2}{(l - 4D)^4}$$

$$+ 12 \frac{(r - \frac{5}{2}D)^2(l - \frac{3}{2}D - r)}{(l - 4D)^4} + 4 \frac{(r - \frac{7}{2}D)^3}{(l - 4D)^4} \theta\left(l - \frac{1}{2}D - r\right)$$

$$= \rho_1(r) + \rho_2(r) + \rho_3(r) + \rho_4(r)$$

Equation 2.7

This is the total density, which when integrated over the interval $[0, l]$, equals the number of nuclei (= 4). The individual densities for the first, second, third and fourth nucleus, $\rho_1(r)$.. $\rho_4(r)$ are plotted in Figure 2.1. The nearest neighbour distance distribution (Figure 2.1) is given by

$$\rho_{nn}(r) = \frac{1}{324} (l - 3D - r)^3 \theta(r - D)$$

Equation 2.8

Acknowledgements

We thank Henk Kieft and Kadir G. Suslu for support in the lab and F. Chang, and P. Tran for strains. In addition we thank Dan McCollum, S. Trautmann, A. Gladfelter, A. Akhmanova, M. Dogterom and T. Ketelaar for helpful discussions. Jeroen de Keijzer for help with MATLAB. The work of B.M.M and JT are part of the research programme of the “Stichting voor Fundamenteel Onderzoek der Materie (FOM)”, which is financially supported by the “Nederlandse Organisatie voor Wetenschappelijk Onderzoek (NWO)”. MEJ was supported by an NWO-middel groot grant.

References

1. Waterman-Storer, C. and E. Salmon, *Endoplasmic reticulum membrane tubules are distributed by microtubules in living cells using three distinct mechanisms*. Current biology, 1998. **8**: p. 798-806.
2. Jain, I.H., V. Vijayan, and E.K. O'Shea, *Spatial ordering of chromosomes enhances the fidelity of chromosome partitioning in cyanobacteria*. Proceedings of the National Academy of Sciences, 2012. **109**(34): p. 13638-13643.
3. Savage, D.F., et al., *Spatially Ordered Dynamics of the Bacterial Carbon Fixation Machinery*. Science, 2010. **327**(5970): p. 1258-1261.
4. Komeili, A., *Molecular mechanisms of compartmentalization and biomineralization in magnetotactic bacteria*. FEMS Microbiology Reviews, 2012. **36**(1): p. 232-255.
5. Metzger, T., et al., *MAP and kinesin-dependent nuclear positioning is required for skeletal muscle function*. 2012. **484**(7392): p. 120-124.
6. Gibeaux, R., et al., *Electron tomography of the microtubule cytoskeleton in multinucleated hyphae of *Ashbya gossypii**. Journal of Cell Science, 2012. **125**(23): p. 5830-5839.
7. Oikawa, K., et al., *CHLOROPLAST UNUSUAL POSITIONING1 Is Essential for Proper Chloroplast Positioning*. The Plant Cell Online, 2003. **15**(12): p. 2805-2815.
8. McNaughton, E. and L. Goff, *The role of microtubules in establishing nuclear spatial patterns in multinucleate green algae*. 1990. **157**(1-3): p. 19-37.
9. Telley, I.A., et al., *Aster migration determines the length scale of nuclear separation in the *Drosophila* syncytial embryo*. The Journal of Cell Biology, 2012. **197**(7): p. 887-895.
10. Foe, V.E., C.M. Field, and G.M. Odell, *Microtubules and mitotic cycle phase modulate spatiotemporal distributions of F-actin and myosin II in *Drosophila* syncytial blastoderm embryos*. Development, 2000. **127**(9): p. 1767-1787.
11. Mattioli, E.p., et al., *Prelamin A-mediated recruitment of SUN1 to the nuclear envelope directs nuclear positioning in human muscle*. 2011. **18**(8): p. 1305-1315.
12. Troxell, C.L., et al., *pk11 + and klp2 +: Two Kinesins of the Kar3 Subfamily in Fission Yeast Perform Different Functions in Both Mitosis and Meiosis*. Molecular Biology of the Cell, 2001. **12**(11): p. 3476-3488.

13. Okazaki, K. and O. Niwa, *Dikaryotic Cell Division of the Fission Yeast <I>Schizosaccharomyces pombe</I>*. Bioscience, Biotechnology, and Biochemistry, 2008. **72**(6): p. 1531-1538.
14. Mana-Capelli, S., et al., *The kinesin-14 Klp2 is negatively regulated by the SIN for proper spindle elongation and telophase nuclear positioning*. Molecular Biology of the Cell, 2012. **23**(23): p. 4592-4600.
15. Nurse, P., P. Thuriaux, and K. Nasmyth, *Genetic control of the cell division cycle in the fission yeast Schizosaccharomyces pombe*. 1976. **146**(2): p. 167-178.
16. Tran, P.T., et al., *A Mechanism for Nuclear Positioning in Fission Yeast Based on Microtubule Pushing*. The Journal of Cell Biology, 2001. **153**(2): p. 397-412.
17. Neumann, F.R. and P. Nurse, *Nuclear size control in fission yeast*. The Journal of Cell Biology, 2007. **179**(4): p. 593-600.
18. Lieb, E.H. and D.C. Mattis, *Mathematical physics in one dimension: exactly soluble models of interacting particles*. Perspectives in physics. 1966: Academic Press.
19. Janson, M.E., et al., *Crosslinkers and Motors Organize Dynamic Microtubules to Form Stable Bipolar Arrays in Fission Yeast*. Cell, 2007. **128**(2): p. 357-368.
20. Carazo-Salas, R.E., C. Antony, and P. Nurse, *The Kinesin Klp2 Mediates Polarization of Interphase Microtubules in Fission Yeast*. Science, 2005. **309**(5732): p. 297-300.
21. Gibeaux, R., et al., *Spindle pole body-anchored Kar3 drives the nucleus along microtubules from another nucleus in preparation for nuclear fusion during yeast karyogamy*. Genes & Development, 2013. **27**(3): p. 335-349.
22. Garner, E.C., et al., *Reconstitution of DNA Segregation Driven by Assembly of a Prokaryotic Actin Homolog*. Science, 2007. **315**(5816): p. 1270-1274.
23. Wilson, M.H. and E.L.F. Holzbaaur, *Opposing microtubule motors drive robust nuclear dynamics in developing muscle cells*. Journal of Cell Science, 2012. **125**(17): p. 4158-4169.
24. Vogel, S.K., et al., *Self-Organization of Dynein Motors Generates Meiotic Nuclear Oscillations*. PLoS Biol, 2009. **7**(4): p. e1000087.
25. Brown, R.C. and B.E. Lemmon, *The cytoskeleton and spatial control of cytokinesis in the plant life cycle*. 2001. **215**(1-4): p. 35-49.
26. Baker, J., W.E. Theurkauf, and G. Schubiger, *Dynamic changes in microtubule configuration correlate with nuclear migration in the preblastoderm Drosophila embryo*. The Journal of Cell Biology, 1993. **122**(1): p. 113-121.

27. Tassin, A.M., B. Maro, and M. Bornens, *Fate of microtubule-organizing centers during myogenesis in vitro*. The Journal of Cell Biology, 1985. **100**(1): p. 35-46.
28. Fridolfsson, H.N. and D.A. Starr, *Kinesin-1 and dynein at the nuclear envelope mediate the bidirectional migrations of nuclei*. The Journal of Cell Biology, 2010. **191**(1): p. 115-128.
29. BALUŠKA, F., D. VOLKMANN, and P.W. BARLOW, *Eukaryotic Cells and their Cell Bodies: Cell Theory Revised*. Annals of Botany, 2004. **94**(1): p. 9-32.
30. Gladfelter, A.S., A.K. Hungerbuehler, and P. Philippsen, *Asynchronous nuclear division cycles in multinucleated cells*. The Journal of Cell Biology, 2006. **172**(3): p. 347-362.
31. Grava, S., et al., *Clustering of Nuclei in Multinucleated Hyphae Is Prevented by Dynein-Driven Bidirectional Nuclear Movements and Microtubule Growth Control in Ashbya gossypii*. Eukaryotic Cell, 2011. **10**(7): p. 902-915.
32. Howard, J., S.W. Grill, and J.S. Bois, *Turing's next steps: the mechanochemical basis of morphogenesis*. 2011. **12**(6): p. 392-398.
33. http://www.sanger.ac.uk/PostGenomics/S_pombe/links.shtml#pombe.
34. http://yeast.lab.nig.ac.jp/nig/index_en.html.
35. Bohnert, K.A., et al., *A Link between Aurora Kinase and Clp1/Cdc14 Regulation Uncovered by the Identification of a Fission Yeast Borealin-Like Protein*. Molecular Biology of the Cell, 2009. **20**(16): p. 3646-3659.
36. Sato, M., et al., *Nucleocytoplasmic transport of Alp7/TACC organizes spatiotemporal microtubule formation in fission yeast*. 2009. **10**(10): p. 1161-1167.
37. Daga, R.R. and F. Chang, *Dynamic positioning of the fission yeast cell division plane*. Proceedings of the National Academy of Sciences of the United States of America, 2005. **102**(23): p. 8228-8232.
38. Tran, P.T., A. Paoletti, and F. Chang, *Imaging green fluorescent protein fusions in living fission yeast cells*. Methods, 2004. **33**(3): p. 220-225.
39. www.mathworks.com.
40. <http://physics.georgetown.edu/matlab/>.

41. Salsburg, Z.W., R.W. Zwanzig, and J.G. Kirkwood, *Molecular Distribution Functions in a One-Dimensional Fluid*. The Journal of Chemical Physics, 1953. **21**(6): p. 1098-1107.



A model for equidistant positioning of multiple nuclei

Juliane Teapal, Leander J. Schuitman, Marcel E. Janson and Bela M. Mulder

Chapter

3

Abstract

A wide range of cells exhibit multiple nuclei that are dispersed throughout the cell. In some cases the internuclear distances are equal, suggesting a well-controlled mechanism behind it. In Chapter 2, we used the multinucleated fission yeast *S. pombe* and provide experimental evidence that repulsive forces generated by dynamic microtubules can control equidistant patterning. To evaluate if these forces are sufficient, we developed a simple 1D stochastic model of a tetranucleated cell. In our model each of the nuclei has its own bipolar microtubule network associated to it, with microtubule ends growing away from the nuclei. We show that the forces of the interdigitating microtubule network between neighbouring nuclei generate an equidistant pattern. The nuclear oscillations and time evolution after pattern perturbation were in agreement with data obtained in *S. pombe* cells. However, an overestimation of the force generation in between nuclei, compared to forces generated between nuclei and cell ends, caused a larger internuclear distance. By introducing the possibility for microtubules to pass the neighbouring nuclei, the force generation is rebalanced and an equidistant nuclear pattern ensues. We conclude that equidistant nuclear positioning can indeed be based on repulsive forces generated by microtubules alone.

3.1. Introduction

The formation of distinct spatial patterns in cells is essential for their function and development. Both reaction diffusion mechanisms and mechanical forces control the organisation of these patterns in cells. One striking pattern is the dispersion of multiple nuclei throughout cells, which is a common occurrence in early embryo stages, myotubes, plants and algae cells [1-5]. These pattern establishments are based on mechanical forces mainly generated by microtubules and associated proteins [6-8], but are not understood at a mechanistic level. In prokaryotic cells nuclei, plasmid DNA, and other micro-compartments are also equidistantly positioned [9-11], suggesting the presence of active control mechanisms.

The crucial role of microtubules for nuclear movement and positioning has been shown in many organisms [12, 13]. Based on their dynamic instability, microtubules are able to explore the entire cell, enabling intracellular transport and organisation. *In vivo* as well as *in vitro* experiments revealed the capability of microtubules to generate forces [14-18]. The polymerization of a microtubule against a physical barrier generates forces based on the Brownian ratchet mechanism [19]. In fission yeast this mechanism is used to position the nucleus to the middle of the cell using pushing forces exerted by growing microtubules in contact with cell poles [12]. Positioning of microtubule organizing centres (MTOC), and associated nuclei, within higher eukaryotic cells is based on a combination of microtubule pushing forces and pulling forces exerted by cortical dynein [13, 17].

No clear mechanism was proposed to explain how multiple nuclei are dispersed equally throughout the cell. In chapter two, we used tetranucleated fission yeast cells and suggest that repulsive forces generated by growing microtubules can distribute nuclei equally. Each of these nuclei has its own bipolar linear microtubule network, similar to single nucleated cells. In addition to generating force against cell walls, microtubules can also impinge into the neighbouring nuclei and generate repulsive forces. However, the question remains if these forces alone are sufficient to disperse nuclei equally throughout the cell. Even a well-characterized model system as fission yeast has non-characterized proteins and processes that may contribute to nuclear positioning.

An increasing number of biological findings is now supported by computer models. Models allow us to deduce whether a limited set of interacting components can explain a biological phenomenon. Thus they demonstrate whether the essence of a regulatory process is captured by the proposed mechanism. Already now, various models explore the dynamic microtubules during interphase (plant cells [20], fission yeast [12], and

ciliated cells [21]) using stochastic methods, based upon interactions between microtubule associated proteins (MAPs) and microtubules.

For our purpose, the model should include a description of the forces at play. These include the force generation of microtubules, and the viscous properties of the cytoplasm that determine the forces required to move the nucleus. Moreover, the dynamics of microtubule growth should be included with sufficient detail.

To test whether repulsive forces generated by dynamic microtubules are sufficient to establish an equidistant nuclear pattern, we created a 1-dimensional model of a simplified multinucleated cell. We included parameters that were required to simulate repulsive force generation (dynamic instability and force generation, but neglected parameters as microtubule buckling and microtubule bundle formation to keep the model simple. The main question we address is whether the dynamics and accuracy of nuclear positioning is in agreement with the measured parameters of dynamic instability. The model reveals that no other forces are required and equidistant positioning of nuclei can indeed be established by microtubule generated repulsive forces alone.

3.2. Formulation of a model

A computer simulation implemented in C++ was set-up to analyse nuclear dispersion as a function of microtubule repulsive forces in interphase fission yeast cells. Step by step we implemented the necessary components of the simulation, starting with the dynamic instability of microtubules, followed by the force generation of microtubules and the mobility of nuclei. All components are modelled based on the outcome of *in vitro* and *in vivo* experiments.

Where possible, we validated simulation results of the model components with existing and newly-derived analytical predictions. Lastly, we integrated the model components into the final model.

Dynamic Instability

In chapter 2 we demonstrated that nuclear dispersion within fission yeast is generated by the repulsive forces of dynamically unstable microtubules. The dynamic instability of microtubules enables continuously switching between growth and shrinkage, where the switch from growth to shrinkage is called a catastrophe and from shrinkage to growth a rescue. These events have been observed *in vivo* as well as *in vitro* using purified tubulin [22-26].

The energy required for dynamic instability is provided by the hydrolysis of tubulin-bound GTP to GDP. GTP-tubulin polymerizes at the tip of the microtubule and establishes a so-called GTP-cap and is later hydrolysed to GDP. The cap stabilizes microtubule growth, while GDP along the remainder length makes the microtubule prone to disassemble [23, 27]. Once the GTP-cap becomes unstable, a microtubule catastrophe is induced. There are three factors influencing dynamic instability: (a) the limitation of the tubulin pool, (b) contacts with physical boundaries within the cell and (c) microtubule associated proteins (MAPs).

In vitro experiments revealed a linear response of growth velocity and catastrophe frequency to the tubulin concentration [26]. While a microtubule is in contact with a physical barrier, the frequency of catastrophes increases as a consequence of the restricted binding of GTP-tubulin to the microtubule tip [16]. Members of the kinesin-8 family alter the dynamic properties of microtubules in a length-dependent matter, by removing tubulin subunits at the tip [28]. Thus, three different mechanisms induce the disassembly of the GTP-cap and induce microtubule catastrophes. The microtubule growth velocity for free growth $v_g^{(0)}$ (without physical boundaries) equals the product of the step size with the difference of the k_{on} and k_{off} rates, where k_{on} is the rate at which new tubulin dimers are added to the microtubule, k_{off} is the rate for disassembly of tubulin dimers and δ is the length of a dimer divided by the 13 protofilaments of the microtubule (8nm/13).

$$v_g^{(0)} = \delta(k_{on} - k_{off})$$

Equation 3.1

Our model of dynamic instability is based on experimental observations in fission yeast cells and will not capture the dynamics of tubulin binding and GTP hydrolysis at a molecular level. Experiments show that microtubules grow at a rate of about 2 $\mu\text{m}/\text{min}$ away from the nucleus, undergo catastrophes followed by shrinkage at a rate of 9 $\mu\text{m}/\text{min}$, and rarely undergo rescues (Table 3.1). In fact, rescues only occur near the nucleus and are treated like the nucleation of a new microtubule in our model [29]. Catastrophes show a small dependency on microtubule length [28]. Based on the available data we choose a catastrophe rate of 0.005/s as a cellular average [28]. Microtubule growth after nucleation was simulated with the given values. The microtubule length distribution in the simulation followed an exponential decay as expected for a length independent catastrophe rate (Figure 3.1). To test whether the simulations are in agreement with the theory we calculated the mean microtubule length L_{MT} , which is given by the reciprocal of the difference between the ratio of the

catastrophe frequency r_c to the growth velocity $v_g^{(0)}$ and the ratio of the rescue frequency r_r to the shrinkage velocity v_s :

$$L_{MT} = \frac{1}{\frac{r_c^{(0)}}{v_g^{(0)}} - \frac{r_r}{v_s}}$$

Equation 3.2

As rescue frequency r_r is zero the following counts:

$$L_{MT} = \frac{v_g^{(0)}}{r_c^{(0)}} = \frac{0.033 \frac{\mu m}{s}}{0.005 \frac{1}{s}} = 6.6 \mu m$$

Equation 3.3

The calculated microtubule mean length of the simulations ($L_{MT} = 6.45 \mu m \pm 0.23$ (S.D.)) is in agreement with the theoretical value. Furthermore, we tested our simulation by changing $v_g^{(0)}$ and r_c , while keeping their ratio constant. Consistent with the fact that the mean microtubule length only depends on the ratio of $v_g^{(0)}$ to r_c , each combination of parameters resulted in the same microtubule mean length (variation of the mean microtubule length <2%) [30].

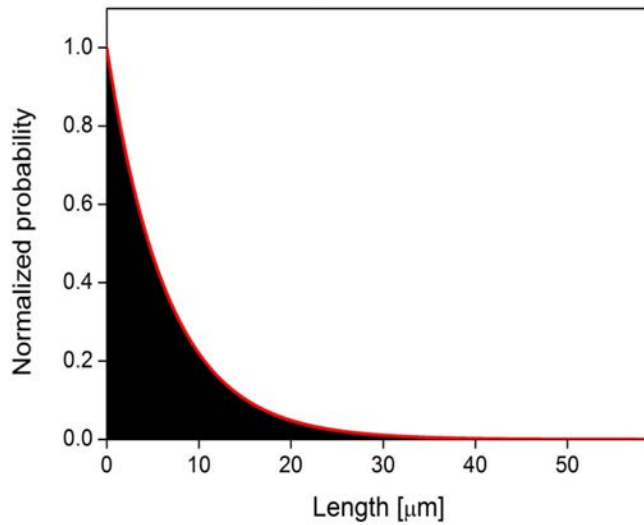


Figure 3.1: Microtubule length distribution for free growth

Simulated length distribution of unconstrained microtubule growth based on parameters measured in fission yeast ($v_g^{(0)} = 0.033 \mu m/s$, $v_s = 0.150 \mu m/s$ and $r_c^{(0)} = 0.005/s$). The microtubule length distribution for bounded growth is characterized by an exponential decay as pictured by the red line. Data are obtained from 10 simulations, where each simulation was run over a 100 min time frame (Number of microtubules $> 1 \cdot 10^6$).

Force generation of microtubules

Confined growth

In fission yeast the microtubule minus-ends are connected to the nucleus and the plus-ends are growing towards the cell tips, which act as physical barriers. The duration of the growth period is determined by the free catastrophe rate and by force-induced catastrophe when microtubules are in contact with the cell poles. In absence of a force all chemical binding energy is available to drive microtubule polymerization whereas in the presence of a physical barrier a part of the energy is converted into work by a mechanism called the Brownian ratchet [19, 31]. This mechanism uses thermal fluctuations to transduce energy in directed motion. Even when the microtubule tip is pressed against a physical barrier, thermal fluctuations at the tip of the microtubule away from the barrier do occur [19, 32, 33]. To allow for continuous growth and force generation, the thermal fluctuations have to open a gap of at least the size of a tubulin dimer.

Microtubules in cells can bend since they are elastic themselves and moreover are in contact with elastic material such as the nuclear envelope and the plasma membrane. When in contact with an object the growing microtubule end experiences a force, which increases slowly as the elastic components become tensed. To model this elasticity in a 1-dimension model we introduce the concept of a stored length, l , which is longer than the true microtubule length L . We can think of this as a microtubule with length l that is compressed to a length L [35, 36]. The corresponding force is modelled as a simple Hookean spring:

$$F = k_m(l - L)$$

Equation 3.4

The constant k_m effectively describes the combined compliance of the microtubule and its connections to the nuclei and cell walls. Following the Brownian ratchet model of force production for negligible monomer off-rate [31], the growth velocity under loading will decrease as

$$v_g(F) = v_g^{(0)} e^{-\beta\delta F}$$

Equation 3.5

where

$$\beta = \frac{1}{k_b T}$$

Equation 3.6

δ the step size of the growth process and $F\delta$ is the required energy to insert one tubulin subunit. Upon compression the instantaneous rate of undergoing a catastrophe increases. The mean waiting time until a catastrophe is defined as follows:

$$\tau_c = \frac{1}{r_c^{(0)}}$$

Equation 3.7

and has for freely growing microtubules, and for microtubules under a load, been shown to be approximately proportional to v_g [16]. Neglecting the small finite mean catastrophe time at stall:

$$r_c^{(0)} \times v_g^{(0)} = r_c(F) \times v_g(F)$$

Equation 3.8

Given the force-velocity relation Equation 3.5, this yields

$$r_c(F) = r_c^{(0)} e^{\beta \delta F}$$

Equation 3.9

which is a simplified version of the one employed in [34].

Compression modulus

The value of the compression modulus k_m used in the simulation is based on the average contact time of a microtubule with the cell pole before it undergoes a catastrophe, which in fission yeast cells is determined to be $\tau_c = 90$ s [12]. Based on the force production model described above, the instantaneous catastrophe rate under compression equals:

$$r_c(l) = r_c e^{\beta \delta k_m (l-L)}$$

Equation 3.10

We now consider the survival probability, S , of a growing microtubule, which first contacts the barrier at $t = 0$. This quantity obeys the equation

$$\frac{d}{dt} S(t|L) = -r_c(t) S(t|L), \quad S(0|L) = 1$$

Equation 3.11

where $r_c(t)$ is the instantaneous catastrophe rate. To determine the latter we first solve for the length at time t , assuming no catastrophe has yet occurred

$$\frac{d}{dt} l(t) = v_g(F(l(t))) = v_g^{(0)} e^{-\beta \delta k_m (l(t)-L)}$$

Equation 3.12

which is readily solved to yield

$$l(t) = L + \frac{1}{\beta \delta k_m} \ln(1 + \beta \delta k_m v_g^{(0)} t)$$

Equation 3.13

Inserting into Equation 3.10 yields

$$r_c(t) = r_c^{(0)} (1 + \beta \delta k_m v_g^{(0)} t)$$

Equation 3.14

i.e. the rate increases linearly in time. This allows us to integrate Equation 3.11 to obtain

$$S(t|L) = e^{-r_c t (1 + \frac{1}{2} \beta \delta k_m v_g^{(0)} t)}$$

Equation 3.15

The waiting time distribution is defined as follow:

$$w(t) = -\frac{dS}{dt}(t) = -r_c^{(0)} \left(1 + \beta \delta k_m v_g^{(0)} t\right) e^{-r_c^{(0)} t (1 + \beta \delta k_m v_g^{(0)} t)} = -r_c^{(0)}(t) S(t)$$

Equation 3.16

From the survival probability we can determine the mean time to catastrophe $\langle \tau_c \rangle$ as

$$\langle \tau_c \rangle = \int_0^{\infty} dt t w(t)$$

Equation 3.17

and taken into account Equation 3.16 can also be shown to be equal to

$$\langle \tau_c \rangle = \int_0^{\infty} dt S(t|L)$$

Equation 3.18

which, using Equation 3.15 becomes:

$$\langle \tau_c \rangle = \frac{1}{r_c} \sqrt{\pi} \sqrt{\frac{r_c}{2\beta\delta k_m v_g^{(0)}}} e^{\frac{r_c}{2\beta\delta k_m v_g^{(0)}}} \text{Erfc} \left(\sqrt{\frac{r_c}{2\beta\delta k_m v_g^{(0)}}} \right)$$

Equation 3.19

where Erfc is the complementary error function [35]

$$\text{Erfc}(z) = \frac{2}{\sqrt{\pi}} \int_z^{\infty} e^{-t^2} dt.$$

Equation 3.20

Equation 3.19 allows k_m to be extracted by numerical inversion from the mean waiting time of 90 seconds at cell ends that is experimentally determined in fission yeast [12].

We then conveniently define the compressibility factor κ , with dimension of inverse length:

$$\kappa = \beta \delta k_m$$

Equation 3.21

We implemented confined growth, stored length and compression in our simulations and analysed the waiting time of microtubules before undergoing catastrophe. The mean waiting time for the simulation (88.9 ± 0.05 s (SE)) is in good agreement with the 90 seconds that went into our analytical model, demonstrating that the simulation works correctly ([36], Figure 3.2).

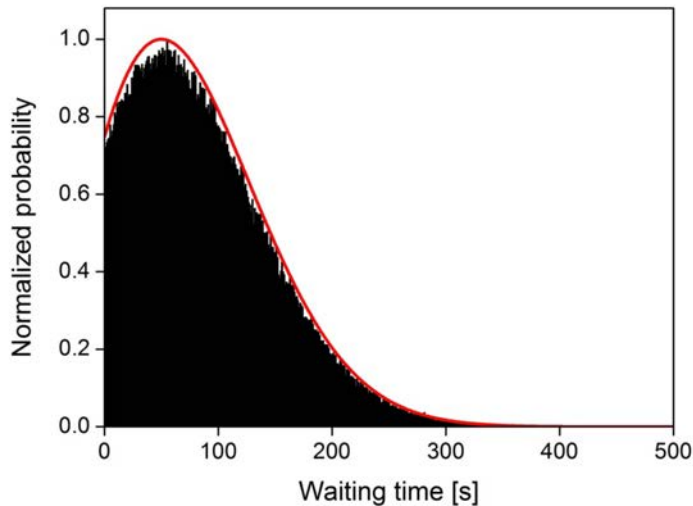


Figure 3.2: Distribution of the waiting time before a microtubule goes under catastrophe

We mimicked microtubule growth from a fixed seed against a distanced barrier in our simulation and analysed the waiting time of microtubules before undergoing a catastrophe. Shown is the average distribution of 10 simulations with 165 microtubule nucleation each. The mean waiting time is 88.9 ± 0.05 s and in good agreement with the waiting time of 90 s observed in fission yeast [36]. Additionally we determined the waiting time distribution analytically (equation 3.16) and plotted it in red.

Microtubule nucleation rate

Microtubule nucleation in fission yeast not only occurs at spindle pole bodies (SPBs) but also along existing microtubules, in the cytoplasm and on the nuclear envelope [37, 38]. Instead of modelling all these processes we modelled nucleation only occurring from nucleation sites on the nuclei. Each nucleation either generates a microtubule growing to the left or to the right as determined by chance. In our 1-dimensional simulation we neglect any bundle formation between microtubules; instead we have individual microtubules, representing the same number of microtubules as in the bundles. It has

been shown that on average 1.5 microtubules are in contact with the cell tips in wild type fission yeast cells with a single nucleus [36, 39]. Therefore, we varied the nucleation rate in a model of a mononucleated cells to achieve an equal number of microtubule-wall interactions. This model includes the mobility of the nucleus that is treated in the next section. For $r_n=0.0275 \text{ s}^{-1}$ approximately 1.5 microtubule-wall interactions were on average detected in the simulation outcome ([36, 39], Figure 3.3 A). We determined an average number of microtubules/nucleus of $n_{MT}=10$ for this nucleation rate. In cells, each nucleus has between three to five bundles, which each consists on average of about three microtubules.

Nuclear mobility

In fission yeast the size of the nucleus takes up most of the cell diameter and its movement will bring flow of viscous cytoplasm through the small remaining space between the nuclear envelope and the plasma membrane. Therefore the viscous drag is the dominating force that counters forces generated by microtubules.

We determined the nuclear mobility using the approach from [34]:

$$\mu^t = \frac{4\varepsilon^2}{9\pi^2\sqrt{2}\eta_{cell}r_{nucleus}}$$

Equation 3.22

with the viscosity of the cytosol η and

$$\varepsilon = \frac{r_{cell} - r_{nucleus}}{r_{nucleus}}$$

Equation 3.23

The mobility is very sensitive to the ratio of the cell radius to the nuclear radius, hence we determined the sizes in single-nucleated fission yeast cells ($r_{cell}=1,75 \mu\text{m}$, $r_{nucleus}=1.5 \mu\text{m}$). With the mobility determined we can use the low Reynolds number equation of motion

$$F_{drag} = \mu^t \times v$$

Equation 3.24

to solve for the nuclear velocity.

For these values we simulated nuclear positions in single nucleated cells and found that the nuclear movement is in agreement with experimental results ([12], Figure 3.1). Our simulation of a single nucleated cell is thus able to predict the experimentally observed motion of nuclei from the dynamics of microtubules, validating our approach.

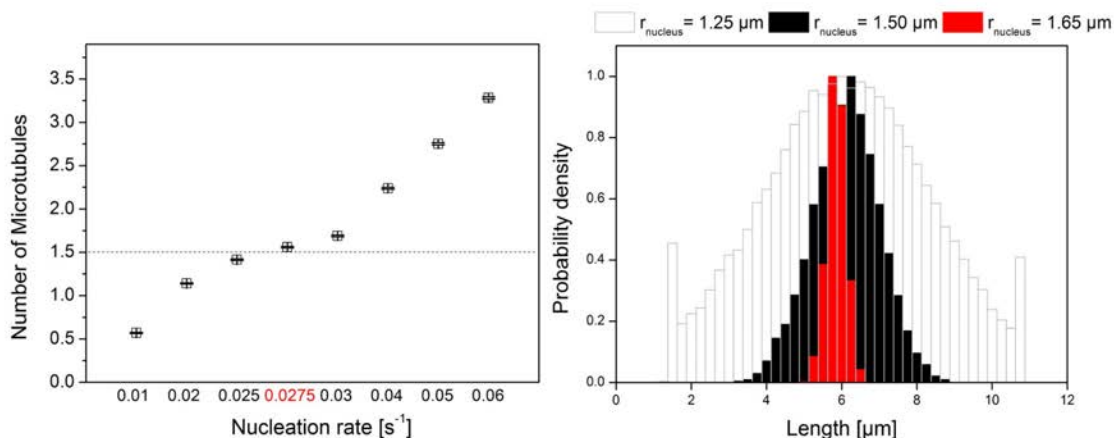


Figure 3.3: Parameter evaluation for single nucleated cells

(A) The nucleation rate in single nucleated cells was varied to determine the amount of microtubules in contact with the cell wall at each given time point. Plotted is the average number of microtubules (+ S.E.) for different nucleation rates. The nucleation rate: 0.0275 s^{-1} (red) was implemented in the final simulations, as the same amount of microtubules are in contact with the membrane as determined in cells (number of microtubules=1.5) [39]. **(B)** The distribution of the nuclear midpoint positions in simulations with different nuclear radii in a cell of $12 \mu\text{m}$ length. Nuclear movement is damped by the drag force when nuclear size increases. Each data set was determined by the average of ten simulations with each simulation lasting over a 100 min.

3.3. Results

Nuclear distribution in multinucleated cells

To test whether the experimentally observed positioning of nuclei can indeed be explained by polymerization forces of dynamically instable microtubules, we simulated nuclear motion within a 1-dimensional cell taking into account, microtubule dynamic instability, viscous forces due to nuclear motion and force generation by microtubules. The model was first implemented for a cell with one nucleus. The nucleation rate of microtubules is the only free parameter in the model and was varied to obtain an average of 1.5 microtubule-wall interactions per cell in agreement with experimental observation [36, 39]. We next extended the model to four nuclei and a cell length of $32 \mu\text{m}$. Previously it was shown that cells with multiple nuclei have a larger nuclei /volume

ratio compared to wild type cells, which causes nuclei to expand and change their mobility [40]. Therefore, we measured the radius of the nuclei and the cell in multi-nucleated cells. While the cell radius remained the same, the nuclear radius ($r_{nucleus} = 1.3 \mu\text{m}$, $n > 100$) is slightly smaller compared to the one in single nucleated fission yeast cells ($r_{nucleus} = 1.5 \mu\text{m}$), which is also in agreement with [40]. We implemented the new parameters into the final model (Figure 3.4 and Table 3.1). Consequently the mobility is increased by a factor of 7.5 in comparison to wild-type cells.

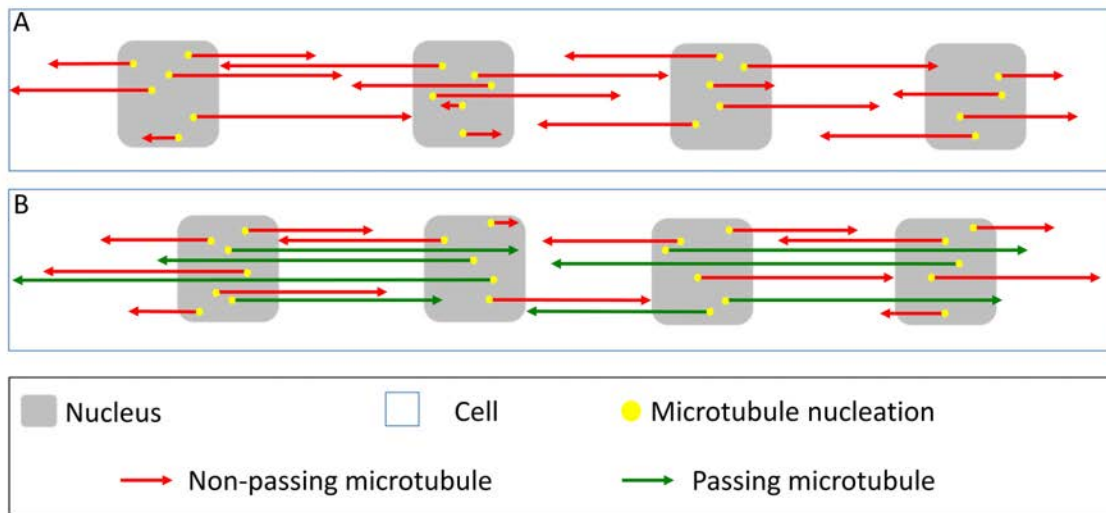


Figure 3.4: Implementation of the model

(A) Tetranucleated cell with dynamic microtubules (arrowhead indicates plus-ends) growing between neighbouring nuclei and towards the cell wall. A constant nucleation rate determines the number of microtubules per nucleus. The direction of growth is decided by chance. Forces are generated either at the cell wall or at the centre of the nuclei. **(B)** same as (A), but the model was extended by the possibility for microtubule to pass the neighbouring nucleus (green microtubules). If a microtubule passes its neighbouring nuclei its growth continues until it reaches the cell wall.

Equidistant nuclear pattern can be based on repulsive forces generated by dynamic instable microtubules

We hypothesized in chapter 2 that the equidistant nuclear patterns in fission yeast can be explained by repulsive forces generated by microtubules. Our simulations confirm that repulsive forces alone are able to generate equidistant patterning as observed in fission yeast cells (Figure 3.5 A). The internuclear spacing, however, was larger than observed in cells. At the same time, the outer nuclei were on average located closer to the cell tips in comparison to tetranucleated *cdc11 klp2Δ* cells. We argued that forces generated in between nuclei may be larger in our simulations compared to forces generated in between the outer nuclei and the cell ends. In fission yeast cells it was observed that growing microtubules are in fact able to pass a nucleus and thereby they reduce the total forces exerted in between nuclei. On the other hand, microtubules cannot pass the cell walls, making force generation at the walls more efficient. To account for this effect, we introduced a probability for the microtubules to pass the nucleus (ρ =passing probability) in the simulation (Figure 3.4 B). We varied the passing probability and analyzed the distribution of nuclei within the tetranucleated cells. A passing probability of $\rho=0.7$ resolved the discrepancy in nuclear positions and yields the same distribution pattern as observed for tetra-nucleated fission yeast cells. We expected that a further increase in passing probability would further decrease the interaction between nuclei, causing nuclei to cluster near the cell center. Indeed, a passing probability of $\rho=1.0$ results in all four nuclei clustered in the middle of the cell (Figure 3.5 C).

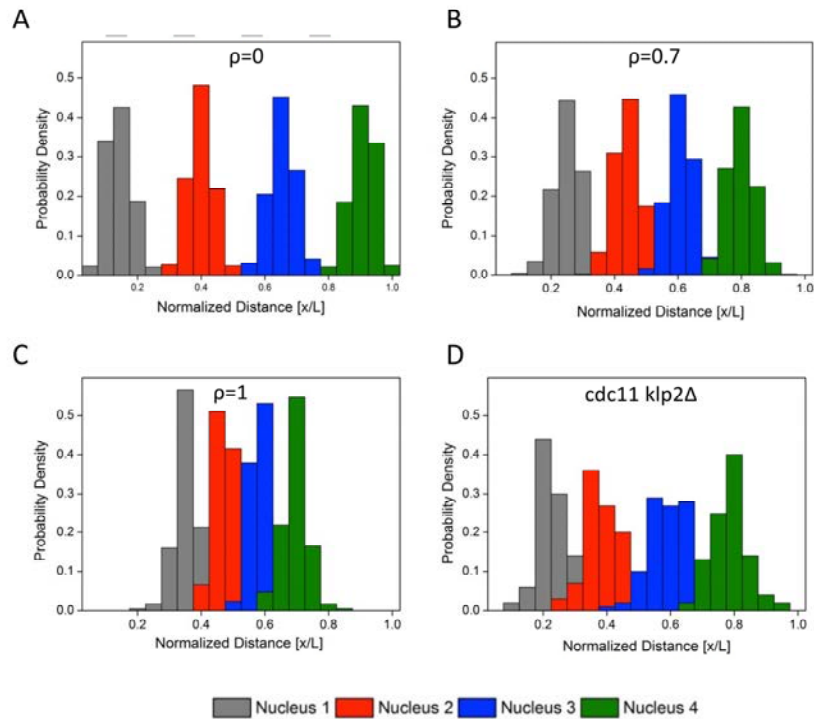


Figure 3.5: Analyses of nuclear midpoint positions

(A) Distribution of nuclear midpoint positions in simulations for tetra-nucleated cells with $\rho=0$ %. (B) Distribution of midpoint positions in simulations with $\rho=0.7$ (C) Same as A and B, but with $\rho=1.0$ ($n > 40$ simulations for each passing probability) (D) Distribution of nuclear midpoint positions in tetra-nucleated *cdc11 klp2 Δ* cells ($n = 109$ cells). All distances are normalized to the cell length.

We next analyzed the amplitude and dynamics of nuclear oscillations. To visualize the dynamics we generated kymographs of the nuclear movement in cells and simulations. Movements in the simulations had a similar appearance as in *cdc11 klp2 Δ* cells, but oscillations appeared to have slightly higher amplitudes and spiking behavior on top of slow oscillations. In agreement, the standard deviation of nuclear positions was S.E. = 2.45 μm in the simulations compared to S.E. = 2.15 μm in tetranucleated cells. Moreover, the halftime of the position autocorrelation function for the simulations ($t_{\text{sim}} = 1,98$ min) is shorter compared to the one in fission yeast cells ($t_{\text{cells}} = 9,6$ min) (Figure 3.6). The dynamics of nuclear positioning appears to be more damped in cells indicating that the mobility may have been slightly overestimated in the simulations.

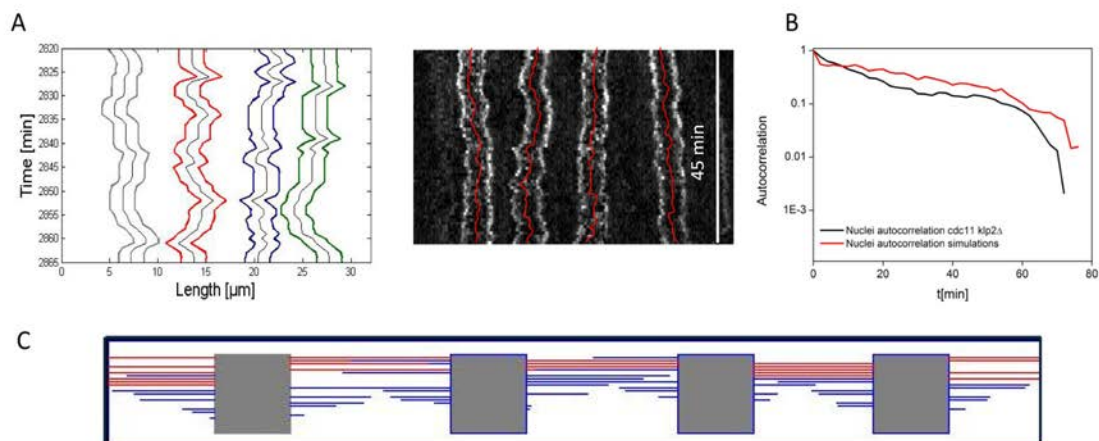


Figure 3.6: Analyses of nuclear oscillations

(A) (Left) Kymograph of nuclear movement generated from the simulated data using Matlab. (Right) Kymograph of nuclear movement in *cdc11 klp2Δ* using the nuclear envelope marker nup107-GFP. Red line represents the position of the nuclear midpoint tracked with a Matlab script (see chapter 2). **(B)** Autocorrelation function of nuclear movement in simulations (red) and *cdc11 klp2Δ* fission yeast cells (black). Nuclear midpoints in *cdc11 klp2Δ* were tracked using the same Matlab script as in (A). Ten autocorrelation functions were averaged to determine the half time. **(C)** Snapshot of one simulation ($\rho=70\%$). Image was generated using Processing visualization language [41]. The nuclei are visualized as a grey box and microtubules as straight lines, the red ones illustrate microtubules exerting a force at the neighboring nuclei, while the blue ones symbolize microtubules passing the nuclei and exerting forces at the cell wall.

Furthermore, we analyzed the repositioning timescale of the nuclei after pattern perturbation by centrifugation forces. For this we positioned all nuclei to one edge of the cell at the start of the simulation (Figure 3.7). The timescale of repositioning was not a strong function of the passing probability but showed good agreement with the experimental data for multinucleated fission yeast cells *cdc11 klp2Δ* (red line).

Evaluation of the model

To evaluate the robustness of the mechanism against variations in parameters, we changed cell length and several parameters that affect microtubule dynamics. All simulations were run with a passing probability of $\rho = 0.7$ and one parameter was varied at a time whilst others remained as stated in table 3.1.

First we varied the growth velocity, which given Equation 3.3 changes the mean microtubule length at constant catastrophe rate. To maintain a wall waiting time of approximately 90 s, we adjusted the compression modulus k_m to the growth velocity

(Table 3.2) as regarding to Equation 3.19 k_m also depends on the growth velocity. The internuclear distance first decreases and then increases with increasing growth velocity (Figure 3.8 A). The smallest distance is obtained at a growth velocity of $0.033 \mu\text{m/s}$, but no large changes are observed for a 10-fold change in growth velocity. Establishment of a nuclear pattern is based on the force equilibrium generated by microtubules in between nuclei and microtubules that interact with the cell wall. The balance of these forces is shifted when parameters of microtubule dynamics are changed. Internuclear distances will be shifted accordingly. We observe that the positional stability, i.e. the standard deviation of each nuclear position, decreases with growth velocity.

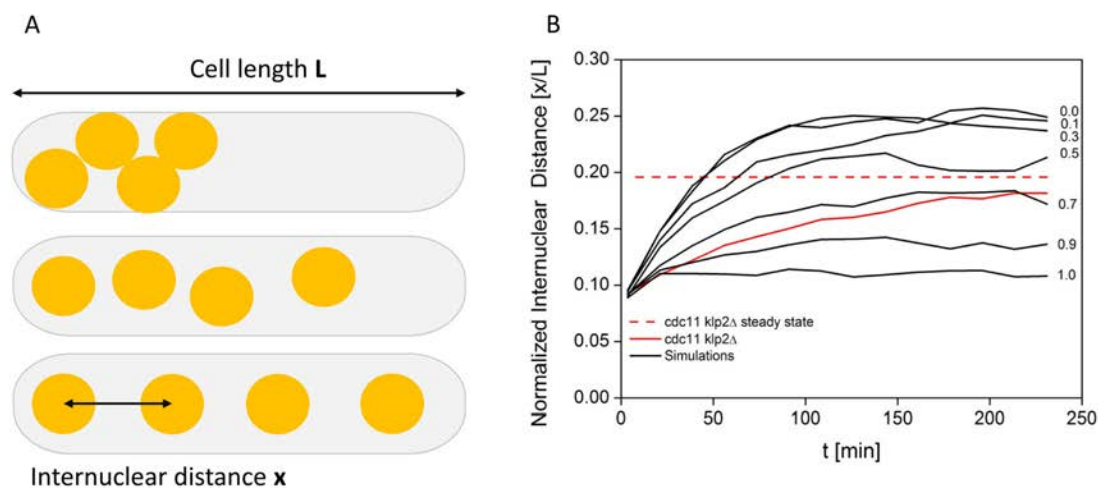


Figure 3.7: Re-establishment of nuclear pattern after perturbation

(A) Cartoon of the start and end point of the simulations of repositioning. **(B)** Simulated time evolution of internuclear distance after cell centrifugation for different passing probabilities ($n > 20$ for each). Nuclei are closed packed at one side of the cell at $t = 0$. Red line shows experimental data for $cdc11 klp2\Delta$ cells after cell centrifugation ($n = 109$) and dashed line for internuclear distances in steady state for a passing probability of 0.7.

Next we investigate the influence on the amount of microtubules by altering the nucleation rate. The internuclear distance itself is not affected by the nucleation rate as the ratio of microtubules interacting with neighbouring nuclei and cell walls remains the same. As more microtubules are in contact with the nuclei, the forces they generate are constantly antagonized by each other, causing only small fluctuations in nuclear positions (Figure 3.8 B). This trend is in agreement with the outcome of an analytical model of positioning of a single microtubule organizing centre in a 1-dimensional geometry [15]. Here it was shown that the positional stability increases with the number of microtubules that interact with the confining geometry.

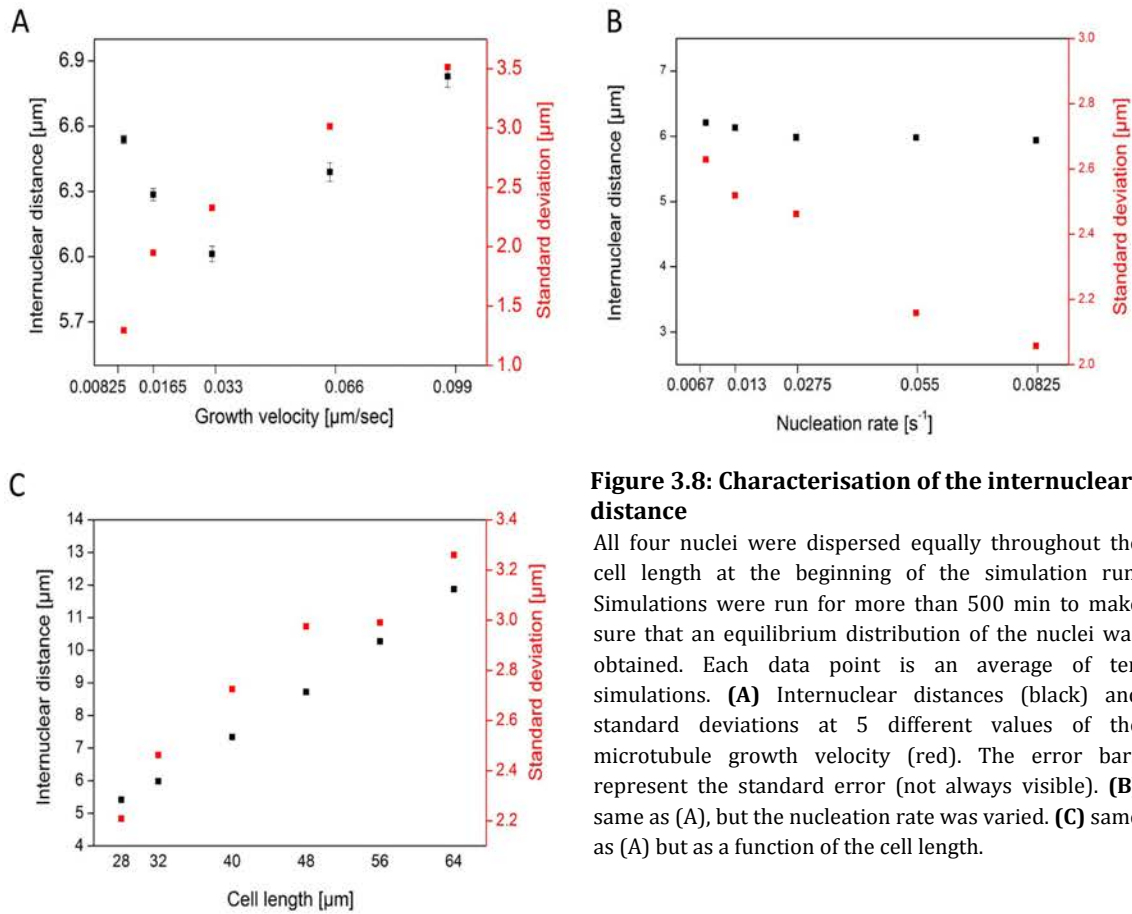


Figure 3.8: Characterisation of the internuclear distance

All four nuclei were dispersed equally throughout the cell length at the beginning of the simulation run. Simulations were run for more than 500 min to make sure that an equilibrium distribution of the nuclei was obtained. Each data point is an average of ten simulations. **(A)** Internuclear distances (black) and standard deviations at 5 different values of the microtubule growth velocity (red). The error bars represent the standard error (not always visible). **(B)** same as (A), but the nucleation rate was varied. **(C)** same as (A) but as a function of the cell length.

As expected, an increase in cell length increased internuclear distances (figure 3.8C). At the same time the stability of the positions themselves decreased. This is likely because fewer microtubules are able to reach their targets, an effect comparable to decreasing the nucleation rate.

Next we analysed the time scale of nuclear motion after positioning all nuclei to one edge of the cell. The same parameters were varied and the time at which 75% of the equilibrium internuclear distance was attained was calculated (Figure 3.9 A). Positioning is slow at low growth velocities but stabilizes at higher growth velocities (Figure 3.9 B). We next varied the nucleation rate. At a reduced nucleation rate of 0.00675/s less than one microtubule was in constant contact with the barrier and repositioning was slow. This is in agreement with earlier work that showed that faster positioning of a single microtubule aster in a 1-dimensional geometry is obtained, when on average one microtubule is in contact with the wall [15]. However, in contrast to this earlier work, our model allows for nuclear movement when microtubules on both sides

of the nucleus are generating forces. Therefore, repositioning does not slow down, when a lot of microtubules are involved in positioning. We conclude that the amount of microtubule interactions is not just important to gain a stable nuclear position but also for the rate at which the equilibrium position is established.

Lastly, we increased the cell length in the simulation. The average microtubule length of $6.6 \mu\text{m}$ in our model closely matches the equilibrium internuclear distance. At increasing cell lengths fewer microtubules are able to reach their targets. Repositioning becomes slower at longer cell length, firstly because longer distances needed to be travelled, but secondly because microtubule-nucleus interactions become more rare (Figure 3.9 D).

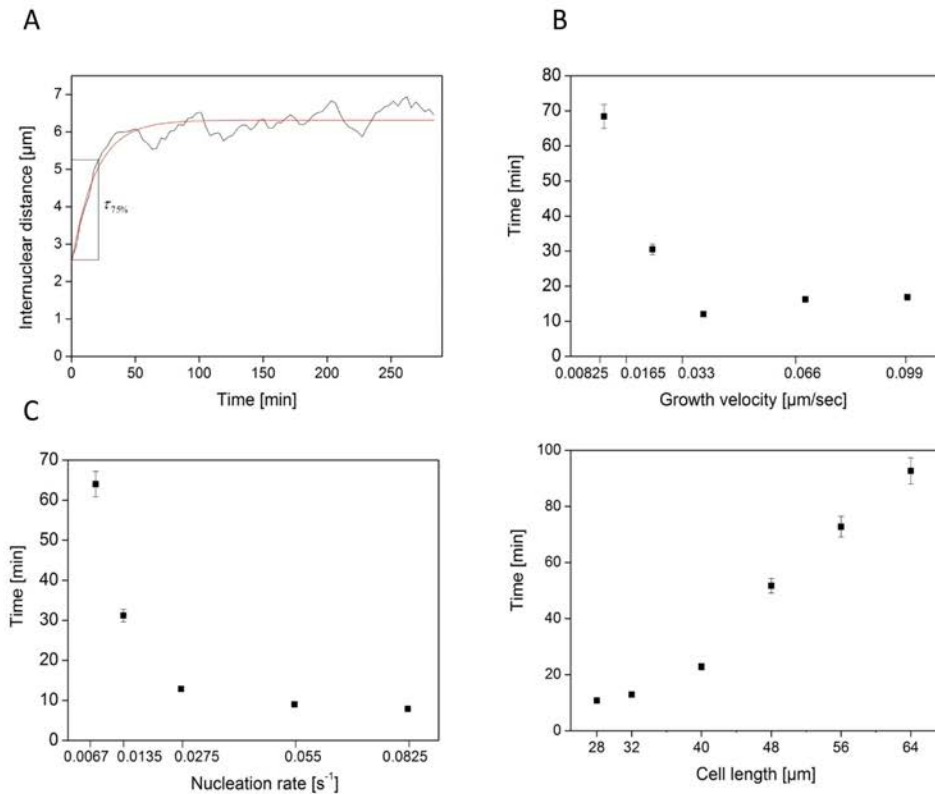


Figure 3.9: Time evolution of internuclear distance after perturbation

(A) Example of single simulated nuclear repositioning event in a tetranucleated cell after positioning all nuclei to one edge of the cell. The internuclear distance in steady state was used to calculate, 75%, the time when 75% of the distance was reached (thin black lines). The time of ten simulations was averaged for each data point in B, C and D. **(B)** $t_{75\%}$ for different microtubule growth velocities as a function of growth velocity. **(C)** Same as B, but for different microtubule nucleation rates and **(D)** for different cell lengths.

3.4. Discussion

Microtubules generate repulsive forces for equidistant nuclear patterns

Equidistant positioning of nuclei in multinucleated cells is observed in various cell types. In the model system fission yeast *S. pombe* it was shown that dynamic unstable microtubules generate repulsive forces in between nuclei (Chapter 2). We set up a simplified model of this system, which we simulated using C++ code, to demonstrate that repulsive forces generated by dynamic unstable microtubules are sufficient for equidistant patterning. The model not only correctly predicts pattern formation, but also the size of positional fluctuations and the dynamics of repositioning are in agreement with experimental data. The results revealed that no other forces are necessary.

In cells, microtubules can bend and they can grow around neighbouring nuclei. Correctly modelling these events in 3 dimensions would require detailed knowledge on mechanical constraints in the cell. For example we have chosen not to model the mechanical details of microtubules that impinge on nuclear envelopes, which might not just lead to nuclear movement but also rotation. This would require knowledge on the friction experienced by microtubule plus-ends on the nuclear envelope and on the stiffness of the attachment of the microtubule minus-ends to the nuclear envelope as well. As such properties have not been measured yet, the extension of the model by these parameters would decrease its simplicity. Instead we chose to build a 1-dimensional model and introduce two concepts to account for events that occur in a 3-dimensional cell. Firstly, microtubules were assigned a compression modulus to account for elastic deformations of microtubules and their attachment points. The compression modulus was chosen such that the wall-interaction time of microtubules under load was similar to observations in cells. Secondly, a passing probability was introduced to take into account that interactions of growing plus ends with cell walls generate on average more force than interactions with neighbouring nuclei. The modelled internuclear distance was in agreement with the experiment for a passing probability of $\rho=0.7$. The passing effect can indeed explain the observed pattern and shows that pushing against nuclei is indeed a rather inefficient force generating mechanism. We do not believe that the estimated passing probability is a good estimate for the true probability of passing. Instead it is a single parameter that summarizes multiple processes that determine the efficiency of force production at nuclear envelopes.

Previously a microtubule pushing-based mechanism has been proposed for the centering of single microtubule asters [17]. These mechanisms were shown to become less efficient if microtubules start buckling. Microtubules that are longer than approximately 10 μm will buckle under their own polymerization forces and will lose

their load bearing property. Moreover, microtubules that buckle may turn around corners in cells and fold back on themselves. It was shown that under these circumstances asters may become trapped at a position other than the center of the bounding geometry. Similarly, buckling of microtubules is expected to influence the positioning mechanism that is proposed here for multiple nuclei. Microtubules were however not observed to turn around at cell ends but they did show some degree of bending. It is therefore likely that longer microtubule relayed less force than modeled in our 1-dimensional approach. However the slender cell shape of *cdc11* cells and the presence of large nuclei confines the bending such that also microtubules longer than 10 μm will generate considerable forces. We therefore believe that our choice to make a 1-D model in which microtubules generate forces independent of their length is justified since our purpose is to demonstrate the feasibility of a positioning mechanism for multiple objects based on polymerization forces alone.

Our results show that repulsive interactions between nuclei can generate an equidistant pattern. The interactions have a long range because microtubules grow away from the nuclei. In fact, the range of the interaction is determined by the mean length of the microtubules as given by Equation 3.3.. The interaction will be weak if the internuclear distance is much larger than the mean microtubule length. Microtubules in between nuclei that are separated far away from each other will more often undergo a catastrophe without generating a pushing event. Because of dynamic instability, the number of productive pushing events in between nuclei increases with decreasing distance. This is why nuclei that are too close to each in comparison to their neighbours move apart. If the mean length of microtubules is much longer than the mean internuclear distance all microtubules that are nucleated will generate a productive pushing event. Then, forces generated in between nuclei will be similar for closely and distantly spaced nuclei, impeding equidistant positioning. This effect may in part explain Figure 3.8A, where the positional accuracy deteriorates with increasing growth velocity. Cells are therefore likely to adapt parameters of dynamic instability to adapt the mean microtubule length to the required internuclear distance. In this way stable equilibrium positions are obtained.

3.5. Material and Methods

The simulated model

We used a C++ program to simulate the repulsive forces generated by dynamic microtubules and the resulting motion of nuclei. The elongated cylindrical geometry of the cell in which the nuclei by virtue of their size are effectively constrained to move only along the long axis and the directed growth of microtubules along the same axis makes the problem at hand nearly 1 dimensional. Therefore, each nucleus in the model has a 1-dimensional position on an interval running from 0 to the length of the cell, and each microtubule end occupies a position on this same interval. The goal of the simulation was to find the minimal conditions that are sufficient to disperse the nuclei equally along the cell axis. We therefore neglected lateral interactions between microtubules and the cell wall, as well as their ability to buckle while growing against a barrier. The simulation evolves the positions of the nuclei and the length of the microtubules with a fixed time step stochastic algorithm. Each simulation generated several output files, which stored, amongst others, the nuclei positions, microtubule length, microtubule contact time and the number of force generating microtubules. Averages were taken over a number of independent runs of the simulation. All parameters used are listed in Table 3.1, with values either taken from the literature or measured / estimated by us.

Table 3.1: Parameters used in the simulations

Parameter		Value	Reference
Growth Velocity	$v_g^{(0)}$	0.033 $\mu\text{m/s}$	[12]
Shrinkage Velocity	v_s	0.150 $\mu\text{m/s}$	[12]
Unconstrained catastrophe rate	$r_c^{(0)}$	0.005 /s	[34]
Nucleation rate	r_n	0.0275 /s	Nr of interacting microtubules
Thermal Energy	kT	0.00411 pN μm	
Cytoplasmic viscosity	η	0.9 pNs/ μm^2	[18]
Effective step size	δ	0.0018461 μm	
Cell radius	r_{cell}	1.75 μm	Measurements/[9]
Thermal compressibility factor	κ	0.560069 / μm	Calculations
Passing probability	ρ	Variable (0-1)	
radius (single)	r_{nucleus_s}	1.5 μm	Measurements
Cell length (single)	l_{c_s}	12 μm	Measurements
radius (multi)	r_{nucleus_m}	1.3 μm	Measurements
Cell length (multi)	l_{c_s}	32 μm	Measurements

Table 3.2: The corresponding k_m and k to the growth velocities taking into account a waiting time of $\tau_c = 90$ s

Growth velocity $v_g^{(0)}$ [$\mu\text{m/s}$]	Compression modulus k_m [$\text{pN}/\mu\text{m}$]	Thermal compressibility factor k [$1/\mu\text{m}$]
0.00825	14.85	2.228893
0.01650	7.42	1.113696
0.033	3.71	0.560069
0.066	1.855	0.278424
0.099	1.235	0.185366

Cell biology

Standard fission yeast techniques were used for gene deletion and gene tagging [42]. The cell lines used to analyse the size of the nuclei, the internuclear distance and nuclear oscillations are listed in Table 3.3. Cell culturing, imaging and the analysis of nuclear position were done as described in chapter two.

Table 3.3: Fission yeast cell lines used in the experiments.

Nr	Strain	note
JT.69	Cdc11-nup107-GFP::kanMx-klp2 Δ 25::ura	This study/ [43]
PT.54	Nup107-GFP::kanMx	[12]

Acknowledgements

We thank F. Chang, and P. Tran for strains. In addition we thank Dan McCollum, S. Trautmann, A. Gladfelter, A. Akhmanova, M. Dogterom and T. Ketelaar for helpful discussions. Jeroen de Keijzer for help with MATLAB. The work of B.M.M and JT are part of the research programme of the “Stichting voor Fundamenteel Onderzoek der Materie (FOM)”, which is financially supported by the “Nederlandse Organisatie voor Wetenschappelijk Onderzoek (NWO)”. MEJ was supported by NWO-middel groot.

References

1. Gibeaux, R., et al., *Electron tomography of the microtubule cytoskeleton in multinucleated hyphae of Ashbya gossypii*. *Journal of Cell Science*, 2012. **125**(23): p. 5830-5839.
2. Jain, I.H., V. Vijayan, and E.K. O'Shea, *Spatial ordering of chromosomes enhances the fidelity of chromosome partitioning in cyanobacteria*. *Proceedings of the National Academy of Sciences*, 2012. **109**(34): p. 13638-13643.
3. Komeili, A., *Molecular mechanisms of compartmentalization and biomineralization in magnetotactic bacteria*. *FEMS Microbiology Reviews*, 2012. **36**(1): p. 232-255.
4. Metzger, T., et al., *MAP and kinesin-dependent nuclear positioning is required for skeletal muscle function*. 2012. **484**(7392): p. 120-124.
5. Oikawa, K., et al., *CHLOROPLAST UNUSUAL POSITIONING1 Is Essential for Proper Chloroplast Positioning*. *The Plant Cell Online*, 2003. **15**(12): p. 2805-2815.
6. Baker, J., W.E. Theurkauf, and G. Schubiger, *Dynamic changes in microtubule configuration correlate with nuclear migration in the preblastoderm Drosophila embryo*. *The Journal of Cell Biology*, 1993. **122**(1): p. 113-121.
7. Elhanany-Tamir, H., et al., *Organelle positioning in muscles requires cooperation between two KASH proteins and microtubules*. *The Journal of Cell Biology*, 2012. **198**(5): p. 833-846.
8. Grava, S., et al., *Clustering of Nuclei in Multinucleated Hyphae Is Prevented by Dynein-Driven Bidirectional Nuclear Movements and Microtubule Growth Control in Ashbya gossypii*. *Eukaryotic Cell*, 2011. **10**(7): p. 902-915.
9. McNaughton, E. and L. Goff, *The role of microtubules in establishing nuclear spatial patterns in multinucleate green algae*. 1990. **157**(1-3): p. 19-37.
10. Savage, D.F., et al., *Spatially Ordered Dynamics of the Bacterial Carbon Fixation Machinery*. *Science*, 2010. **327**(5970): p. 1258-1261.
11. Telley, I.A., et al., *Aster migration determines the length scale of nuclear separation in the Drosophila syncytial embryo*. *The Journal of Cell Biology*, 2012. **197**(7): p. 887-895.

12. Tran, P.T., et al., *A Mechanism for Nuclear Positioning in Fission Yeast Based on Microtubule Pushing*. The Journal of Cell Biology, 2001. **153**(2): p. 397-412.
13. Vogel, S.K., et al., *Self-Organization of Dynein Motors Generates Meiotic Nuclear Oscillations*. PLoS Biol, 2009. **7**(4): p. e1000087.
14. Dogterom, M., et al., *Force generation by dynamic microtubules*. Current Opinion in Cell Biology, 2005. **17**(1): p. 67-74.
15. Dogterom, M. and B. Yurke, *Microtubule dynamics and the positioning of microtubule organizing centers*. Physical Review Letters, 1998. **81**(2): p. 485-488.
16. Janson, M.E., M.E. de Dood, and M. Dogterom, *Dynamic instability of microtubules is regulated by force*. The Journal of Cell Biology, 2003. **161**(6): p. 1029-1034.
17. Laan, L., et al., *Force-generation and dynamic instability of microtubule bundles*. Proceedings of the National Academy of Sciences, 2008. **105**(26): p. 8920-8925.
18. Tolić-Nørrelykke, I.M., et al., *Positioning and Elongation of the Fission Yeast Spindle by Microtubule-Based Pushing*. Current Biology, 2004. **14**(13): p. 1181-1186.
19. Bier, M., *Brownian ratchets in physics and biology*. Contemporary Physics, 1997. **38**(6): p. 371-379.
20. Deinum, E.E. and B.M. Mulder, *Modelling the role of microtubules in plant cell morphology*. Current Opinion in Plant Biology, 2013. **16**(6): p. 688-692.
21. Kruse, K., S. Camalet, and F. Jülicher, *Self-Propagating Patterns in Active Filament Bundles*. Physical Review Letters, 2001. **87**(13): p. 138101.
22. Cassimeris, L., N.K. Pryer, and E.D. Salmon, *Real-time observations of microtubule dynamic instability in living cells*. The Journal of Cell Biology, 1988. **107**(6): p. 2223-2231.
23. Mitchison, T. and M. Kirschner, *Dynamic instability of microtubule growth*. 1984. **312**(5991): p. 237-242.
24. Sammak, P.J. and G.G. Borisy, *Direct observation of microtubule dynamics in living cells*. 1988. **332**(6166): p. 724-726.
25. Schulze, E. and M. Kirschner, *New features of microtubule behaviour observed in vivo*. 1988. **334**(6180): p. 356-359.

26. Walker, R.A., et al., *Dynamic instability of individual microtubules analyzed by video light microscopy: rate constants and transition frequencies*. The Journal of Cell Biology, 1988. **107**(4): p. 1437-1448.
27. Flyvbjerg, H., T.E. Holy, and S. Leibler, *Microtubule dynamics: Caps, catastrophes, and coupled hydrolysis*. Physical Review E, 1996. **54**(5): p. 5538-5560.
28. Tischer, C., D. Brunner, and M. Dogterom, *Force- and kinesin-8-dependent effects in the spatial regulation of fission yeast microtubule dynamics*. 2009. **5**.
29. Bratman, S.V. and F. Chang, *Stabilization of Overlapping Microtubules by Fission Yeast CLASP*. Developmental Cell, 2007. **13**(6): p. 812-827.
30. Dogterom, M. and S. Leibler, *Physical aspects of the growth and regulation of microtubule structures*. Physical Review Letters, 1993. **70**(9): p. 1347-1350.
31. Dogterom, M. and B. Yurke, *Measurement of the Force-Velocity Relation for Growing Microtubules*. Science, 1997. **278**(5339): p. 856-860.
32. Hill, T.L. and M. Kirschner, *Bioenergetics and kinetics of microtubule and actin filament assembly-disassembly*. Int. Rev. Cytol, 1982.
33. Mogilner, A. and G. Oster, *The Polymerization Ratchet Model Explains the Force-Velocity Relation for Growing Microtubules*. European Biophysics Journal, 1999. **11/1998**.
34. Foethke, D., et al., *Force- and length-dependent catastrophe activities explain interphase microtubule organization in fission yeast*. 2009. **5**.
35. Abramowitz, M.S., Irene A, *Handbook of Mathematical Functions With Formulas, Graphs, and Mathematical Tables*. 1964.
36. Daga, R.R., A. Yonetani, and F. Chang, *Asymmetric Microtubule Pushing Forces in Nuclear Centering*. Current Biology, 2006. **16**(15): p. 1544-1550.
37. Samejima, I., et al., *Fission Yeast Mto1 Regulates Diversity of Cytoplasmic Microtubule Organizing Centers*. Current Biology, 2010. **20**(21): p. 1959-1965.
38. Sawin, K.E., P.C.C. Lourenco, and H.A. Snaith, *Microtubule Nucleation at Non-Spindle Pole Body Microtubule-Organizing Centers Requires Fission Yeast Centrosomin-Related Protein mod20p*. Current Biology, 2004. **14**(9): p. 763-775.
39. Daga, R.R., et al., *Self-organization of microtubule bundles in anucleate fission yeast cells*. 2006. **8**(10): p. 1108-1113.

40. Neumann, F.R. and P. Nurse, *Nuclear size control in fission yeast*. The Journal of Cell Biology, 2007. **179**(4): p. 593-600.
41. Processing.org.
42. Bähler, J., et al., *Heterologous modules for efficient and versatile PCR-based gene targeting in Schizosaccharomyces pombe*. Yeast, 1998. **14**(10): p. 943-951.
43. http://yeast.lab.nig.ac.jp/nig/index_en.html.





Microtubule growth and sliding are coupled processes that regulate spindle assembly

Juliane Teapal, Jouke Sjollema and Marcel E. Janson

Chapter

4

Abstract

Microtubules together with various microtubule associated (MAPs) proteins form the mitotic spindle to segregate the chromosomes. Interdigitating microtubules form an overlap in the middle of the spindle and template the formation of a midzone. Members of the Map65/PCR1/Ase1 family of microtubule crosslinkers specifically localize to the zone of interdigitation and recruit other midzone proteins. We investigated mechanisms that control the size of the midzone during spindle elongation in fission yeast. Spindle elongation is driven by relative sliding of interdigitating microtubules and simultaneous growth at microtubule plus-ends. Investigations of midzone length regulation have mainly focussed upon the hypothesis that a balance of opposing molecular motors may regulate spindle elongation rate. In wild type fission yeast cells, microtubule plus-ends grew away from the midzone towards the opposite pole, demonstrating that spindle elongation rate is limited by the speed at which motors slide interdigitating microtubules. Our results show that overextension of the interdigitation zone by microtubule growth is prevented by a high microtubule catastrophe rate and limited availability of ase1p. In cells with decreased microtubule growth velocity, the spindle elongation rates were reduced by a 4-fold. This shows that spindle elongation was limited by microtubule growth velocity, demonstrating that microtubule sliding and microtubule growth are coupled processes. Further we hypothesize that ase1p crosslinkers generate forces that oppose spindle elongation, when microtubule growth is insufficient. The highlighted role of microtubule dynamics will aid future investigations into the complex interactions between microtubule related processes at the midzone.

4.1. Introduction

The mitotic spindle is a subcellular machine that uses microtubule based force generation for chromosome segregation [1]. During mitosis microtubules take on different functions and are named accordingly: kinetochore microtubules connect the spindle poles with kinetochores on chromosomes, astral microtubules position the spindle in the cell through interactions with the cell cortex, and interpolar microtubules form connections between the two spindle poles to maintain bipolar organization. The interpolar microtubules form a highly organized array of overlapping microtubules, called the midzone, which emerges during anaphase. Apart from maintaining overall spindle architecture, the midzone regulates cleavage furrow positioning in animal cells [2]. At the onset of anaphase bundling proteins of the Ase1/Pcr1/MAP65 family localize specifically to the antiparallel microtubule overlap [3, 4]. Ase1p acts as a major scaffolding protein and recruits MAPs and other regulatory proteins to the midzone [4-7] in a phosphor-dependent manner [4, 8]. Yet the mechanism by which the overlaps are positioned in the centre within the spindle and the length control of overlaps are poorly understood.

A major role of the midzone is to regulate the rate of spindle elongation during anaphase-B. Antiparallel microtubules slide apart to increase the distance between spindle poles and their associated chromosomes before cytokinesis commences. Plus-end directed motors of the Kinesin-5, Kinesin-6, and Kinesin-12 [9-12] families generate forces in between overlapping microtubules to drive spindle elongation. Moreover, minus-end directed dynein motors positioned at the cortex are believed to generate additional forces for spindle elongation by pulling on astral microtubules in *Drosophila* embryos and *C. elegans* [13, 14]. Other studies, however, suggest that dynein may also generate forces that counteract spindle elongation by acting on interpolar microtubules [9, 12, 15, 16]. Similarly, minus-end directed Kinesin-14 motors have been proposed to generate counteracting forces that slow down spindle elongation in budding yeast and mammalian cells [14, 17, 18]. It was shown that deletion of Kinesin-14 can rescue the phenotype of Kinesin-5 deletion to a large degree suggesting that a balance of outward forces (plus-end motors) and inward-forces (minus-end motors) may regulate spindle elongation [16]. However, *in vitro* assays with antagonistic Kinesin-14 and Kinesin-5 motors acting on microtubules showed that a stable force balance between both motors cannot be achieved [19]. Instead, directional instability, a phenomena in which microtubules occasionally switch sliding direction, is observed when motor forces are balanced [20]. It is therefore unclear how the activities of motors of opposite directionality can be coordinated to drive robust spindle elongation.

During metaphase microtubules have a high dynamic instability to aid the search and capture mechanism [21, 22] for the alignment of the chromosomes on the bipolar spindle. The construction of the midzone in anaphase however is accompanied with a change into more stable microtubules [23, 24]. Later it was shown that Clasp proteins, which are microtubule rescue factors, localize specifically to the midzone through association with the microtubule crosslinkers of the Ase1/PRC1/Map65 family [5]. The resulting local inhibition of microtubule disassembly in the midzone enables lasting connections between antiparallel microtubules to sustain microtubule sliding for spindle elongation. It is at present unknown how the combined activities of microtubule dynamics and microtubule sliding control the size of the midzone. Observations in bipolar spindles in animals and bipolar phragmoplasts in plants show that both the size and position of the overlap is well regulated [25-27].

The fission yeast, *S. pombe*, serves as an excellent model system to study microtubule dynamics and organization. Photobleaching experiments of GFP-tubulin reveal that the poleward-microtubule flux mechanism observed in other organisms is lacking in *S. pombe* [28]. Astral microtubules maintain only the spindle orientation and are not believed to aid spindle elongation [29]. On the other hand, many of the genes and features like microtubule bundles and a well-defined spindle midzone are shared with more complex mammalian spindles. Moreover, the thin cell diameter and genetic modification by homologous recombination makes it a suitable tool for microscopy.

In order to understand the regulation of midzone length we visualized the midzone using GFP-tagged *ase1p* and perturbed the microtubules genetically and pharmacologically. The results show that spindle elongation velocity depends on midzone organization and velocities respond to changes in microtubule growth velocity.

4.2. Results

Zone of microtubule interdigitation is wider than the midzone

The bundling protein ase1p is a prominent midzone-associated protein. We expressed GFP-ase1p in fission yeast to visualize the midzone during the fast phase of spindle elongation corresponding to anaphase-B. As described previously, GFP-ase1p localized to microtubules at the centre of the spindle and near spindle poles bodies (SPBs) i.e. the yeast functional analogue of centrosomes in which all microtubule minus -ends are embedded ([30, 31], Figure 4.1 A and B). The signal near the SPB corresponds to astral microtubules that associate to the cytoplasmic side of the SPB. The length of the central GFP-ase1p zone remained remarkably constant throughout anaphase-B. This constant midzone length of about 1.8 μm suggests that the zone of microtubule interdigitation, which is thought to be the template for ase1p binding and midzone formation, is well controlled in size.

To visualize the zone of microtubule interdigitation directly, we imaged cells expressing GFP-tubulin (Figure 4.1 B). Spindle microtubules are visible as a bright bundle in between the SPBs. The pre-anaphase-B spindle consists of kinetochore microtubules and interdigitating microtubules [32]. Electron microscopy has shown that all kinetochore microtubules have shortened to the SPBs when the spindle has reached a length of 6 μm . At this length the spindle is composed out of about ten interdigitating microtubules and the zone of overlap becomes visible as a brighter central region in fluorescent images ([32]; Figure 4.1 B). To quantify the distribution of microtubules, we generated line scans of the GFP-tubulin signal along spindles with a length of 6 μm (Figure 4.1C). The signal at the spindle centre was almost twice the signal near the spindle poles. This indicates that microtubules must extend beyond the spindle centre, but do not run all the way towards the other SPB. This is in agreement with electron microscopy reconstructions of anaphase-B spindles [32]. A comparison of GFP-tubulin line scans and line scans of GFP-ase1p indicated that the zone of microtubule interdigitation is wider than the midzone itself, defined as the zone of ase1 localization (Figure 4.1 C).

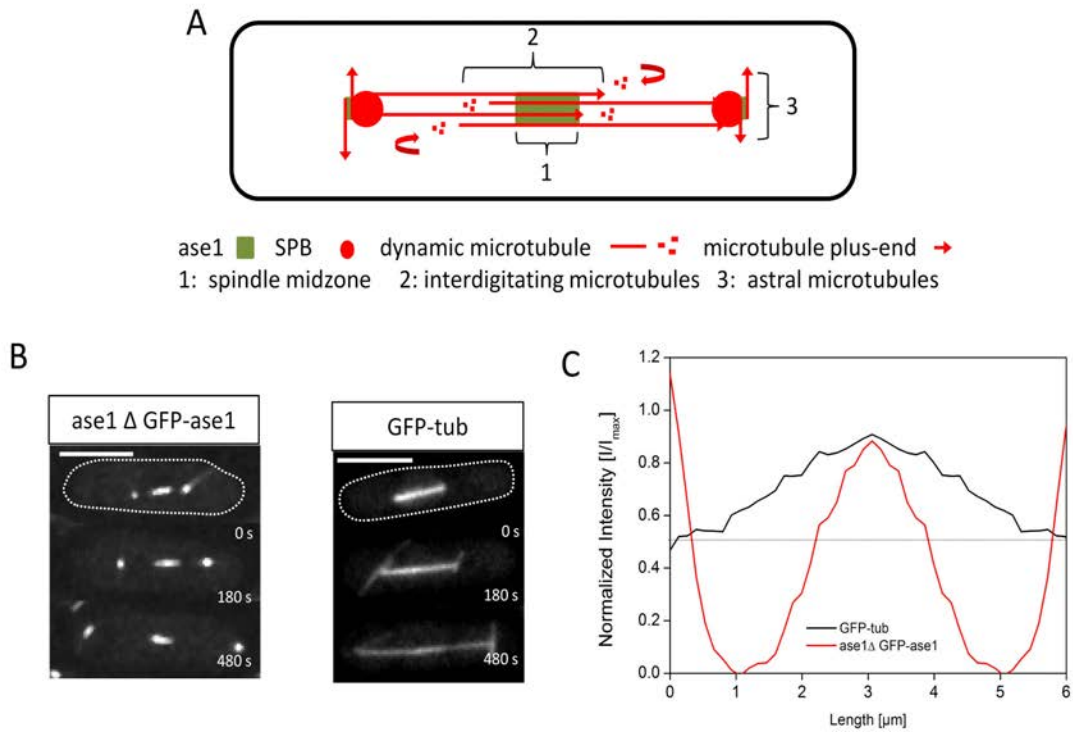


Figure 4.1: Visualizing of microtubule networks in fission yeast

(A) Cartoon of a spindle during anaphase B with dynamic microtubules (red lines). Red circles represent the SPBs, the nucleation centre for microtubules. Green blocks symbolize the crosslinker *ase1*, binding to the spindle midzone and to astral microtubules. Microtubules grow towards the opposite SPB and interdigitate with each other. The spindle midzone is determined by the binding of the crosslinker *ase1*. **(B)** Time series of cells expressing GFP-*ase1* (left) and GFP-tub. Time point 0 represents the start of anaphase B and the last time point the maximum spindle length. **(C)** Intensity plot of the GFP-*ase1* and GFP-tubulin signal measured at the spindle length of 6 μm . The intensities of the GFP-signals were normalized to the maximum signal at the midzone and represent the average of 15 individual spindles. The zone of interdigitating microtubule (black) is wider than the midzone, defined by the localisation of *ase1* (red).

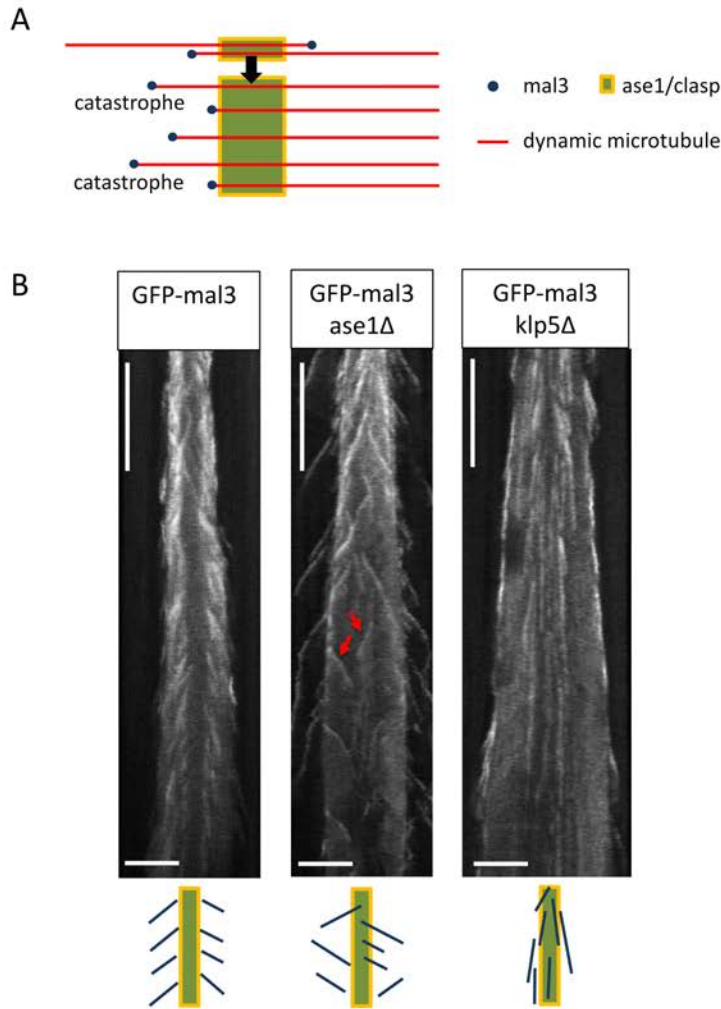


Figure 4.2: Organisation of the spindle midzone

(A) Cartoon of a dynamic microtubule within the spindle. Microtubule growth occurs at the plus-end away from the spindle midzone. Upon a catastrophe the microtubule shrinks until it encounters the midzone, where a rescue occurs and growth recommences. **(B)** Kymographs (top) of cells expressing the microtubule plus-end tracking protein GFP- mal3 and cartoons to visualize microtubule dynamics within the spindle. Left: GFP-mal3 expressed in wild type cells. A clear midzone is visible in which growing microtubule ends are absent. Short periods of growth only occur away from the midzone towards the SPBs. Middle: GFP-mal3 expressed in cells lacking *ase1p*. Microtubule growth is bidirectional along the full length of the spindle. Right: Cells lacking *klp5p* have extended periods of microtubule growth. Growth is unidirectional. Scale bars: top 5 min, bottom : 5 μ m

Microtubules in anaphase-B undergo brief length oscillations back and forth to the midzone

The confined zone of microtubule interdigitation indicates that microtubule length is well regulated in the spindle. To investigate the mechanisms involved we set out to visualize microtubule dynamics in the spindle. We were unable to visualize the dynamics of individual microtubules in the spindles using GFP-tubulin expression because of the large microtubule density (data not shown). Microtubule growth in dense networks has however been successfully visualized in cells using the microtubule-end binding proteins EB1 or its homologues [33, 34]. These proteins recognize and selectively bind to features at growing microtubule plus-ends while shrinking microtubule plus-ends are not targeted. The fission yeast homologue GFP-mal3p (Figure 4.2 B left) formed dim moving spots in spindles and this localisation appeared as diagonal lines in kymographs that were constructed from time-lapsed movies. The mean

growth velocity was $1.8 \pm 0.08 \mu\text{m}/\text{min}$ ($\pm\text{SE}$, $N=102$). Growth events in each spindle half were unidirectional directed away from the midzone in agreement with our earlier finding that all microtubule plus-ends must have passed the spindle centre. The central region of the spindle, i.e. the presumed location of the midzone, is deficient of microtubule plus-ends and new growth events, corresponding to switches between the shrinkage and the growth state (rescues), appear to be initiated at the boundaries of this zone. Growth events are brief suggesting that a high catastrophe rate limits the extent to which microtubules grow away from the midzone in order to prevent overextension of the zone of microtubule interdigitation. Our combined observations thus demonstrate that individual microtubules in anaphase-B cells undergo brief length oscillations away and towards the spindle midzone as schematically illustrated in Figure 4.2 A. This interpretation is in agreement with direct visualization of microtubules in longer spindles of about $10 \mu\text{m}$ in length. At this stage most microtubules have disassembled towards the SPBs but the 2-3 remaining interdigitating microtubules were shown to oscillate in length without shrinking past the midzone [35].

To explain the brief microtubule length oscillation back and forth to the midzone, we hypothesized that a catastrophe factor and a midzone-localized rescue factor are minimal requirements. Previously, anaphase spindle microtubules were shown to depolymerize all the way to the SPB in absence of *cls1p*, a homologue of the microtubule rescue factor CLASP [5]. *Cls1p* localizes at the midzone through a physical interaction with *ase1p*. In absence of *ase1p*, rescues no longer occurred selectively near the spindle centre but were observed all over the spindle (Figure 4.2 B middle), in agreement with the diffuse spindle localization of *cls1p* in *ase1Δ* cells [5]. Consequently, microtubule growth was no longer unidirectional in each spindle half. The *ase1p/cls1p* module is thus required to create a strong spatial gradient in rescues near the midzone. The kinesins *kfp5p* and *kfp6p* are strong candidates for the catastrophe factor that limits the extent of growth away from the midzone. *Kfp5p* has previously been shown to induce catastrophes in interphase cells and localizes along the spindle [36]. In agreement with these results, we observed that the duration of growth events was prolonged in *kfp5Δ* cells (Figure 4.2 B right).

Next, we questioned why the *ase1p/cls1p* module is only recruited to a zone of limited length in the spindle. Microtubules grow away from the midzone in wild type cells and thus extend the zone of interdigitation. But *ase1p* does not bind to this wider zone and therefore cannot recruit *cls1p* to stabilize an ever-growing zone of interdigitation (Figure 4.1 C). In contrast, microtubule growth within microtubule bundles in interphase fission yeast cells immediately recruits *ase1p* to the new microtubule segments [37]. We hypothesized that since the mobility of *ase1p* on microtubules is down-regulated during

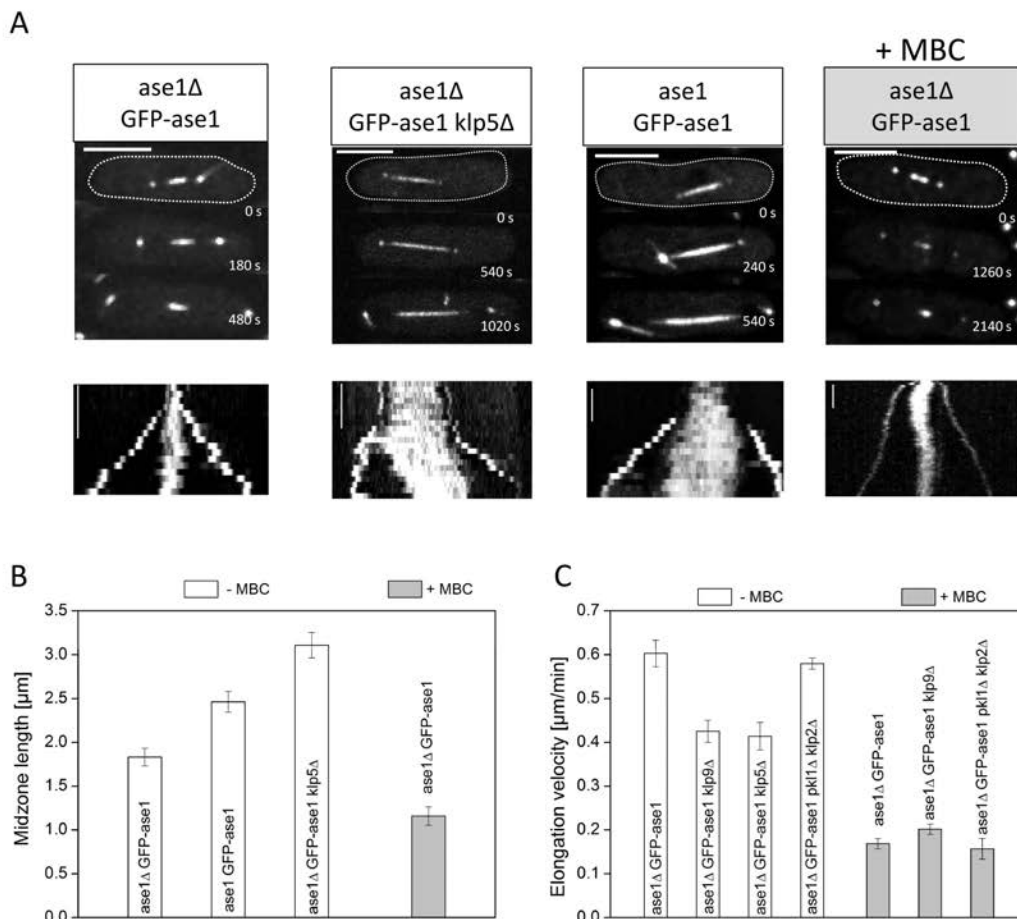


Figure 4.3: Analyses of midzone length and spindle elongation

(A) Time series and kymographs of cells expressing GFP-ase1. Scale bar: 5 min. **(B)** Midzone length established from the GFP-ase1 signal at a spindle length of 6 μm . The intensity of the signal was normalized to the maximum signal at the spindle midzone and midzone length was determined at 50% signal intensity. The average length of at least 15 spindles is plotted with the standard error. **(C)** Quantification of the spindle elongation velocity. The average elongation rates that are plotted were determined for at least 15 spindles for elongation from 5 μm to 7 μm . Standard errors are plotted.

anaphase, nearly all available *ase1p* may be immobilized at the midzone, preventing binding of *ase1p* to a new zone of interdigitation [30]. In such a scenario the available amount of *ase1p* should correlate with midzone length. We therefore imaged cells that express both GFP-*ase1p* and *ase1p* under the native *ase1* promoter. Midzones in these cells were about 40% longer and are so in agreement with length control by *ase1* availability (*ase1Δ GFP-ase1*: $1.8 \pm 0.10 \mu\text{m}$ (\pm SE); N=15, *ase1 GFP-ase1*: $2.5 \pm 0.12 \mu\text{m}$ (\pm SE); N=15; Fig. 4.3B).

To further investigate regulation of midzone length we imaged midzones in cells with perturbed microtubule dynamics. Compared to wild type cells, the zone of GFP-ase1p localization was 75% longer in *klp5Δ* cells with reduced catastrophe rates (Fig. 4.3.B). The extended midzone in *klp5Δ* cells however demonstrates that the available ase1p does not by itself organize into a compact midzone but that sufficient catastrophes are required to confine ase1 to a tight central zone. We noticed that the zone of GFP-ase1p localization was already extended at the metaphase to anaphase transition, the moment at which ase1p affinity to microtubuli is up-regulated (Figure 4.3 A). Possibly, in *klp5Δ* cells, ase1p and cls1p condense onto a large zone of interdigitation that is already established in metaphase. Due to the stabilizing properties of cls1p the midzone may not be able to shorten afterwards. We next perturbed microtubule growth by adding the depolymerizing drug MBC to the cells. Interphase microtubules depolymerized immediately after addition of the drug but surprisingly the midzone remained intact. Although midzones were decreased in length (by 37 % with N=15 for both treated and untreated cells; Fig 4.3 B) they remained approximately constant in length as the spindle further elongated demonstrating that microtubule growth continued. We conclude that the midzone length is not only determined by the limited pool of ase1p but also by microtubule dynamics. Nonetheless, the stability of the midzone upon treatment with MBC shows that midzone length is remarkably robust against strong perturbation of microtubule dynamics.

Spindle elongation rate responds to changes in microtubule dynamics

Spindle elongation requires simultaneous sliding and microtubule elongation. In wild type cells microtubules grow away from the midzone suggesting that the rate of spindle elongation is not limited by microtubule growth but the rate at which microtubules slide apart from each other. Such a notion is supported by an observed decrease in spindle elongation rate when the sliding motor *klp9p* is knocked out (Figure 4.3 C). In these cells sliding is thought to be powered by the remaining cut7 motors of the Kinesin-5 family [4]. We noticed that many microtubules do not grow away from the midzone in *klp5Δ* cells suggesting that microtubule growth velocity is about half of the measured spindle elongation rate ($0.41 \pm 0.03 \mu\text{m}/\text{min}$ ($\pm\text{SE}$); N = 15). This results in vertical instead of diagonal lines in the GFP-mal3 kymograph (Figure 4.2 B, right). Microtubule growth velocity is thus decreased in *klp5Δ* cells possibly because overextension of microtubules in absence of catastrophes lowers the free concentration of tubulin. A decrease in elongation rate upon slower growth velocity is in agreement with cells in which the function of *xmap215*-homologue (*alp14*) is perturbed which also show slower elongation rate [38]. In the MBC experiment we see an extreme slowdown of the elongation rate upon a strong decrease in microtubule growth velocity (Figure 4.3 C, wild type = $0.60 \pm 0.03 \mu\text{m}/\text{min}$ ($\pm\text{SE}$); N = 15, + MBC = $0.17 \pm 0.01 \mu\text{m}/\text{min}$ ($\pm\text{SE}$); N = 15). Additional knockout of *klp9p* does not further decrease elongation velocity in agreement with elongation being limited by microtubule growth under MBC conditions

(Figure 4.3 C). These results show that sliding and microtubule dynamics are coupled processes. Sliding velocity slows down when microtubule growth cannot keep up.

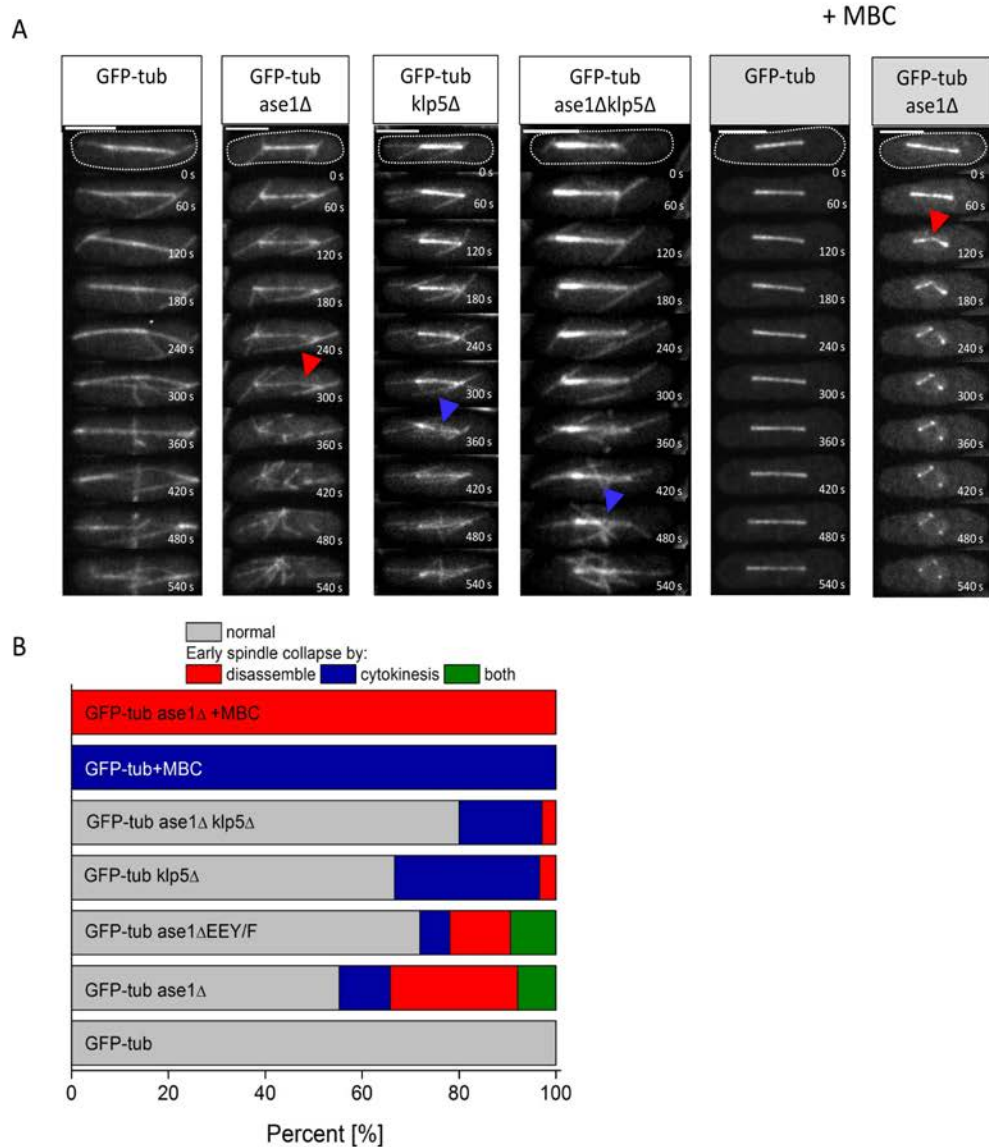


Figure 4.4: Interference of the midzone leads to early spindle collapse

(A) Time series of z-projections ($10 \times 0.5 \mu\text{m}$) of cells expressing GFP-tubulin. For each mutant a cell with a clear phenotype was chosen. For display, time point 0 is chosen such that all spindles have approximately equal length. **(B)** Spindle elongation and spindle collapse was investigated during the last phase of anaphase B. We quantified the occurrence of spindle breakage and spindle severing by the cytokinetic machinery ($N > 10$). Red arrow head indicates spindle collapse by disassemble, blue by the cytokinetic ring. Scale bar: $5 \mu\text{m}$

How can the elongation rate slow down in response to changes in microtubule dynamics? It has been suggested that a balance of plus- and minus-end directed motors may set sliding rate [17, 39]. It is possible that this balance is somehow changed in mutants with different microtubule dynamics. We knocked out two minus-end directed kinesin motors but found that they do not affect spindle elongation rate and are not required to slow down elongation upon addition of MBC (Figure 4.3 C). We next investigated whether *ase1p* itself may slow down spindle elongation for example by generating friction forces that oppose sliding. Severe overexpression of *ase1p* was shown previously to slow down elongation [40]. In this case, overexpressed *ase1p* localized throughout the complete spindle. Our strain that expresses GFP-*ase1* next to the endogenous *ase1p* does not show a slowdown in elongation velocity (Figure 4.3 C). Moreover deletion of *ase1* in cells expressing GFP-tubulin does not speed up elongation (wild type = $0,67 \pm 0.03 \mu\text{m}/\text{min}$ (\pm SE); N = 15, *ase1* Δ = $0.6 \pm 0.05 \mu\text{m}/\text{min}$, (SE); N = 16). *Ase1p* may thus only act as a brake on sliding under strongly perturbed conditions.

The function of the midzone

To further understand the function of the midzone in fission yeast we visualized spindle elongation and spindle break down at the end of anaphase B in cells expressing GFP-tubulin. In wild type cells, spindles first disassemble before the cytokinetic machinery contracts in the cell centre (Figure 4.4 A). The onset of siltation was visible because it causes a small indentation in background fluorescence in the cell centre. In cells treated with MBC, cytokinesis commenced before spindles disassembled, causing severing of spindles by the cytokinetic machinery (Figure 4.4 B). The start of cytokinesis is however delayed compared to the wild type (wild type = $11.2 \pm 0.47 \text{ min}$ (\pm SE), N = 10; MBC = $24,6 \pm 0.89 \text{ min}$ (\pm SE), N=8) suggesting that the timing of cytokinesis is delayed by the slower rate of spindle elongation in MBC cells. The absence of a midzone in *ase1* Δ cells causes spindles to break into two halves before they fully elongate (Figure 4.4 A and B), an effect that was strongly enhanced by the addition of MBC. Moreover, cytokinesis in *ase1* Δ cells frequently commenced before spindle breakdown. This spindle-breaking-phenotype could be partly rescued by removing the microtubule destabilizer *klp5* Δ , supposedly because microtubules become longer due to lower catastrophe rates and the two opposing sets of microtubules increase their interdigitation zone. Possibly this allows motor proteins to slide SPBs sufficiently apart from each other without a proper midzone. This prevented spindle breakage (Figure 4.4 B) but premature severing still occurred. Also cells with *ase1p* but lacking *klp5p* showed premature spindle severing. Lack of catastrophes in *klp5* Δ cells may thus hinder timely spindle disassembly. These experiments suggest that the major role of a well-organized midzone is coordinating spindle elongation, spindle breakdown, and cytokinesis (Figure 4.4).

4.3. Discussion

Length control of the midzone

The zone of microtubule interdigitation that forms the template for midzone formation is affected by microtubule dynamics and inter-microtubule sliding. Microtubule growth and shrinkage will respectively elongate and shorten the zone of interdigitation and the action of plus-end directed motors, klp9p and cut7p will slide interdigitating microtubules apart from each other, decreasing the overlap. Microtubule growth in wild type bipolar spindles occurs at a speed of $1.8 \mu\text{m}/\text{min}$ and could in principle drive spindle elongation at a rate that is twice as high: $3.6 \mu\text{m}/\text{min}$. In contrast, spindle elongation occurs at $0.6 \mu\text{m}/\text{min}$, demonstrating that elongation is limited by the rate of motorized sliding. This is in agreement with *in vitro* experiments that suggest that kinesin-5 motors are slow motors [41]. Due to the mismatch in microtubule growth velocity and elongation rate, dynamic microtubules in wild type cells grow away from the midzone and return after a catastrophe. Growth away from the midzone is less clearly observed in cells that lack the catastrophe factor klp5p. Instead, spindle elongation rates were decreased to $0.41 \mu\text{m}/\text{min}$. Based on the vertical lines in mal3-GFP kymographs of klp5 Δ cells, we propose that under these conditions spindle elongation rate is about equal to twice the microtubule growth velocity. In other words: elongation is limited by microtubule growth. The same is probably true for spindle elongation under MBC conditions. Mal3-GFP did not bind to microtubule ends under these conditions (data not shown) but a very well demarcated zone of GFP-ase1 in these cells suggests that microtubules do not grow away from the midzone. The elongation rate is reduced to $0.17 \mu\text{m}/\text{min}$ in this case. Our results thus demonstrate that sliding and microtubule dynamics are strongly coupled processes. Coupling prevents that spindle halves can separate by sliding when microtubule growth is perturbed.

Mechanism to control spindle elongation

What is slowing down the elongation rate when microtubule growth becomes too low to sustain elongation at wild type velocities? As motors are prime candidates to regulate elongation velocity, minus-end motors that oppose spindle elongation might generate more force when the midzone becomes too short. It is however unclear how feedback between midzone length and motor activity may be regulated at a molecular level. Our results show that two minus-end directed kinesins, klp2p and pkl1p, are not involved in this feedback. Minus-end directed dynein motors may be involved, however they do not localize to midzones and their deletion does not change spindle elongation rate [13, 42, 43]. Recent *in vitro* work showed that the kinesin-5 Cin8 motor from budding yeast can act both as a plus-end and minus-end directed motor [44], unusual in comparison to other members of the family (cut7, Eg5). Interestingly, large populations of cin8 motors drive plus-end directed motility whereas smaller pools drive minus-end directed motility. Kinesin-5 motors might thus switch to minus-end-directed motility when the overlap becomes too small due to limited growth of microtubules. It is however unclear

if such a mechanism could also work if there are additional motors of the Kinesin-6 family around, which is the case for fission yeast *klp9p*.

The role of *ase1p*

Moderate overexpression of *ase1p* demonstrated that the length of the midzone may be limited by the availability of *ase1p*. The affinity of *ase1p* for interdigitating microtubules is very large and the cytoplasmic concentration of *ase1p* is therefore low. *Ase1p* may thus not be recruited to microtubules that grow away from the midzone. Consequently, new zones of interdigitation are not immediately stabilized by CLASP proteins and microtubules can undergo sequences of growth and shrinkage. *In vitro* experiments have shown that *ase1p* crosslinkers can slow down motorized microtubule sliding in particular when they become closely packed within overlaps [45, 46]. *Ase1p* bound to overlaps is able to diffuse along the microtubules. The binding of *ase1p* and homologues to overlaps may therefore generate only a limited friction force that opposes motorized sliding [47]. The ends of microtubules, however, act as a diffusion barrier to the diffusion of *ase1p* proteins within overlaps. Consequently, *ase1p* proteins are highly confined to an overlap and the available proteins in an overlap become compacted when the overlap is shortened by motorized sliding. Compaction of *ase1p* may generate an opposing force through multiple mechanisms. Firstly, when an overlap shortens, the amount of associated *ase1p* will stay constant whereas the amount of bound motor proteins may decline [45]. This will lead to a relative increase of friction forces by *ase1p* over motor forces that drive spindle elongation. Secondly, if *ase1p* becomes closed packed in the overlap, further shortening may require *ase1p* to leave the overlap at the boundaries of the overlap. The breakage of bonds involved will generate a force that opposes overlap shortening. Thirdly, unpublished data has shown that a compacted pool of *ase1p* generates entropic forces that act to expand an overlap, again opposing spindle elongation. In wild type cells, microtubules grow for the most of their time away from the *ase1p* zone. Therefore it is not expected that they act as a barrier to *ase1p* diffusion in the overlap. In agreement, spindle elongation does not speed up in absence of *ase1p*. However, when microtubule growth is slowed down, microtubule ends will corner the pool of *ase1p* at the midzone. This may occur in *klp5Δ* cells (Figure 4.2 B) in which microtubule plus do not grow away from the midzone but instead are localized throughout the midzone. The same may be true for cells treated with MBC. Under conditions of limited microtubule growth it is expected that deletion of *ase1p* should speed up spindle elongation. Deletion of *ase1p* under MBC conditions however causes spindle disassembly. Deletion of *ase1p* in cells lacking *klp5Δ* causes a very small increase in spindle elongation rate (GFP-tub *ase1Δ klp5Δ* = 0.55 ± 0.05 (SE) $\mu\text{m}/\text{min}$, N=19; GFP-tub *klp5Δ* = 0.48 ± 0.03 (SE) $\mu\text{m}/\text{min}$, N=16). Further studies are required to find additional proof.

The role of clasp (cls1p)

The cls1p/ase1p module is essential for a stable and constant midzone. Cls1p initiates microtubule rescues at the midzone, and lack of a central cls1p zone causes microtubules to shrink past the central region of the spindle all the way to the SPB where new nucleation can occur. Counterintuitively, cls1p is an essential protein, whereas ase1, the protein that is targeted by cls1p, is not. In absence of ase1, cls1p localisation is however homogenously over the spindle [5]. Our results suggest that this diffuse pool of cls1p is able to generate sufficient rescues to create long microtubules. Without cls1p, microtubule length is solely determined by the high rate of klp5p/klp6p-induced catastrophes. Consequently, microtubules may remain too short to elongate a spindle. In agreement, the use of temperature sensitive cls1-mutant demonstrated that spindles disassemble in absence of functional clsp1 [5]. Interestingly, this phenotype is comparable to cells lacking ase1p in presence of MBC (Figure 4.4 C). Possibly, the diffuse pool of cls1p is not able to generate sufficient rescues in presence of MBC. When ase1p is around, cls1p is concentrated at the midzone and is able to prevent microtubule depolymerisation. The essential function of clsp1 for the midzone formation holds for fission yeast but in human cells clasp proteins are not essential. Here, the stabilization of microtubules in the midzone is likely taken over by kinesin-4 proteins that are recruited by the ase1p homologue PRC1 [48-50]. Fission yeast has no homologues of the kinesin-4 family. Possibly, the cls1p/ase1p module works well in fission yeast because there is only a single region of microtubule overlap organized. Higher eukaryotes have multiple regions of overlap whose position needs to be coordinated amongst each other.

Role of the midzone in coordinating elongation and mitotic exit

In mammalian cells midzones are proposed to play a role in regulating the contraction of the cell cortex for cytokinesis. The ability of a cell to organize a well-defined midzone may be crucial to orchestrate this process. Likewise, midzone-like regions of microtubule overlap in phragmoplasts of plants were proposed to aid in recruitment of cell wall material to build a new cell wall in the cell centre [51]. Here the spatial organization of microtubule overlaps may need to be well regulated to pattern a straight cell wall. The role of the midzone in fission yeast is less clear. Cells without ase1p do not form a midzone, and premature disassembly of short spindles was observed as a result of spindle breakage. Our results on cells lacking both ase1p and the catastrophe factor klp5 Δ show that breakage can be largely prevented by stimulating microtubule growth. A well-organized midzone may thus not be required for spindle elongation. Cells lacking a well-organized midzone (klp5 Δ , ase1 Δ , and ase1 Δ klp5 Δ) do however show a cytokinesis defect in which cytokinesis commences before spindles are disassembled. The midzone may thus synchronize spindle breakdown and cytokinesis. Timing of cytokinesis involves signalling between midzone localized chromosomal passenger proteins and proteins localized at the spindle pole bodies [52]. How the functioning of

this biochemical network relies on proper midzone organization remains to be investigated.

4.4. Material and Methods

Generation of strains

Standard fission yeast techniques were used for gene tagging or gene deletion. All cell lines used for the experiments are listed in Table 4. 1. Some strains were kindly provided by P. Tran (University of Pennsylvania, US & Institute Curie, France) and F.Chang (Columbia University, US). The identities of all strains were confirmed by PCR. Recipes for media and culturing the yeast cells are described in [53].

Table 4. 1 Fission yeast strains used for the experiments

Nr	Strain	Figure	note
JT.54	ura4-294::promoter ase1-GFP-ase1-nmt1 stop ase1Δ::KanMX6	h+	[30, 37]
JT.55	leu1-32::pSV-40-GFP-atb2(leu+)	h-	[5]
JT.60	ase1-mcherry: NatMX leu1-32::pSV-40-GFP- atb2(leu+)	h+	This study; [5]
JT.151	leu1-32::pSV-40-GFP-atb2(leu+) ase1Δ::KanMX6	h-	This study, [5, 30]
JT.157	leu1-32::pSV-40-GFP-atb2(leu+)ade6-leu1- 32 ura4-d18 ase1-ΔEEYY(Cap-Gly)	h-	This study, [5]
JT.173	nmt1-GFP-mal3::KanMX6 klp5Δ:: ura4-294	h-	This study, [54]
JT.194	ura4-294::promoter ase1-GFP-ase1-nmt1 stop	h+	This study, [30]
JT.198	ura4-294::promoter ase1-GFP-ase1-nmt1 stop ase1Δ::KanMX6 pkl1Δ ::his klp2Δ ::ura	h-	This study, [30, 55, 56]
JT.198	nmt1-GFP-mal3::KanMX6 ase1Δ::KanMX6	h+	This study, [57]
JT.201	ura4-294::promoter ase1-GFP-ase1-nmt1 stop ase1Δ::KanMX6 klp5Δ:: ura4-294	h-	This study, [30, 54]
JT.206	ura4-294::promoter ase1-GFP-ase1-nmt1 stop ase1Δ::KanMX6 klp9Δ:: KanMX6	h+	This study, [4, 30]
JT.208	leu1-32::pSV-40-GFP-atb2(leu+) ase1Δ::KanMX6 klp5Δ:: ura4-294		This study [5,20]
JT.209	leu1-32::pSV-40-GFP-atb2(leu+)klp5Δ:: ura4-294		This study [5,20]
PT.306	Ase1::GFP-KanMX6	h+	[30]
PT.602	nmt1-GFP-mal3::KanMX6	h-	[54]

Cell Culture

Before imaging, the fission yeast cells were grown in YE5S media at 30°C overnight. Cells expressing genes under the nmt-promoter were cultured in EMM5S media with 15 mg/ml thiamine (Sigma).

MBC-experiments

MBC (25 µg/ml in DMSO, Sigma) experiments were carried out similar as described previously [58], but cells were just incubated in EMM5S media with concavelin A (10 mg/ml sigma) for 15 min and added to the cell flow. After another 5 min incubation, remaining cells in the bulk were washed out. MBC was added shortly before imaging started.

Microscopy

Fission yeast cells were imaged on thin EMM agar pads as described [59] or in the flow cells [58]. Imaging was always done at 25°C and performed as described in chapter two.

Imaging analyses

Images and kymographs are compiled from maximum intensity projections of 10 confocal planes spaced 0.5 µm apart. Spindle elongation rates were measured for elongation from 5 to 7 µm and spindle midzone length were measured at spindle length of 6 µm. For MBC experiments, only cells were analysed for which MBC was added before anaphase commenced and imaging was started within 1 min after MBC addition.

Acknowledgements

We thank F. Chang, and P. Tran for strains. Henk Kieft and Lieuwe Biewenga for support in the Lab. The work of JT is part of the research programme of the “Stichting voor Fundamenteel Onderzoek der Materie (FOM)”, which is financially supported by the “Nederlandse Organisatie voor Wetenschappelijk Onderzoek (NWO)”. MEJ was supported by NWO-middel groot.

References

1. Goshima, G. and J.M. Scholey, *Control of Mitotic Spindle Length*. Annual Review of Cell and Developmental Biology, 2010. **26**(1): p. 21-57.
2. McCollum, D., *Cytokinesis: The Central Spindle Takes Center Stage*. Current Biology, 2004. **14**(22): p. R953-R955.
3. Schuyler, S.C., J.Y. Liu, and D. Pellman, *The molecular function of Ase1p: evidence for a MAP-dependent midzone-specific spindle matrix*. The Journal of Cell Biology, 2003. **160**(4): p. 517-528.
4. Fu, C., et al., *Phospho-Regulated Interaction between Kinesin-6 Klp9p and Microtubule Bundler Ase1p Promotes Spindle Elongation*. Developmental Cell, 2009. **17**(2): p. 257-267.
5. Bratman, S.V. and F. Chang, *Stabilization of Overlapping Microtubules by Fission Yeast CLASP*. Developmental Cell, 2007. **13**(6): p. 812-827.
6. Gruneberg, U., et al., *KIF14 and citron kinase act together to promote efficient cytokinesis*. The Journal of Cell Biology, 2006. **172**(3): p. 363-372.
7. Zhu, C. and W. Jiang, *Cell cycle-dependent translocation of PRC1 on the spindle by Kif4 is essential for midzone formation and cytokinesis*. Proceedings of the National Academy of Sciences of the United States of America, 2005. **102**(2): p. 343-348.
8. Khmelinskii, A., et al., *Cdc14-regulated midzone assembly controls anaphase B*. The Journal of Cell Biology, 2007. **177**(6): p. 981-993.
9. Tanenbaum, M.E., et al., *Dynein, Lis1 and CLIP - 170 counteract Eg5 - dependent centrosome separation during bipolar spindle assembly*. The EMBO Journal, 2008. **27**(24): p. 3235-3245.
10. Tanenbaum, M.E., et al., *Kif15 Cooperates with Eg5 to Promote Bipolar Spindle Assembly*. Current Biology, 2009. **19**(20): p. 1703-1711.
11. Tanenbaum, M.E. and R.H. Medema, *Mechanisms of Centrosome Separation and Bipolar Spindle Assembly*. Developmental Cell, 2010. **19**(6): p. 797-806.
12. Tanenbaum, M.E., et al., *Cytoplasmic dynein crosslinks and slides anti-parallel microtubules using its two motor domains*. eLife, 2013. **2**.
13. Gönczy, P., et al., *Cytoplasmic Dynein Is Required for Distinct Aspects of Mtoc Positioning, Including Centrosome Separation, in the One Cell Stage Caenorhabditis elegans Embryo*. The Journal of Cell Biology, 1999. **147**(1): p. 135-150.

14. Sharp, D.J., G.C. Rogers, and J.M. Scholey, *Microtubule motors in mitosis*. 2000. **407**(6800): p. 41-47.
15. Ferenz, N.P., et al., *Dynein Antagonizes Eg5 by Crosslinking and Sliding Antiparallel Microtubules*. *Current Biology*, 2009. **19**(21): p. 1833-1838.
16. Mitchison, T.J., et al., *Roles of Polymerization Dynamics, Opposed Motors, and a Tensile Element in Governing the Length of Xenopus Extract Meiotic Spindles*. *Molecular Biology of the Cell*, 2005. **16**(6): p. 3064-3076.
17. Mountain, V., et al., *The Kinesin-Related Protein, Hset, Opposes the Activity of Eg5 and Cross-Links Microtubules in the Mammalian Mitotic Spindle*. *The Journal of Cell Biology*, 1999. **147**(2): p. 351-366.
18. Nédélec, F., *Computer simulations reveal motor properties generating stable antiparallel microtubule interactions*. *The Journal of Cell Biology*, 2002. **158**(6): p. 1005-1015.
19. Hentrich, C. and T. Surrey, *Microtubule organization by the antagonistic mitotic motors kinesin-5 and kinesin-14*. *The Journal of Cell Biology*, 2010. **189**(3): p. 465-480.
20. Tao, L., et al., *A Homotetrameric Kinesin-5, KLP61F, Bundles Microtubules and Antagonizes Ncd in Motility Assays*. *Current Biology*, 2006. **16**(23): p. 2293-2302.
21. Huang, B. and T.C. Huffaker, *Dynamic microtubules are essential for efficient chromosome capture and biorientation in S. cerevisiae*. *The Journal of Cell Biology*, 2006. **175**(1): p. 17-23.
22. Tanaka, K., et al., *Molecular mechanisms of kinetochore capture by spindle microtubules*. 2005. **434**(7036): p. 987-994.
23. Kline-Smith, S.L. and C.E. Walczak, *Mitotic Spindle Assembly and Chromosome Segregation: Refocusing on Microtubule Dynamics*. *Molecular Cell*, 2004. **15**(3): p. 317-327.
24. Mallavarapu, A., K. Sawin, and T. Mitchison, *A switch in microtubule dynamics at the onset of anaphase B in the mitotic spindle of Schizosaccharomyces pombe*. *Current Biology*, 1999. **9**(23): p. 1423-1428.
25. Fridman, V., et al., *Midzone organization restricts interpolar microtubule plus - end dynamics during spindle elongation*, ed. V. Fridman, et al. Vol. 10. 2009. 387-393.

26. Khmelinskii, A. and E. Schiebel, *Assembling the spindle midzone in the right place at the right time*. *cc*, 2008. **7**(3): p. 283-286.
27. Zhu, C., et al., *Spatiotemporal control of spindle midzone formation by PRC1 in human cells*. *Proceedings of the National Academy of Sciences*, 2006. **103**(16): p. 6196-6201.
28. Khodjakov, A., S. La Terra, and F. Chang, *Laser Microsurgery in Fission Yeast: Role of the Mitotic Spindle Midzone in Anaphase B*. *Current Biology*, 2004. **14**(15): p. 1330-1340.
29. Oliferenko, S. and M.K. Balasubramanian, *Astral microtubules monitor metaphase spindle alignment in fission yeast*. 2002. **4**(10): p. 816-820.
30. Loïodice, I., et al., *Ase1p Organizes Antiparallel Microtubule Arrays during Interphase and Mitosis in Fission Yeast*. *Molecular Biology of the Cell*, 2005. **16**(4): p. 1756-1768.
31. Yamamoto, A., et al., *A Cytoplasmic Dynein Heavy Chain Is Required for Oscillatory Nuclear Movement of Meiotic Prophase and Efficient Meiotic Recombination in Fission Yeast*. *The Journal of Cell Biology*, 1999. **145**(6): p. 1233-1250.
32. Ding, R., K.L. McDonald, and J.R. McIntosh, *Three-dimensional reconstruction and analysis of mitotic spindles from the yeast, Schizosaccharomyces pombe*. *The Journal of Cell Biology*, 1993. **120**(1): p. 141-151.
33. Salaycik, K.J., et al., *Quantification of microtubule nucleation, growth and dynamics in wound-edge cells*. *Journal of Cell Science*, 2005. **118**(18): p. 4113-4122.
34. Stepanova, T., et al., *Visualization of Microtubule Growth in Cultured Neurons via the Use of EB3-GFP (End-Binding Protein 3-Green Fluorescent Protein)*. *The Journal of Neuroscience*, 2003. **23**(7): p. 2655-2664.
35. Sagolla, M.J., S. Uzawa, and W.Z. Cande, *Individual microtubule dynamics contribute to the function of mitotic and cytoplasmic arrays in fission yeast*. *Journal of Cell Science*, 2003. **116**(24): p. 4891-4903.
36. Tischer, C., D. Brunner, and M. Dogterom, *Force- and kinesin-8-dependent effects in the spatial regulation of fission yeast microtubule dynamics*. 2009. **5**.
37. Janson, M.E., et al., *Crosslinkers and Motors Organize Dynamic Microtubules to Form Stable Bipolar Arrays in Fission Yeast*. *Cell*, 2007. **128**(2): p. 357-368.

38. Garcia, M.A., N. Koonrugsa, and T. Toda, *Two Kinesin-like Kin I Family Proteins in Fission Yeast Regulate the Establishment of Metaphase and the Onset of Anaphase A*. *Current Biology*, 2002. **12**(8): p. 610-621.
39. Sharp, D.J., et al., *Antagonistic microtubule-sliding motors position mitotic centrosomes in Drosophila early embryos*. 1999. **1**(1): p. 51-54.
40. Yamashita, A., et al., *The Roles of Fission Yeast Ase1 in Mitotic Cell Division, Meiotic Nuclear Oscillation, and Cytokinesis Checkpoint Signaling*. *Molecular Biology of the Cell*, 2005. **16**(3): p. 1378-1395.
41. Kapitein, L.C., et al., *The bipolar mitotic kinesin Eg5 moves on both microtubules that it crosslinks*. 2005. **435**(7038): p. 114-118.
42. Goshima, G. and R.D. Vale, *The roles of microtubule-based motor proteins in mitosis: comprehensive RNAi analysis in the Drosophila S2 cell line*. *The Journal of Cell Biology*, 2003. **162**(6): p. 1003-1016.
43. Grishchuk, E.L. and J.R. McIntosh, *Microtubule depolymerization can drive poleward chromosome motion in fission yeast*. *The EMBO Journal*, 2006. **25**(20): p. 4888-4896.
44. Roostalu, J., et al., *Directional Switching of the Kinesin Cin8 Through Motor Coupling*. *Science*, 2011. **332**(6025): p. 94-99.
45. Braun, M., et al., *Adaptive braking by Ase1 prevents overlapping microtubules from sliding completely apart*. 2011. **13**(10): p. 1259-1264.
46. Lansky, Z., et al., *Diffusible crosslinkers generate directed forces in microtubule networks*. 2014.
47. Subramanian, R., et al., *Insights into Antiparallel Microtubule Crosslinking by PRC1, a Conserved Nonmotor Microtubule Binding Protein*. *Cell*, 2010. **142**(3): p. 433-443.
48. Bieling, P., I.A. Telley, and T. Surrey, *A Minimal Midzone Protein Module Controls Formation and Length of Antiparallel Microtubule Overlaps*. *Cell*, 2010. **142**(3): p. 420-432.
49. Hu, C.-K., et al., *KIF4 Regulates Midzone Length during Cytokinesis*. *Current biology : CB*, 2011. **21**(10): p. 815-824.
50. Kurasawa, Y., et al., *Essential roles of KIF4 and its binding partner PRC1 in organized central spindle midzone formation*. *The EMBO Journal*, 2004. **23**(16): p. 3237-3248.

51. de Keijzer, J., B.M. Mulder, and M.E. Janson, *Microtubule networks for plant cell division*. 2014: p. 1-8.
52. Rozelle, D.K., S.D. Hansen, and K.B. Kaplan, *Chromosome passenger complexes control anaphase duration and spindle elongation via a kinesin-5 brake*. *The Journal of Cell Biology*, 2011. **193**(2): p. 285-294.
53. Sanger. http://www.sanger.ac.uk/PostGenomics/S_pombe/links.shtml#pombe).
54. Busch, K.E. and D. Brunner, *The Microtubule Plus End-Tracking Proteins mal3p and tip1p Cooperate for Cell-End Targeting of Interphase Microtubules*. *Current Biology*, 2004. **14**(7): p. 548-559.
55. Pidoux, A.L., M. LeDizet, and W.Z. Cande, *Fission yeast pkl1 is a kinesin-related protein involved in mitotic spindle function*. *Molecular Biology of the Cell*, 1996. **7**(10): p. 1639-1655.
56. Troxell, C.L., et al., *pkl1 +andklp2 +: Two Kinesins of the Kar3 Subfamily in Fission Yeast Perform Different Functions in Both Mitosis and Meiosis*. *Molecular Biology of the Cell*, 2001. **12**(11): p. 3476-3488.
57. West, R.R., T. Malmstrom, and J.R. McIntosh, *Kinesins klp5+ and klp6+ are required for normal chromosome movement in mitosis*. *Journal of Cell Science*, 2002. **115**(5): p. 931-940.
58. Janson, M.E., et al., *Efficient formation of bipolar microtubule bundles requires microtubule-bound γ -tubulin complexes*. *The Journal of Cell Biology*, 2005. **169**(2): p. 297-308.
59. Tran, P.T., A. Paoletti, and F. Chang, *Imaging green fluorescent protein fusions in living fission yeast cells*. *Methods*, 2004. **33**(3): p. 220-225.

General discussion and future research directions

Juliane Teapal

Chapter

5

Abstract

In this thesis, *S. pombe* was used as a model system to investigate mechanisms for microtubule based pattern generation. We revealed how dynamic microtubules can set a length scale that is required for nuclear dispersion. Further, we showed how molecular motors can trigger reorganisation of nuclei. In this chapter, thus I will discuss how cytoskeletal filaments and their associated proteins in general may induce switches in organelle organisation. Next I will debate which requirements are needed to actively control nuclear dispersion over larger distances. In chapter 4 we focused on the regulation of spindle midzone length. Here, I will discuss possible mechanisms for the stability and the positioning of the midzone. To understand the role of *ase1p*, we examined the turnover *in vitro* with FRAP (Fluorescence Recovery After Photobleaching)-experiments and reveal a dependency on the number of microtubules in the bundle for the recovery time. We take these results into account to discuss the role of *ase1p* in the spindle overall.

5.1. Organelle patterns in eukaryotes

In chapter two and three we revealed a mechanism that disperses multiple nuclei throughout the cell. The length scale is set by microtubule dynamics, which causes microtubules to generate repulsive forces by impinging into neighboring nuclei. Yet, in the presence of the minus-end directed motor klp2p attractive forces dominate, resulting in the formation of a cluster of nuclei in the cell center. Up- and down regulation of klp2p is used in single nucleated fission yeast to control nuclear positions during mitosis and meiosis [1, 2]. Whereas during mitosis the SIN pathway deactivates klp2p to prevent nuclear congression [1], in meiosis klp2p is required for nuclei fusion to form diploid nuclei [2]. More often organelle and organelle-like structures require a switch from clustering to dispersion to change cellular functions. Even though the exact mechanisms are often poorly understood, the involvement of the cytoskeleton (especially microtubules and actin filaments) and its associated proteins has been shown [5-7]. For example, the development of muscle tissues requires spatial nuclear reorganization. Upon the fusion of single nucleated myoblasts to myotubes the microtubule network rearranges from an astral network to an antiparallel network [8]. Melanophores are cells which contain pigment and light reflecting organelles. These organelles are either aggregated or homogeneously dispersed through the cytoplasm. The configurations are hormone dependent and allow animals to display color change. In this case a combination of microtubules and actin filament with their associated motors are involved. The dispersion requires the microtubule plus-end directed motor kinesin-2 and the actin motor myosin-V, while the aggregation is powered by the minus-end directed motors dynein [9]. Localization of the motors at the membrane of the organelles allows the switch of the configuration and thus facilitates transport along the cytoskeleton.

Also actin filaments alone are involved in organelle positioning, i.e. chloroplast localization. The light-induced reorganization of the chloroplasts for optimizing photosynthetic light absorption in higher plants and algae is actin dependent. Up- and down regulation of a minus-end directed motor like myosin might induce this regulation. Indeed two kinesin-like proteins mediate chloroplast movement, and *in vitro* their interaction with actin filaments is shown [10]. Also, dispersion of mitochondria in protoplasts is actin dependent to ensure unbiased inheritance during cell division [11]. In *C. elegans* and *Drosophila* SUN-KASH proteins anchor the nucleus to the surrounding actin filaments or support the centrosome connection to the nucleus during pronuclear migration [12]. Interestingly, KASH proteins are in addition suggested to support the formation of an actin-like basket around the nucleus. Various cell types obtain these structures (insect cells, amoeba and fungi) [13]. The formation of actin-baskets around nuclei could generate a steric hindrance between interdigitating actin networks, thus disperse nuclei and also other organelles throughout the cell.

Interestingly, similar to what we revealed in multinucleated fission yeast cells, organelle patterns can be obtained through cytoskeletal filaments, but often require the support of associated proteins. The functions of these proteins, however, may be very diverse (e.g. bundling, sliding, and coupling) and to understand the overall mechanisms further research is necessary.

5.2. Organelle dispersion based on repulsive forces

Nuclear dispersion in fission yeast is based on forces generated by dynamically unstable microtubules in between neighbouring nuclei. As revealed in chapter 2 multinucleated fission yeast cells have a linear microtubule network in between the nuclei. A similar network is observed in myotubes; microtubules are connected to the nucleus and form an interdigitating network of antiparallel microtubules. However, the internuclear distances are larger as in the multinucleated fission yeast cells and the question remains if microtubule dynamics are sufficient to disperse the nuclei. Microtubule dynamics differs for each cell type, but in general the average microtubule length increases with cell size [15, 16, 17]. In muscle cells the microtubule plus-end protein EB1 stabilizes microtubules [14] and this control of microtubule dynamics might be sufficient enough to generate the required microtubule length for nuclear dispersion. Nonetheless, *in vitro* studies showed longer microtubules tend to buckle more and generate smaller compressive forces [15]. Yet, investigation of cytoplasmic microtubules in single nucleated cardiac myocytes and kidney cells revealed strong curvatures that suggest high compression forces. Furthermore, neighbouring microtubules tend to have the same curvature pattern, indicating a mechanical coupling by a surrounding elastic network of actin and intermediary filaments [16]. Multinucleated myotubes have a distinct actin network co-localising with the microtubules, which could indeed mechanically support microtubules [17]. Hence, a long microtubule could withstand higher forces before buckling and generate sufficient forces to disperse nuclei over a larger length scale [18]. However, the generated forces might still not be sufficient and additional mechanisms may be required to control nuclear dispersion over larger length scales.

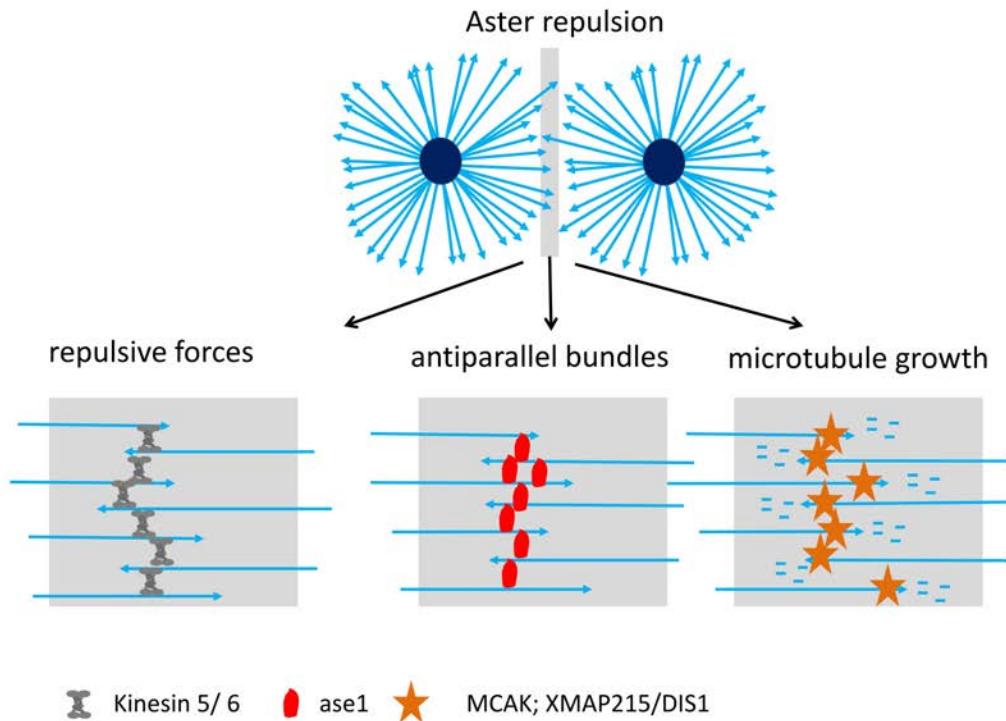


Figure 5.1: Possible mechanism to control microtubule aster repulsion

Repulsion of microtubule asters is required for positioning. Microtubules of neighbouring asters generate antiparallel overlaps. Spatial coordination of molecular motors and microtubule associated proteins might be essential for the repulsion of the asters. Plus-end directed motors of the kinesin 5 or 6 families can induce sliding of antiparallel microtubules and generate the distance to keep asters apart. The crosslinker ase1 bundles antiparallel microtubules, but also recruits essential motors to the spindle midzone required for spindle elongation. Further microtubule growth into the opposite aster should be regulated.

For larger systems it has been proposed that plus-end directed motors generate forces to keep microtubule asters apart from each other, very much similar to how forces are generated in the midzone of anaphase B spindles [19]. However, it is not clear how these forces would depend on the inter-aster spacing. In chapter 2 and 3 we showed that for multinucleated fission yeast cells it is essential that repulsion forces decay with length. It is not clear yet, how this works when microtubules form a stable midzone, in which microtubules ends are stabilized against catastrophes. These midzones may generate forces independent of spindle length. Asters might repel each other just because they interdigitate and microtubules from opposing poles cause steric interactions (Figure 5.1, [20]). These forces will increase when you push the asters together just like when you

would push two sea urchins against each other. In addition, the increased amount of interdigitation when asters are moved together will allow plus-end motors to generate more bipolar connections between microtubules for force generation. Ase1p could play a role in organizing these bipolar contacts with binding to bipolar microtubules that are best positioned to push asters away. Ase1p may then recruit molecular motors to these sites, which are required to generate the repulsive forces, as suggested by reported interactions between kinesin-5 (Cin8) [21] and kinesin-6 (MKLP1/kif23) [22] with ase1 family members. Ase1p and plus-end motors may thus form a two-component module that together forms force-generating overlaps. Such a system will prevent motors from engaging in inefficient force generation between parallel microtubules or microtubules from two asters that cross under large angles. It has been shown for Eg5p [23] that crosslinking motors on their own will engage in such interactions. For such a mechanism to work, it will also be important to limit the extent of the microtubule asters by regulating dynamic instability. The length scale of the microtubules should be on the order of the desired inter-aster spacing.

In that case microtubule growth of the asters has to be actively controlled and good candidates would be the microtubule depolymerizer MCAK [24, 25] and the polymerizer family XMAP215/Dis1 [26, 27]. Opposite to Kif4, which forms a complex with PRC1 and only controls microtubule dynamics in bundles, the function and localisation of MCAK and XMAP215 are independent of the PRC1/MAP65/ase1 family. Most of the XMAP215/Dis1 [28-30] and MCAK [31, 32] are plus-end tracking proteins and dynamics of single microtubules can be regulated.

The combination of plus-end directed motors and controlled microtubule dynamics ensues that the amount of force-generating overlaps are a function of the inter aster distance. To further understand the positioning of the asters, localisation of the PRC1/MAP65/ase1 family with possible candidates of plus-end directed motors should be investigated first. Additionally, motors and MAPs (microtubule associated proteins) should be perturbed to invest the changes in inter-aster distances.

We tried to express a plus-end directed motor in tetranucleated fission yeast cells to investigate whether the dynamics of nuclear positioning would change. The additional expression of the plus-end directed motor may increase the dynamics of nuclear repositioning after pattern perturbation, but also stabilize the position of each nucleus leading to less nuclear oscillations. Fission yeast cells have two plus-end directed motors, the kinesin-6 klp9p and the kinesin-5 cut7p [33, 34]; both molecular motors are only expressed during mitosis. As cut7p is an essential motor, we used the ELM-server to identify the possible nuclear localisation signal (NLS) of klp9p. We expressed GFP-klp9 Δ NLS in fission yeast cells lacking the endogenous klp9p. Unfortunately, klp9 Δ NLS was still only expressed in the nucleus and also extended removal of the sequences around the NLS-motif did not lead to expression of klp9p during interphase. It would

have been interesting to see how the internuclear distances would adjust. We would expect that in presence of a plus-end directed motor the internuclear distance between nuclei increases. The distance between outer nuclei and the cell tips would decrease, as the unidirectional microtubule growth towards the cell membrane would not lead motor activity. In that case the dispersion of the nuclei might be not equidistant anymore.

All these experiments would help to understand how organelle dispersion can actively be controlled over larger distances, where microtubule dynamics alone might not be sufficient and motors play additional roles.

5.3. Regulation of the spindle midzone

Stability control of the spindle midzone

In chapter 4 we investigated mechanisms which control the midzone length of the mitotic spindle. Perturbation of the microtubule dynamics revealed that the length of the spindle midzone was remarkably resistant to those changes. This raised the question which mechanisms are responsible to maintain spindle integrity and elongation.

Experiments where the overlap length is reduced either by microtubule growth perturbation (MBC experiments, Figure 4.3 C) or by microtubule sliding [35] show that ase1p becomes compacted and does not leave the overlap. Ase1p has a higher affinity to antiparallel overlaps than to single microtubules [36]. Additionally, sliding of microtubules forms a barrier to ase1p, similar as described for dam1p, which tracks along the depolymerizing ends of microtubules [37]. The sweeping at the microtubule ends thus compacts ase1p in shortening overlaps and acts as a diffusion barrier, preventing microtubule to slide apart [35]. The experiments were carried out with a minus-end directed motor; however the sweeping mechanism should be independent from the direction of the motor. Thus, the midzone stability could be controlled by the diffusion barrier build-up of the ase1p sweeping. In that case the diffusion barrier restricts microtubule sliding by plus-end directed motors and the midzone remains stable.

Follow up *in vitro* experiments (unpublished data [36]) revealed that ase1p cannot just act as a diffusion barrier, but that it is actually able to induce sliding by itself. Ase1p was confined in an overlap of antiparallel microtubules with the help of molecular motors. In absence of the molecular motors, ase1p expands and these expansion forces are strong enough to induce microtubule sliding.

It has been shown before [38] that lateral steric confinement of proteins can generate forces, in that case to induce spontaneous formation of lipids and tubules, which are

required for polarizing of membranes. Here, the energy required to deform the membrane could be based on the expansion forces of the spatially confined proteins [38]. As described in [36] (unpublished data) the amount of generated forces is entirely determined by the entropy of ase1p, when the number of ase1p in the overlap remains constant. FRAP experiments of ase1p at the spindle midzone revealed a very low recovery rate, indicating that the exchange of ase1 is low [39]. Therefore ase1p could not just act as a diffusion barrier but also generate sliding forces to antagonize forces generated by plus-end directed motors. However, the force measurements by optical trapping were in the range of 1pN, most likely not sufficient to counter forces of a plus-end directed motor of several pN (reviewed in [40], [41]).

A closer look at the protein structure of ase1p revealed different motifs leading to different functions [4, 42, 43]. In absence of the C-terminus microtubule bundling is disrupted and even spindle disassemble is observed [4, 42]. Interestingly, in fission yeast the C-terminus contains the EEY/F domain [44] that is proposed to function in binding CAPGLY proteins. Pombe has two CAPGLY ssm4p and tip1p, both reported to be absent from the spindle [45]. In absence of tip1, however, cells show a delay in metaphase and exhibit a high percentage of lagging chromosomes but the spindle elongation rate is indistinguishable from the wild type [46]. This raises the question what the possible function of the EEY/F domain could be, as the domain is not evolutionarily conserved. In all other proteins of the PCR1/MAP65/ase1 family the motif is absent. Interestingly, we find a disorganized zone of interdigitation and a spindle breakage phenotype as strong as for the ase1 Δ phenotype in absence of the EEY/F domain (Figure 5.2). This indicates a cell's attempt to uncouple regulatory functions and bundling functions. Previously, a 67 AA truncation of clasp by [4] was shown to decouple roles in bundling and microtubule stabilization. Further, experiments on the molecular structure might give insights into protein interactions required for a stable midzone.

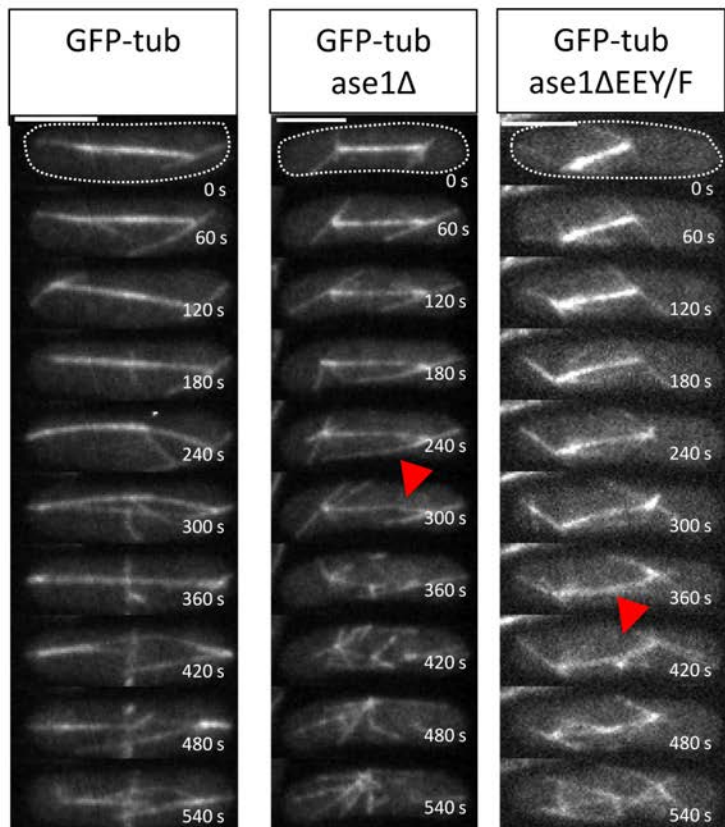


Figure 5.2: EEY/F motif of *ase1* stabilises the spindle midzone

Time series of z-projections ($10 \times 0.5 \mu\text{m}$) of cells expressing GFP-tubulin. For each mutant a cell with a clear phenotype was chosen. Red arrow head indicates spindle collapse. Experimental set up: Standard fission yeast technologies were used for gene tagging and deletion [3]. The GFP-tub strain was kindly provided by [4]. Imaging was performed as described in chapter 2.

Next, we analysed whether antagonizing forces generated by minus-end directed motors control midzone stability. The co-depletion of the minus-end directed motor *klp2p* and *pkl1p* did decrease the length slightly, albeit it again remained constant during spindle elongation. However, fission yeast has three minus-end directed motors. Next to *klp2p* and *pkl1p*, also dynein is expressed during mitosis and might as well contribute to antagonizing forces generation. So far no significant differences in spindle positioning, orientation or elongation kinetics were detected in absence of dynein [47-49] and even the triple-deletion of all three minus-end directed motors in fission yeast grows well [50]. However in various organisms it has been shown that the function of dynein is essential for spindle elongation [51-54].

Therefore it is essential to analyse the spindle elongation velocity in the cells with triple-depletion of all three minus-end motors, when microtubule dynamics are perturbed. In that case one can investigate the function of minus-end directed motors when the midzone length is decreased in such a way that the spindle might collapse. At the 58th Annual Meeting of the Biophysical Society 2014, it was shown in budding yeast that dynein is transported by plus-end directed motors to the microtubule tips, similar as *tea2p* transports *tip1p* during interphase in fission yeast [55]. The mechanism in

budding yeast requires a protein from the tea2 family and a tip1 homologue. Moreover it has been shown *in vitro* that dynein can act as a brake when it is pulled towards the microtubule minus-end [56] and strong suggestions were made that dynein antagonizes the force of Eg5 in epithelial cells [51]. A possible control mechanism in fission yeast could be as follows: if microtubule growth is perturbed and spindle elongation by cut7p/klp9p continues, dynein at the plus-ends could be pulled to the minus-end and acts like a brake to prevent spindle collapse. But if microtubule growth is faster than the sliding of cut7p/klp9, dynein will be pulled to the plus-end no breaking mechanism is activated.

In vitro work of the kinesin-5 Cin8p showed, depending on the ionic strength, that this in general plus-end directed motor can switch its motility to minus-end directed [57, 58]. Under certain circumstances a switch could be initiated in cells and forces can be generated to prevent spindle disassembly during elongation.

Possibly a combination of active forces by minus-end directed motors and passive forces by ase1 contribute to generate antagonizing forces to ensure a constant stable spindle elongation.

Positioning of the spindle midzone

So far, our prime investigations were focussed on dissecting mechanisms that control the spindle midzone length, but we have not discussed how the midzone gets its central position. Disruption of the midzone leads to severe disruption of cytokinesis because the position controls the cleavage furrow in animal cells [59] and cell plate formation in plant cells [60]. In several organisms it has been shown that controlling microtubule dynamics during anaphase B is important for the midzone length regulation [61-63], which we confirmed for fission yeast in chapter 4. In multiple organisms the minus-ends of the microtubules are stabilized [64-66], indicating the importance of understanding microtubule dynamics at the plus-end. To ensure spindle elongation the microtubules polymerize at their plus-end and their dynamics are tightly controlled by the kinesin 4 member kif4p [61-63]. The kinesin-4 family is absent in fission yeast, instead the two component protein module of ase1p-clp1p is essential to generate rescues specifically at the midzone [4]. At the onset of anaphase ase1 binds to the interdigitating microtubules in the spindle middle and recruits clp1p to the midzone. In this way the clp1p prevents microtubules from having a catastrophe. How does this mechanism generate the positioning of the spindle midzone? Ase1p may seek a configuration in which the limited pool of ase1p can make the maximal number of associations with antiparallel overlaps. This is at the spindle centre, where microtubules nucleated from opposite SPBs interdigitate (Figure 5.3 A).

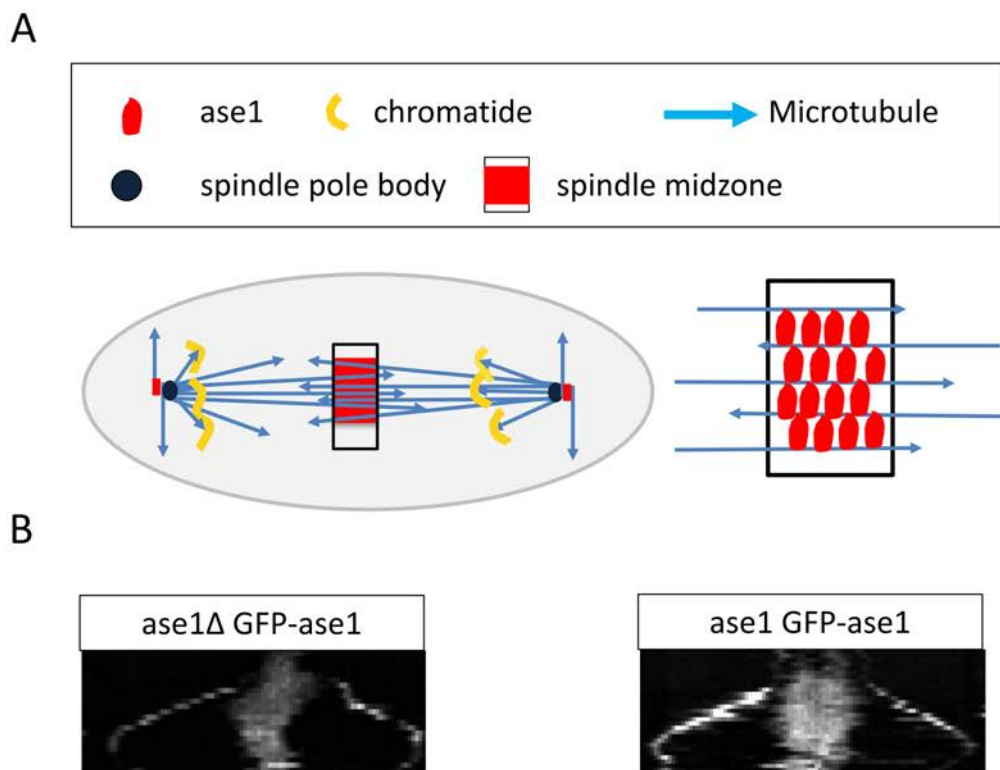


Figure 5.3: The crosslinker ase1 determines the size of the spindle midzone

(A) Left: Cartoon of an anaphase B spindle, where ase1p binds specifically to the spindle midzone, where the highest density of antiparallel microtubules is. Right: Zoom in on the spindle midzone. Ase1p stays within the spindle midzone, and does not associate with microtubules growing in an antiparallel manner out of the spindle midzone. (B) Left: Kymograph of fission yeast cell expressing GFP-ase1, but lacking the endogenous ase1. Right: Overexpression of ase1 in cells expressing the endogenous ase1 with an additional copy of GFP-ase1. The overexpression of ase1 leads to an increase of the spindle midzone length, suggesting a limited pool of ase1p in fission yeast cells.

In vitro work shows evidence for a mechanism of localized ase1p multimerization. The mechanism is concentration dependent, but interestingly the threshold decreases in microtubule overlaps [67]. The multimerization of ase1p thus limits the diffusion within the bundle and may explain the high affinity to antiparallel microtubules. Additionally, we investigated whether the midzone length depends on the amount of ase1p. We added an additional copy of GFP-ase1 to the endogenous ase1p. Overexpression increases the midzone length by approximately 20 % and demonstrates that it is likely that the limitation of the ase1 pool is important (Figure 5.3 B).

FRAP experiments of ase1p in mitotic spindles revealed a very low recovery rate, indicating that the exchange of ase1 is low, compared to exchange of ase1 during interphase [39], suggesting a mechanism that prevents fast dissociation of ase1p into solution. We set up experiments *in vitro* to study the ase1p recovery rate in antiparallel bundles using FRAP experiments. We generated antiparallel microtubule bundles with ase1-GFP and analysed the recovery rate as a function of the number of microtubules in the bundle. Ase1-GFP within bundles of two microtubules recovered much faster as ase1-GFP within bundles of three or four microtubules (Figure 5.4).

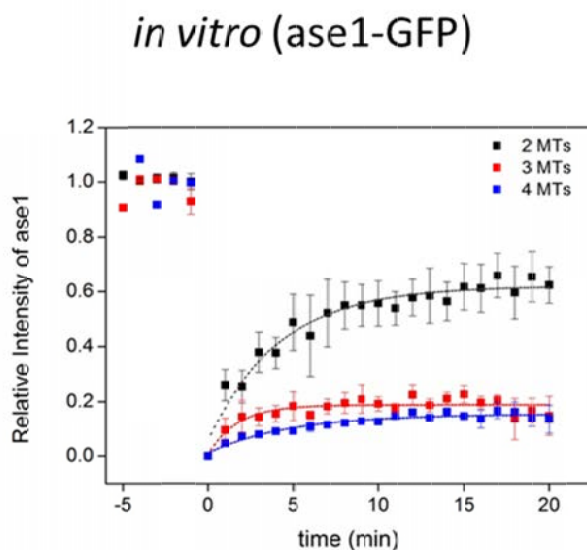


Figure 5.4: In vitro FRAP recovery rate of ase1p in microtubule bundles.

FRAP recovery of ase1-GFP as a function of microtubule numbers within a bundle. The number of microtubules was determined by measuring the intensity of rhodamin-labelled microtubules reduced by the background intensity. The average of normalized recovery curves (FRAP experiments for each bundle size $n > 10$) is plotted with the standard error. Experimental set up: For the *in vitro* experiments the flow chambers and rhodamin-labelled microtubules were prepared as previous described [68]. Ase1-GFP was purified as described in [69] and bundles obtaining multiple microtubules were generated by repeating the steps described in [36]. FRAP experiments were performed as described in [35], with one frame per minute as post-FRAP acquisition rate. Intensities are not corrected for bleaching.

Overall, this indicates a lower dissociation rate of ase1p in bundles containing more microtubules. Thus, rebinding of ase1p to a surrounding microtubule is more likely than dissociation into solution. Indeed FRAP experiments of ase1p along single microtubules *in vitro* revealed a higher dissociation rate compared to ase1 in bundles [35]. Whereas ase1p can dissociate from a single microtubule via one of its two heads, ase1 within a bundle has to dissociate with a two-steps mechanism (Figure 5.5 A and B).

First it will dissociate with one head and afterwards it can either rebind or dissociate into solution by unbinding the second head.

This indicates multistep kinetics for the dissociation of ase1p as previously reported by [70] for DNA binding proteins. Thus, we assume the dissociation rate of ase1 (K_{off}^D) into solution is defined by a multistep kinetic

$$K_{off}^D = K_{off}^{2 \rightarrow 1} * \left(\frac{K_{off}^{1 \rightarrow 0}}{K_{on}^{1 \rightarrow 2} + K_{off}^{1 \rightarrow 0}} \right)$$

Equation 1

With our experiments we measured the dissociation of the complete ase1p into solution. As we see a decrease in recovery of ase1p with increasing numbers of microtubules, it indicates that actually more ase1p molecules re-associate with the second head to a surrounding microtubule, than dissociate into solution. The probability of rebinding increases when more microtubules are within the bundle. The number of microtubules within a mitotic spindle is larger as in our experimental set ups (maximum number of microtubules = 4). This may lead to no dissociation of ase1p into solution (Figure 5.5 C). This means that the localisation of ase1p is set by the interaction of a larger number of microtubules that averages out the fluctuations of individual microtubules growing out of the spindle midzone. The centring ase1p is likely a collective effect that stems from the interaction with many microtubules. Therefore this may be an intrinsic accumulation of ase1p at the spindle centre that also limits the extension of cls1p accumulation.

To directly investigate the influence of the number of microtubules a simple model could be generated, as all models until now [33, 69] are using a constant K_{off}^D independent of the amount of microtubules in the bundle. This model could determine the possibility of rebinding of ase1p after one head is detached as a function of the binding possibilities given by the surrounding microtubules. In this manner, the role of immobilization of ase1p within the spindle and its possible functioning in centring the midzone can be better understood.

Overall ase1p is a key player for the localisation of the spindle midzone. Therefore we conclude three aspects of ase1p are essential: 1.) high affinity of ase1p for antiparallel microtubules, 2.) limited ase1p pool and 3.) the low dissociation rate into solution. How important each single parameter is needs still to be determined, where again a simple model would be of good help.

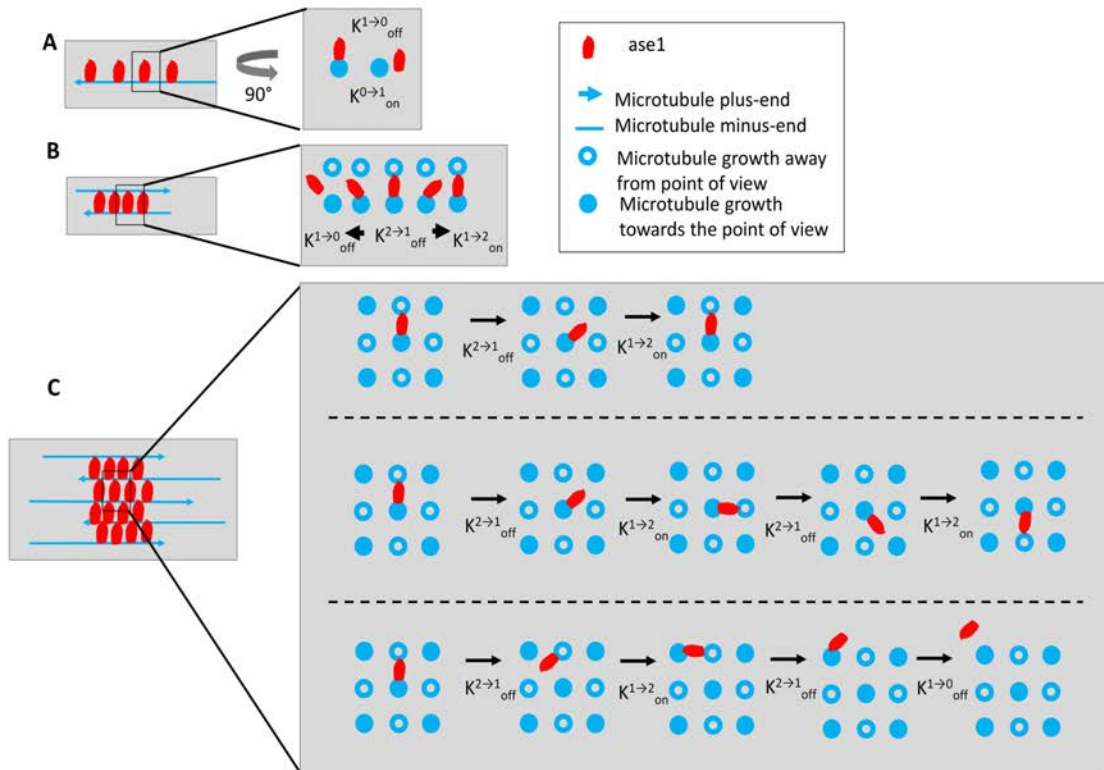


Figure 5.5: The dissociation of ase1 depends on the number of surrounding microtubules

Ase1p (for simplification shown as on molecule) can bind with one of its head to a single microtubule and its dissociation follows a simple one-step kinetics. Within antiparallel microtubule bundles both heads of ase1 are attached to the microtubules, in that case the dissociation follows a two-step kinetic. To picture the kinetics the microtubule bundles has been turned by 90°, so the ends of the microtubules are visible. **(A)** Association and dissociation of ase1 along a single microtubule. **(B)** Association and dissociation of ase1p to an overlap of antiparallel microtubules consisting out of two microtubules. Dissociation of ase1p into solution not only depends follows a two-step kinetic. **(C)** If ase1 is surrounded by a large number of microtubules the probability of ase1 to dissociate into solution is decreasing even further because rebinding in multiple configurations becomes possible.

References

1. Mana-Capelli, S., et al., *The kinesin-14 Klp2 is negatively regulated by the SIN for proper spindle elongation and telophase nuclear positioning*. *Molecular Biology of the Cell*, 2012. **23**(23): p. 4592-4600.
2. Troxell, C.L., et al., *pk11 +andklp2 +: Two Kinesins of the Kar3 Subfamily in Fission Yeast Perform Different Functions in Both Mitosis and Meiosis*. *Molecular Biology of the Cell*, 2001. **12**(11): p. 3476-3488.
3. Bähler, J., et al., *Heterologous modules for efficient and versatile PCR-based gene targeting in Schizosaccharomyces pombe*. *Yeast*, 1998. **14**(10): p. 943-951.
4. Bratman, S.V. and F. Chang, *Stabilization of Overlapping Microtubules by Fission Yeast CLASP*. *Developmental Cell*, 2007. **13**(6): p. 812-827.
5. Al-Mehdi, A.-B., et al., *Perinuclear Mitochondrial Clustering Creates an Oxidant-Rich Nuclear Domain Required for Hypoxia-Induced Transcription*. *Science Signaling*, 2012. **5**(231): p. ra47.
6. Metzger, T., et al., *MAP and kinesin-dependent nuclear positioning is required for skeletal muscle function*. 2012. **484**(7392): p. 120-124.
7. Staiger, C.J., et al., *Roles for Actin Filaments in Chloroplast Motility and Anchoring*, in *Actin: A Dynamic Framework for Multiple Plant Cell Functions*. 2000, Springer Netherlands. p. 203-212.
8. Tassin, A.M., B. Maro, and M. Bornens, *Fate of microtubule-organizing centers during myogenesis in vitro*. *The Journal of Cell Biology*, 1985. **100**(1): p. 35-46.
9. Levi, V., et al., *Organelle Transport along Microtubules in Xenopus Melanophores: Evidence for Cooperation between Multiple Motors*. *Biophysical Journal*, 2006. **90**(1): p. 318-327.
10. Suetsugu, N., et al., *Two kinesin-like proteins mediate actin-based chloroplast movement in Arabidopsis thaliana*. *Proceedings of the National Academy of Sciences*, 2010. **107**(19): p. 8860-8865.
11. Van Gestel, K., R.H. Köhler, and J.P. Verbelen, *Plant mitochondria move on F - actin, but their positioning in the cortical cytoplasm depends on both F - actin and microtubules*. *Journal of Experimental Botany*, 2002. **53**(369): p. 659-667.

12. Starr, D.A. and H.N. Fridolfsson, *Interactions Between Nuclei and the Cytoskeleton Are Mediated by SUN-KASH Nuclear-Envelope Bridges*. Annual Review of Cell and Developmental Biology, 2010. **26**(1): p. 421-444.
13. Munter, S., et al., *Actin polymerisation at the cytoplasmic face of eukaryotic nuclei*. BMC Cell Biology, 2006. **7**(1): p. 23.
14. Zhang, T., et al., *Microtubule plus-end binding protein EB1 is necessary for muscle cell differentiation, elongation and fusion*. Journal of Cell Science, 2009. **122**(9): p. 1401-1409.
15. Dogterom, M. and B. Yurke, *Measurement of the Force-Velocity Relation for Growing Microtubules*. Science, 1997. **278**(5339): p. 856-860.
16. Brangwynne, C.P., et al., *Microtubules can bear enhanced compressive loads in living cells because of lateral reinforcement*. The Journal of Cell Biology, 2006. **173**(5): p. 733-741.
17. McCarthy, A.M., et al., *Loss of cortical actin filaments in insulin-resistant skeletal muscle cells impairs GLUT4 vesicle trafficking and glucose transport*. American Journal of Physiology - Cell Physiology, 2006. **291**(5): p. C860-C868.
18. Guerin, C.M. and S.G. Kramer, *Cytoskeletal remodeling during Myotube assembly and guidance: Coordinating the actin and microtubule networks*. cib, 2009. **2**(5): p. 452-457.
19. Sharp, D.J., G.C. Rogers, and J.M. Scholey, *Microtubule motors in mitosis*. 2000. **407**(6800): p. 41-47.
20. Mitchison, T., et al., *Growth, interaction, and positioning of microtubule asters in extremely large vertebrate embryo cells*. Cytoskeleton, 2012. **69**(10): p. 738-750.
21. Khmelinskii, A., et al., *Phosphorylation-Dependent Protein Interactions at the Spindle Midzone Mediate Cell Cycle Regulation of Spindle Elongation*. Developmental Cell, 2009. **17**(2): p. 244-256.
22. Mishima, M., S. Kaitna, and M. Glotzer, *Central Spindle Assembly and Cytokinesis Require a Kinesin-like Protein/RhoGAP Complex with Microtubule Bundling Activity*. Developmental Cell, 2002. **2**(1): p. 41-54.
23. Kapitein, L.C., et al., *The bipolar mitotic kinesin Eg5 moves on both microtubules that it crosslinks*. 2005. **435**(7038): p. 114-118.
24. Desai, A., et al., *Kin I Kinesins Are Microtubule-Destabilizing Enzymes*. Cell. **96**(1): p. 69-78.

25. Hunter, A.W., et al., *The Kinesin-Related Protein MCAK Is a Microtubule Depolymerase that Forms an ATP-Hydrolyzing Complex at Microtubule Ends*. *Molecular Cell*, 2003. **11**(2): p. 445-457.
26. Brouhard, G.J., et al., *XMAP215 Is a Processive Microtubule Polymerase*. *Cell*, 2008. **132**(1): p. 79-88.
27. Zanic, M., et al., *Synergy between XMAP215 and EB1 increases microtubule growth rates to physiological levels*. 2013. **15**(6): p. 688-693.
28. Hestermann, A. and R. Graf, *The XMAP215-family protein DdCP224 is required for cortical interactions of microtubules*. *BMC Cell Biology*, 2004. **5**(1): p. 24.
29. Nakaseko, Y., et al., *M phase-specific kinetochore proteins in fission yeast: Microtubule-associating Dis1 and Mtc1 display rapid separation and segregation during anaphase*. *Current Biology*, 2001. **11**(8): p. 537-549.
30. van Breugel, M., D. Drechsel, and A. Hyman, *Stu2p, the budding yeast member of the conserved Dis1/XMAP215 family of microtubule-associated proteins is a plus end-binding microtubule destabilizer*. *The Journal of Cell Biology*, 2003. **161**(2): p. 359-369.
31. Howard, J. and A.A. Hyman, *Dynamics and mechanics of the microtubule plus end*. 2003. **422**(6933): p. 753-758.
32. Jiang, K., et al., *TIP150 interacts with and targets MCAK at the microtubule plus ends*. *EMBO reports*, 2009. **10**(8): p. 857-865.
33. Fu, C., et al., *Phospho-Regulated Interaction between Kinesin-6 Klp9p and Microtubule Bundler Ase1p Promotes Spindle Elongation*. *Developmental Cell*, 2009. **17**(2): p. 257-267.
34. Hagan, I. and M. Yanagida, *Kinesin-related cut 7 protein associates with mitotic and meiotic spindles in fission yeast*. 1992. **356**(6364): p. 74-76.
35. Braun, M., et al., *Adaptive braking by Ase1 prevents overlapping microtubules from sliding completely apart*. 2011. **13**(10): p. 1259-1264.
36. Lansky, Z., et al., *Diffusible crosslinkers generate directed forces in microtubule networks*. 2014.
37. Gestaut, D.R., et al., *Phosphoregulation and depolymerization-driven movement of the Dam1 complex do not require ring formation*. 2008. **10**(4): p. 407-414.

38. Stachowiak, J.C., C.C. Hayden, and D.Y. Sasaki, *Steric confinement of proteins on lipid membranes can drive curvature and tubulation*. Proceedings of the National Academy of Sciences, 2010. **107**(17): p. 7781-7786.
39. Loiodice, I., et al., *Ase1p Organizes Antiparallel Microtubule Arrays during Interphase and Mitosis in Fission Yeast*. Molecular Biology of the Cell, 2005. **16**(4): p. 1756-1768.
40. Jülicher, F., *Force and motion generation of molecular motors: A generic description*, in *Transport and Structure*. 1999, Springer Berlin Heidelberg. p. 46-74.
41. Valentine, M.T., et al., *Individual dimers of the mitotic kinesin motor Eg5 step processively and support substantial loads in vitro*. 2006. **8**(5): p. 470-476.
42. Mollinari, C., et al., *PRC1 is a microtubule binding and bundling protein essential to maintain the mitotic spindle midzone*. The Journal of Cell Biology, 2002. **157**(7): p. 1175-1186.
43. Yamashita, A., et al., *The Roles of Fission Yeast Ase1 in Mitotic Cell Division, Meiotic Nuclear Oscillation, and Cytokinesis Checkpoint Signaling*. Molecular Biology of the Cell, 2005. **16**(3): p. 1378-1395.
44. Server, E. <http://elm.eu.org/links.html>.
45. Brunner, D. and P. Nurse, *CLIP170-like tip1p Spatially Organizes Microtubular Dynamics in Fission Yeast*. Cell, 2000. **102**(5): p. 695-704.
46. Goldstone, S., et al., *Tip1/CLIP-170 Protein Is Required for Correct Chromosome Poleward Movement in Fission Yeast*. PLoS ONE, 2010. **5**(5): p. e10634.
47. Khodjakov, A., S. La Terra, and F. Chang, *Laser Microsurgery in Fission Yeast: Role of the Mitotic Spindle Midzone in Anaphase B*. Current Biology, 2004. **14**(15): p. 1330-1340.
48. Tolić-Nørrelykke, I., *Push-me-pull-you: how microtubules organize the cell interior*. 2008. **37**(7): p. 1271-1278.
49. Yamamoto, A., et al., *A Cytoplasmic Dynein Heavy Chain Is Required for Oscillatory Nuclear Movement of Meiotic Prophase and Efficient Meiotic Recombination in Fission Yeast*. The Journal of Cell Biology, 1999. **145**(6): p. 1233-1250.
50. Grishchuk, E.L. and J.R. McIntosh, *Microtubule depolymerization can drive poleward chromosome motion in fission yeast*. The EMBO Journal, 2006. **25**(20): p. 4888-4896.

51. Ferenz, N.P., et al., *Dynein Antagonizes Eg5 by Crosslinking and Sliding Antiparallel Microtubules*. Current Biology, 2009. **19**(21): p. 1833-1838.
52. Tanenbaum, M.E., et al., *Dynein, Lis1 and CLIP - 170 counteract Eg5 - dependent centrosome separation during bipolar spindle assembly*. The EMBO Journal, 2008. **27**(24): p. 3235-3245.
53. Tanenbaum, M.E., et al., *Kif15 Cooperates with Eg5 to Promote Bipolar Spindle Assembly*. Current Biology, 2009. **19**(20): p. 1703-1711.
54. Vanneste, D., et al., *The Role of Hklp2 in the Stabilization and Maintenance of Spindle Bipolarity*. Current Biology, 2009. **19**(20): p. 1712-1717.
55. Busch, K.E., et al., *Tea2p Kinesin Is Involved in Spatial Microtubule Organization by Transporting Tip1p on Microtubules*. Developmental Cell, 2004. **6**(6): p. 831-843.
56. Tanenbaum, M.E., et al., *Cytoplasmic dynein crosslinks and slides anti-parallel microtubules using its two motor domains*. eLife, 2013. **2**.
57. Gerson - Gurwitz, A., et al., *Directionality of individual kinesin - 5 Cin8 motors is modulated by loop 8, ionic strength and microtubule geometry*. Vol. 30. 2011. 4942-4954.
58. Thiede, C., et al., *Regulation of bi-directional movement of single kinesin-5 Cin8 molecules*. BioArchitecture, 2012. **2**(2): p. 70-74.
59. Glotzer, M., *Cleavage furrow positioning*. The Journal of Cell Biology, 2004. **164**(3): p. 347-351.
60. Verma, D.P.S., *CYTOKINESIS AND BUILDING OF THE CELL PLATE IN PLANTS*. Annual Review of Plant Physiology and Plant Molecular Biology, 2001. **52**(1): p. 751-784.
61. Hu, C.-K., et al., *KIF4 Regulates Midzone Length during Cytokinesis*. Current biology : CB, 2011. **21**(10): p. 815-824.
62. Kurasawa, Y., et al., *Essential roles of KIF4 and its binding partner PRC1 in organized central spindle midzone formation*. The EMBO Journal, 2004. **23**(16): p. 3237-3248.
63. Nunes Bastos, R., et al., *Aurora B suppresses microtubule dynamics and limits central spindle size by locally activating KIF4A*. The Journal of Cell Biology, 2013. **202**(4): p. 605-621.

64. Anders, A. and K.E. Sawin, *Microtubule stabilization in vivo by nucleation-incompetent γ -tubulin complex*. Journal of Cell Science, 2011. **124**(8): p. 1207-1213.
65. Goodwin, S.S. and R.D. Vale, *Patronin Regulates the Microtubule Network by Protecting Microtubule Minus Ends*. Cell, 2010. **143**(2): p. 263-274.
66. Marcette, J.D., et al., *The Caenorhabditis elegans microtubule minus-end binding homolog PTRN-1 stabilizes synapses and neurites*. Vol. 3. 2014.
67. Kapitein, L.C., et al., *Microtubule-Driven Multimerization Recruits ase1p onto Overlapping Microtubules*. Current Biology, 2008. **18**(21): p. 1713-1717.
68. Fink, G., et al., *The mitotic kinesin-14 Ncd drives directional microtubule-microtubule sliding*. 2009. **11**(6): p. 717-723.
69. Janson, M.E., et al., *Crosslinkers and Motors Organize Dynamic Microtubules to Form Stable Bipolar Arrays in Fission Yeast*. Cell, 2007. **128**(2): p. 357-368.
70. Graham, J.S., R.C. Johnson, and J.F. Marko, *Concentration-dependent exchange accelerates turnover of proteins bound to double-stranded DNA*. Nucleic Acids Research, 2011. **39**(6): p. 2249-2259.

Summary

A brief look at the animal and plant kingdom shows a large variety of spatial patterns like the periodic stripes of zebras and the arrangement of flower petals. Interestingly, a microscopic look at tissues and single cells reveals very well structured organisations at smaller length scales as well. In this thesis I provide mechanistic insights into the organization of such patterns.

To build complex structures, cells require mechanism to set a length scale. Apart from mechanisms based on the reaction and diffusion of interacting molecules, mechanical processes like the growth of cytoskeletal filaments can set length scales at the subcellular level. The cytoskeleton mechanically supports cells but more importantly for our purpose generates forces that can change cellular architecture. In eukaryotic cells the contribution is based on three filaments (microtubules, actin and intermediate filaments), but in this thesis the focus is set on microtubules. Microtubules are stiff and dynamic filaments that enable them to play a prominent role in cellular organization.

Microtubules are composed of tubulin heterodimers that arrange longitudinally and laterally to form a slender hollow tube with high rigidity. Microtubules in cells grow away from specialized nucleation sites and have a certain probability to undergo a transition to a state of shortening. This switching mechanism, termed dynamic instability, determines how far microtubules grow away from their nucleation site. This length regulating mechanism aids the positioning of cellular components in cooperation with molecular motors that transport material along microtubules and forces generated by growing and shrinking microtubules in contact with cellular objects (organelles, membrane). The role of microtubules in intercellular positioning mechanisms is reviewed in chapter 1.

In chapter 2 and 3 we investigated the role of microtubules in positioning nuclei in cells. Eukaryotic but also prokaryotic cells disperse organelles and micro-compartments throughout the cellular space. The spacing between compartments is in many cases regulated and equidistant patterns have been described in particular for the case of

nuclei in multinucleated cells. The spacing between nuclei is regulated to control the patterning of cells in developing embryos but the occurrence of irregular patterns in large multinucleated muscle cells also correlates with muscle diseases. In chapter 2 we used fission yeast cells with a cytokinetic defect to generate a model multinucleated cell. Fission yeast cells are easy to genetically modify and the organization of their microtubule network is well understood. Cells had a cluster of nuclei at their centre but in absence of the minus-end directed motor klp2p the pattern changed to an arrangement in which the nuclei were well dispersed and positioned at equidistant intervals. Patterning depended on the presence of microtubules and we observed the growth of microtubules away from the envelope of nuclei towards neighbouring nuclei. We hypothesized that impingement of microtubules onto neighbouring nuclei generates nuclear repulsive forces. The net effect of microtubule interactions with cell walls and nuclei may be a force field in which nuclei are stably positioned at equidistant positions. However dominant forces generated by klp2p cause sliding between microtubules originating from sister nuclei that pull nuclei together. Our studies thus suggest a mechanism for equidistant positioning of organelles and a way to switch between patterns. Switching behaviour is observed in biology for example during light induced redistribution of chloroplasts in plant cells.

An increasing number of biological findings are now supported by computer models, as it allows to deduce whether a limited set of interacting components can explain a biological phenomenon. To evaluate whether repulsive pushing forces by dynamic unstable microtubules in between nuclei are sufficient to pattern nuclei we developed a simple 1D stochastic model of microtubule growth and nuclear motion in a tetranucleated cell. Our model demonstrated that the dynamics and accuracy of nuclear positioning in fission yeast cells is in agreement with the measured parameters of dynamic instability of microtubules. For this we compared nuclear oscillations and nuclear redistribution after pattern perturbation in experiments and simulations. An overestimation of the force generation between nuclei in our model caused a larger internuclear distance than experimentally observed. This discrepancy disappeared when we took into account that force generation at cell walls is more efficient than at nuclear envelopes. The model in chapter 3 thus clearly revealed that equidistant nuclear positioning can be explained by force generation of microtubules undergoing dynamic instability.

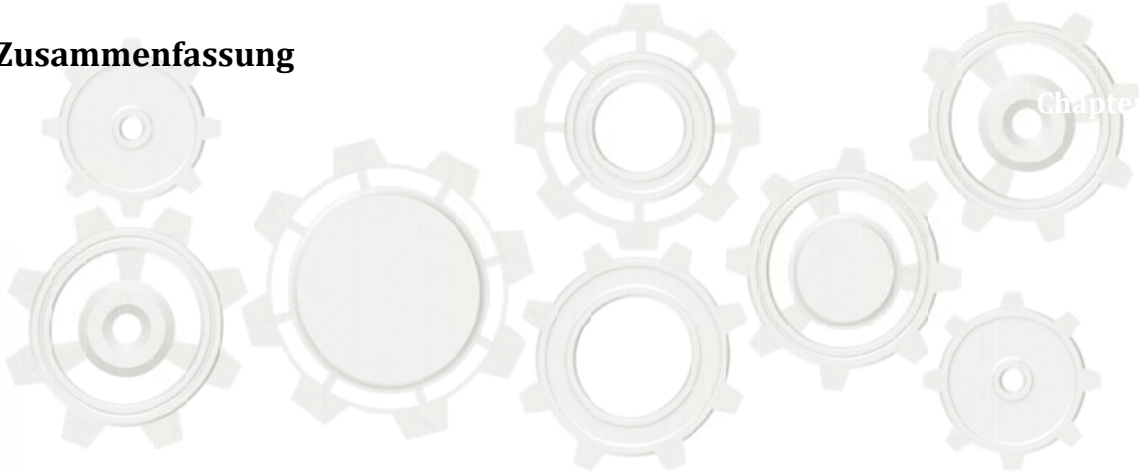
In chapter 4 we investigated the role of microtubule dynamics in the regulation of spindle elongation. During mitosis, microtubules form the mitotic spindle that segregates chromosomes to different cell halves. Microtubules from two spindle halves interdigitate at the spindle centre and template a multi protein assembly called the spindle midzone. Microtubules within the midzone grow and slide relative to each other causing spindle elongation. Moreover, the midzone regulates cytokinesis and as such mechanism that control midzone assembly are of interest to identify new targets for

cancer therapy. In chapter 4 we investigated, using fission yeast as a model, the mechanism that regulates the length of the midzone during spindle elongation. We demonstrate that spindle elongation velocity is limited by the speed at which motors push overlapping microtubules apart. However, under conditions of reduced microtubule growth, the elongation is being limited by microtubule growth. These results show that sliding and microtubule growth are coupled to prevent that spindle halves can separate from each other by sliding alone. This insight will help to reveal the function of a myriad of protein interactions that take place at the midzone.

This thesis reveals mechanically insights into pattern formation based on microtubule dynamics. In chapter 5 we discuss the relevance of our findings for the patterning of nuclei in larger eukaryotic cells. Preliminary results on the binding of the major midzone protein ase1p show that the binding affinity of ase1p microtubule crosslinkers depends on the number of microtubules that it can potentially bind to. These results suggest how ase1p may be recruited to the centre of mitotic spindles, where microtubule interdigitation is strongest.



Zusammenfassung



Bereits ein kurzer Blick in die Tier und Pflanzenwelt offenbart eine große Vielfalt an Strukturen z. B. die Streifen eines Zebras oder die Organisation der Blütenblätter. Bei einem Blick durch ein Mikroskop erkennt man das auch Gewebe und selbst einzelne Zellen in einem hohen Maß organisiert sind. Dies ist essential für die Funktionen jeder Zelle und der daraus bestehenden Gewebe.

Eukaryotische und prokaryotische Zellen sind sogar in der Lage bestimmte Zellkomponenten gleichmäßig in der Zelle zu verteilen. Dabei ist der Abstand zwischen diesen Komponenten durch die Zelle streng kontrolliert. In dieser Doktorarbeit war ich besonders daran interessiert Mechanismen zu finden, die mehrkernigen Zellen anwenden um die Kerne in den Zellen zu organisieren. Verschiedene Zellarten (z. B. Muskelzellen) besitzen mehrere Zellkerne um unter anderem eine ausreichende Menge an Proteinen zu produzieren. Zudem besitzt jede Zelle direkt vor der Zellkernteilung mehrere Kerne. Die Positionen der Kerne als auch deren Abstände zueinander spielen eine bedeutende Rolle für die Entwicklung und Funktionen der Zellen. In gesunden Muskelzellen z. B. sind die Kerne gleichmäßig in der gesamten Zelle verteilt, während eine ungleichmäßige Verteilung zu verschiedenen Muskelkrankheiten wie Muskeldystrophie des Typs Duchenne oder Becker-Kiener führt. Auch neu generierten Zellkerne müssen vor der Zellteilung einen möglichst großen Abstand voneinander haben, um zwei gleiche Tochterzellen zu erzeugen. Dafür benötigt die Zelle Mechanismen, um diese verschiedenen Abstände zu erzeugen. Diese Mechanismen können unter anderem auf das Wachstum von Filamenten des Zellskeletts basieren. Das Zellskelett eukaryotischer Zellen (Mikrotubuli, Aktine und Intermediär Filamente) ist für die mechanische Stabilisierung der Zelle verantwortlich. Es ist in der Lage Kräfte zu erzeugen, welche die Architektur der Zelle verändern können. In dieser Doktorarbeit habe ich mich im Speziellen mit den Mikrotubuli beschäftigt. Aufgrund ihrer strukturellen und kinetischen Polarität (dynamische Instabilität) übernehmen sie eine entscheidende Rolle bei der zellulären Strukturierung. Mikrotubuli bestehen aus

Heterodimeren, die ein röhrenförmiges Filament mit hoher Stabilität bilden. Sie wachsen von speziellen Startpunkten, den sogenannten Mikrotubuli-organisierenden Zentren und unterliegen infolge ihrer dynamischen Instabilität einem ständigen Auf- und Abbau. Diese Eigenschaft bestimmt die Länge der Mikrotubuli und ist zusammen mit Motorproteinen für die Positionierung von verschiedenen Zellkomponenten verantwortlich. Während Motorproteine entlang der Mikrotubuli laufen und Zellkomponenten wie Vesikel und Organellen transportieren, können dynamische Mikrotubuli bei direktem Kontakt mit den Zellkomponenten selber Kräfte erzeugen und so Komponente in der Zelle positionieren.

Bis jetzt sind die Mechanismen zur Abstandsregulierung der Zellkerne noch nicht vollständig aufgeklärt, jedoch haben Untersuchungen den Mikrotubuli eine entscheidende Rolle zugeteilt. Wir veränderten eine Spaltheife (*S.pombe*) in der Art und Weise, das sie anstatt eines Zellkernes mehrere aufwies. Die Spaltheife ist ein sehr guter Modelorganismus weil es einfach genetisch zu manipulieren ist und die Organisation von Mikrotubuli bereits gut untersucht ist. Ich visualisierte sowohl die Kerne als auch die Mikrotubuli, um die Zellen mikroskopisch zu analysieren. Die mehrkernigen Zellen zeigten eine Anhäufung von Kernen in der Zellmitte. In Abwesenheit eines Motorproteins (*klp2*) sind die Kerne allerdings gleichmäßig in der Zelle verteilt. Ich analysierte die Mikrotubuli in Abwesenheit des Motorproteins. Die Ergebnisse zeigen, dass Aufgrund des Kontaktes von Mikrotubuli mit den Zellkernen und der Zellwand Abstoßungskräfte erzeugt werden, die in der Lage sind Zellkerne gleichmäßig zu verteilen. In Anwesenheit des Motorproteins gleitet dieser entlang Mikrotubuli und zieht benachbarten Zellkernen zusammen. Die Ergebnisse verdeutlichen nicht nur einen Mechanismus um Organellen in gleichem Abstand zu positionieren, sondern auch eine Möglichkeit die Position von Organellen durch (De-) Aktivierung eines Motorproteins zu verändern. Dies könnte beispielsweise erklären, wie sich die Chloroplasten bei Lichteinfall in pflanzlichen Zellen verteilen.

Seit mehreren Jahren werden biologische Forschungsergebnisse mit Computermodellen unterstützt. Hierbei kann direkt bestimmt werden, welche Faktoren für biologische Phänomene verantwortlich sind. Ich entwickelte ein Modell, um zu untersuchen, ob die abstoßenden Kräfte von dynamischen Mikrotubuli ausreichend, sind um die Kerne gleichmäßig in der Zelle zu verteilen. Anhand einer vierkernigen Modellzelle konnte ich zeigen, dass sowohl die Bewegungen der Zellkerne als auch deren Abstände ausschließlich auf dem Parameter der dynamischen Instabilität der Mikrotubuli basieren. Bei der Analyse stellten wir allerdings fest, dass die Abstände zwischen den Zellkernen größer als in den Spaltheifezellen waren. Diese Überschätzung beruhte darauf, dass die abstoßenden Kräfte zwischen den Zellkernen weniger effizient sind, als die zwischen den äußeren Zellkernen und der Zellwand. Mit dieser Anpassung in unserem Model konnten wir anhand von unserem einfachen stochastischen Model

zeigen, dass die Kräfte von dynamischen Mikrotubuli ausreichend für die gleichmassige Verteilung der Zellkerne sind.

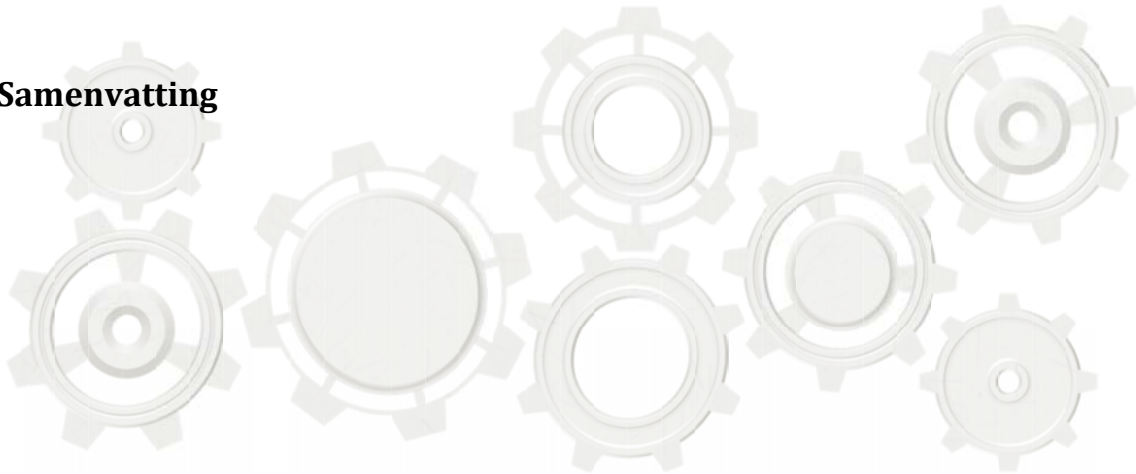
Wie bereits erwähnt, ist auch der Abstand von neu generierten Zellkernen sehr bedeutend für die Erzeugung von gleichen Tochterzellen. Dafür ist der Spindelapparat verantwortlich. Der Abstand der neu generierten Zellkerne zwischen den Polen verlängert sich zunehmend (*Spindle Elongation*), um vor der Zellteilung ein größ möglichen Abstand zu generieren. Das Finden von Mechanismen für Organisation des Spindelapparates ist von hoher Bedeutung in der Krebsforschung. Insbesondere durch eine zielgerichtete Veränderung der Dynamik von Mikrotubuli kann eine korrekte Zellteilung verhindert werden. Die sogenannten Mitosegifte können damit das Wachstum von Tumoren und Metastasen abwenden.

Der Spindelapparat besteht aus zwei Hälften wobei die Mikrotubuli sich zwischen den Hälften im Spindelzentrum überlappen. Das Spindelzentrum ist essential für die Zellteilung und Target für die Bindung von verschiedenen Proteinen, die unter anderem für die Elongation der Spindel verantwortlich sind. Interessanterweise bleibt die Länge des Spindelzentrums während der *Elongation* konstant, obwohl die Mikrotubuli weiterhin dynamisch sind und Motorproteine die Mikrotubuli auseinandergleiten. Mein Interesse war es, mögliche Mechanismen zu identifizieren, welche die Länge des Spindelzentrums und die Spindel Elongation regulieren. Ich benutzte abermals die Spaltheft und zeige, dass die Elongationsgeschwindigkeit der Spindel durch Motorproteine limitiert ist. Ist die Dynamik der Mikrotubuli allerdings beeinflusst, ist das der limitierende Faktor für die Geschwindigkeit. Daraus lässt sich schließen, dass die Elongationsgeschwindigkeit der Spindel sowohl von Motorproteinen als auch von der Dynamik der Mikrotubuli abhängt. Dadurch wird vermieden, dass das Spindelzentrum reduziert wird und die Spindel während der Elongation auseinanderfällt.

Im letzten Kapitel diskutierten wir mögliche Anwendungen der Resultate für andere Zellen. Unsere Ergebnisse könnten unter anderem beitragen, den Mechanismus der gleichmäßigen Verteilung der Zellkerne in Muskelzellen besser zu verstehen. Abschließend präsentiere ich erste Resultate von weiteren Experimenten, um die Organisation des Spindelapparates noch besser zu verstehen. Die Rekrutierung von Proteinen zum Spindelzentrum ist oft durch das Protein Ase1 reguliert, welches wiederum die Mikrotubuli der Spindelhälften miteinander verbindet. Dabei bindet das Protein Ase1 exklusiv im Spindelzentrum. Unsere Ergebnisse zeigen, dass die Bindungseffizienz von Ase1 an Mikrotubuli von deren Anzahl bestimmt wird. Je mehr Mikrotubuli im Spindelzentrum sind, umso geringer ist die Möglichkeit das Ase1 anderweitig zu binden. Damit versichert die Zelle das Proteine, welche essentiell für die *spindle Elongation* sind, nur im Spindelzentrum binden. Zusätzlich präsentiere ich Ideen für ein Computermodell, das dieses Ergebnis unterstützen würde.

Zusammenfassend zeigt diese Arbeit Mechanismen, wie dynamischen Mikrotubuli Zellkernen in der Spalthefe organisieren können.

Samenvatting



Een blik op de dieren- en plantenwereld laat een grote verscheidenheid aan structuren zien zoals de strepen van een zebra en de organisatie van bloemblaadjes. Ook wanneer wij door een microscoop kijken, kun je structuren op verschillende niveaus waarnemen; zelfs enkele cellen vertonen een hoge graad van organisatie. Deze organisatie is essentieel voor de functie van weefsels en de cellen waaruit zij bestaan. In dit proefschrift beschrijf ik fundamentele inzichten in het ontstaan en de instandhouding van dergelijke patronen.

Om complexe structuren te bouwen hebben cellen een mechanisme nodig om afstand te kunnen bepalen. Naast mechanismen die gebaseerd zijn op de reactie-diffusie van interacterende moleculen kunnen ook processen zoals de groei van filamenten van het cytoskelet afstanden reguleren. Het cytoskelet is verantwoordelijk voor de mechanische stabiliteit van de cel en kan krachten produceren die de vorm van de cel beïnvloeden. Hoewel het cytoskelet uit drie typen filamenten (microtubuli, actinefilamenten en intermediaire filamenten) bestaat heb ik mij in dit proefschrift geconcentreerd op de bijdrage van de microtubuli. Door hun structurele en kinetische polariteit (dynamische instabiliteit) spelen ze een belangrijke rol in de organisatie binnen de cel.

Microtubuli zijn opgebouwd uit tubuline heterodimeren die een slank buisvormig filament met een hoge stabiliteit vormen. Ze groeien vanuit specifieke uitgangspunten, de zogenaamde microtubuli organiserende centra, en ondergaan vanwege hun dynamische instabiliteit een permanente afwisseling van afbraak en groei. Deze eigenschap bepaalt de lengte van de microtubuli en samen met motoreiwitten zijn ze verantwoordelijk voor het positioneren van verschillende componenten. Terwijl motoreiwitten langs microtubuli “lopen” en componenten zoals vesikels en bepaalde organellen vervoeren, kunnen dynamische microtubuli bij direct contact met de componenten zelf krachten genereren en deze in de cel positioneren.

In hoofdstuk 2 en 3 van dit proefschrift wordt de functie van microtubuli bij het positioneren van celkernen beschreven.

Zowel eukaryoten en prokaryoten verspreiden organellen en microcompartimenten door de cel. De afstand tussen deze compartimenten is in veel gevallen gereguleerd en patronen van gelijke afstand zijn in het bijzonder beschreven voor kernen in meerkernige cellen. De afstand tussen de kernen wordt gereguleerd om patronen te sturen in zich ontwikkelende embryo's maar aan de andere kant correleert het voorkomen van onregelmatig patronen in grote meerkernige spiercellen met spierziekten.

Splijtgist cellen zijn ideaal om als model mee te werken aangezien ze gemakkelijk genetisch te modificeren zijn en de organisatie van hun microtubuli goed beschreven is. In hoofdstuk 2 gebruiken we splijtgist cellen met een defect in cytokinese als model voor meerkernige cellen. De cellen hebben een cluster van kernen in het midden van het cel maar in afwezigheid van het motoreiwit klp2p verandert het patroon zodat de kernen mooi op gelijke afstand van elkaar verdeeld zijn.

In cellen zonder de eiwit heb ik de groei van microtubuli tussen de kernen in afwezigheid van het motoreiwit geanalyseerd. Door de interacties van microtubuli met de celwand en kernen ontstaat er waarschijnlijk een krachtenveld dat er voor zorgt dat de kernen stabiel en gelijkmatig van elkaar gepositioneerd zijn. Als de motor echter wel aanwezig is worden de kernen naar elkaar toe getrokken door de krachten die de motor genereert.

Onze resultaten verhelderen niet alleen een mechanisme om organellen op dezelfde afstand te positioneren, maar ook een manier waarom deze positionering door motoreiwitten kan worden beïnvloed. Een dergelijk schakelmechanisme wordt vaker waargenomen in de natuur, bijvoorbeeld bij de door licht geïnduceerde herordening van chloroplasten in plantencellen.

Door de alsmaar toenemende rekenkracht worden onderzoeksresultaten steeds vaker ondersteund door computermodellen. Deze modellen stellen ons in staat te herleiden of een specifiek aantal factoren een biologisch fenomeen kunnen verklaren. Om te onderzoeken of de afstotende krachten van dynamische microtubuli voldoende zijn om kernen gelijkmatig te verdelen, heb ik een model ontwikkeld dat de groei van microtubuli en bewegingen van de kern simuleert. Gebaseerd op een vier-kernige cel konden we aantonen dat de dynamische instabiliteit van microtubuli voldoende is om zowel de bewegingen van de kernen als hun onderlinge afstand te controleren. Uit de analyses bleek echter dat de afstanden tussen de kernen groter waren dan gevonden in de splitgistcellen. Deze overschatting is gebaseerd op het feit dat de afstotende krachten tussen de celkernen minder efficiënt zijn dan die tussen de buitenste celkernen en de celwand. Door deze waarneming mee te nemen in ons model beschreven in hoofdstuk 3 laten we zien dat de krachten van dynamische microtubuli alleen voldoende zijn voor een gelijkmatige verdeling van de celkernen.

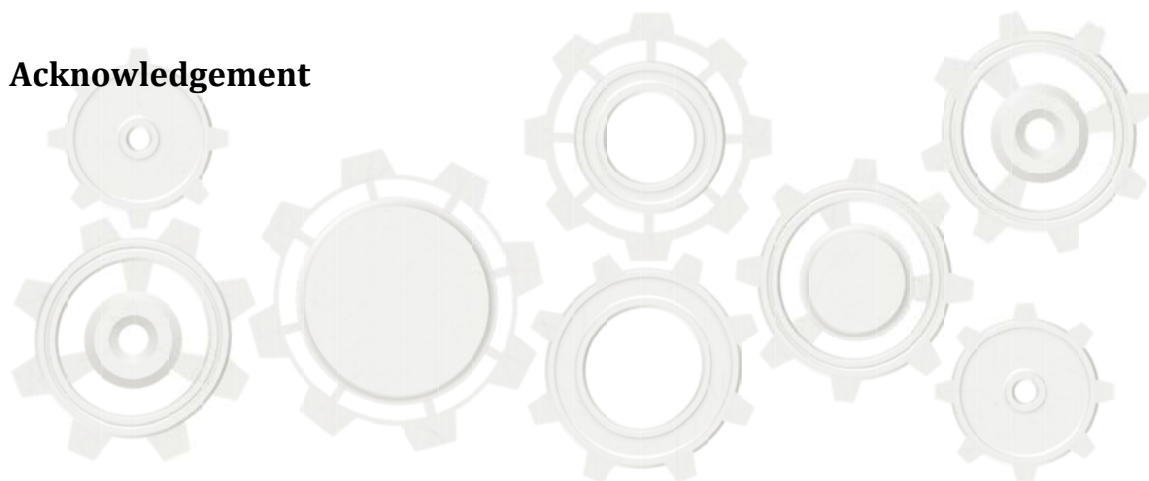
De afstand van de celkernen tijdens de celdeling is belangrijk voor de productie van identieke dochtercellen en wordt gereguleerd door de spoelfiguur. In hoofdstuk 4 onderzoek ik de functie van dynamische microtubuli bij de regulatie van de spoelfiguur. Microtubuli vormen twee spoelhelften vanuit twee polen die samenkomen in het spoelcentrum (polaire microtubuli). Een deel van de microtubuli zetten zich vast aan de chromosomen en trekken deze naar de celpolen om later de celkern te vormen. Tijdens de celdeling vergroot de spoelfiguur de afstand tussen de polen. Microtubuli in het spoelcentrum groeien en glijden ten opzichte van elkaar en veroorzaken samen met motoreiwitten op deze manier verlenging van de spoel. Bovendien reguleert het spoelcentrum de celdeling en daarom is een goed begrip van de werking ook van belang om nieuwe targets voor kankertherapie te ontwikkelen.

Opnieuw heb ik de splijtgist gebruik en laat zien dat de snelheid van de spoelverlenging door motoreiwitten bepaald wordt. Als de dynamica van microtubuli beïnvloed wordt, is dit de beperkende factor voor de snelheid. Hieruit concludeer ik dat de snelheid van de spoelverlenging zowel door de motoreiwitten als door de dynamiek van de microtubuli bepaald wordt.

In hoofdstuk 5 besprek ik de mogelijke toepassingen van onze resultaten op kernen in andere cellen. De resultaten kunnen onder meer helpen om een beter inzicht te krijgen in het mechanisme voor gelijkmatige verdeling van kernen in spiercellen.

Daarnaast tonen voorlopige resultaten van andere experimenten beter inzicht in de organisatie van de spoelfiguur. Het eiwit ASE1 verbindt de microtubuli van de spoelhelften in het centrum en reguleert de rekrutering van andere (motor)eiwitten naar het spoelcentrum. Daarbij bindt Ase1 uitsluitend aan microtubuli in het spoelcentrum. De resultaten tonen aan dat deze specifieke binding van ASE1 wordt bepaald door het aantal van microtubuli. Hoe meer microtubuli in het spoelcentrum zijn, des te lager is de mogelijkheid dat ASE1 ergens anders bindt. Op deze manier verzekert de cel de binding van eiwitten die essentieel zijn voor de spoelfiguurverlenging, alleen in het spoelcentrum. Daarnaast beschrijf ik een idee voor een mogelijk computermodel dat dit resultaat zou kunnen ondersteunen.

Acknowledgement



“Nobody said it was easy, but nobody said it was this hard ...”(The scientist, Coldplay)

However with a lot of support from colleagues, friends and family I was able to produce the book laying in your hand right now.

I would like to thank my promotor Prof. Dr. Marcel Janson who offered me to be his first PhD student. I am grateful for all the scientific discussions, which often resulted in constructive solutions or advice.

Bela Mulder thanks for being my second promotor and your guidance through the C++ world. I really appreciated your constant enthusiasm, which creates a pleasant environment to work in.

I started as a PhD student in PCB (plant cell biology group) which name was later changed into CLB (cell biology), however independent of the name it was a pleasure working with all of you. Annie Mie, even though I was not your PhD, your door was always open for me. Thank you very much. As soon as I had any questions regarding molecular biology Thijs you were the person to go to. Thank you for sharing your always working protocols. Jan Vos, my first room and bench mate. I learned a lot from you while working next to you. I appreciated your (thanks to Peter as well) help and advice also outside of the scientific world. When I started my PhD all others were plant scientist, a research field I was not totally excited about. However, Hannie, Jelmer, Andre, Henk and Ying showed me the beauty of being a plant scientist. Further, Hannie thanks for all the help in the wet lab and Jelmer introducing the SD. The only not plant person by that time, Zdenek thanks especially for letting me enter the ase1 and TIRF world, but also for starting up the movie nights with Jelmer, ending with me usually falling asleep. Ying, you taught me so much (not just how to make good Chinese food), the song “For good” from the musical Wicked describes it best. I miss you a lot and wish you all the best for your future. With you leaving, the area of PCB ended and the CLB area started bringing

along new people. Olya we just started a few months apart and hopefully will also end our PhD time just a few month apart. A lot of things connected us, thanks for all the talks. Now we both starting a new life with a lot of challenges, this time just few days apart (so excited about it). Good luck with finishing. Within a few month the CLB triplets started Aniek, Jeroen and Kris (even though the guys were not really newbies). You guys cannot get enough from each other and even spent vacation together. I enjoyed having you around a lot during the last 3 years of my PhD, thanks especially to the entertaining 10:30 being a real PhD student-banana breaks and the 15:30 Kiwi breaks.

Throughout my PhD time I supervised several students (Jouke, Lieuwe, Andreas and Kadir). Thank you for your good work and company. Even though you were not “my” students Anneke, Elysa, Lisa, Gonda and Kiki (thanks for teaching me knitting) I really enjoyed your company.

So there are two persons left of CLB, if they wouldn't be there nothing would work out anymore. Marie-Jose you are so much more than a secretary, thanks for constantly helping me out. Norbert the guide of our microscope world, although you are constantly busy you could always spare some time for me.

After moving to the radix we could not only enjoy the open workspace but also new neighbours- molecular biology and plant developmental biology. We shared plenty of lunch and coffee breaks (with way too much cake), lab trips and occasionally some dancing events. Special thanks to Henk and Olya (you are the cutes couple ever), Marijke Ting Ting and Sabine.

Although I was used to live abroad being away from my family and friends is always tough. But then you meet amazing people from various cultures who make the distance more bearable. Surprisingly, living in Wageningen turned out to be great. You meet a mix of different cultures; some of the people already left, whereas some of them are still here.

It all started with a bus trip and very fast I was surrounded by a bunch of lovely people. Together with Lily and Elske (my random bus friend),we set up a lot of good dinners in the cold or too hot kitchen. Usually guided by a few beers here and there (ending often in the International with different fashion styles). Thanks to both of you I had a wonderful start in Wageningen, all the best to you. Lily kindly introduced me to the KeyGene crew who all become very good friends of mine as well (and included me as KeyGene by association)- Mike (never met somebody as crazy as you), Bibna (the Zumba queen with an addiction to red wine), Jeab (“whaaaaatss upppp”), Pernelle, Gunnar, Feyruz and GMO (I think Kristin will never allow us to go out again). Special thanks also to the SkiGene -team especially to Harrie and to Yvonne.

Thanks to EPS and Kristin I met some brilliant german girls- Tila, Jacqui and Lea (thanks super perfectionist Kristin). I really enjoyed your company, dinners and our London trip. May plenty of them follow.

Firat and Merei – ohh did I enjoy our trips to all the castles in the Netherlands, even though the original purpose was not successful yet. Iliana and Jordi we met way too late, again thanks to Kristin and EPS, but luckily you are still around. All the best for you and lets spoil our kids together. Bjorn and Siska thanks goes especially to Bjorn for his endless support and interest in my work. Pierre I really enjoyed your company and the many nice conversations we had.

I did not spend a lot of time in Germany, but every time my visits were guided by the company of good old friends- Schulli, Doreen, Anja, Ina, Aline, Diana, Gaby and Rayko. Thanks for not forgetting me.

Before I come to thank my family I want to thank people that actually become family for me over the last years. Henk, I don't really know how to thank you best. You were always there for me giving me the support I needed. All the best for you and I am very happy that you stand next to me. Peter and Lorena I could always count on you in good and bad times. Thanks for always being there for me. I am so looking forward to join you guys in the new adventure.

You go abroad leaving your family behind, but then you meet somebody special and his family becomes yours. I never had any siblings but now I have two brothers Robert and PB, a sister in law Katrin and adorable nephews Floris and Max. This is topped by great parents in law Jan and Letty. Thank you all for constantly supporting me and the nice family time we spend together. I could have not done it without you.

(Je vertrekt naar het buitenland je familie achterlatend maar dan ontmoet je een special persoon en wordt zijn familie (ineens)ook een beetje jouw familie.. Zelf heb ik nooit een broer of zus gehad maar nu heb ik twee broers; Robert en Pieter-Bas, een schoonzus Katrin en twee schitterende neefjes Floris en Max. Tenlotte heb ik nog twee geweldige schoonouders Jan en Letty. Dank jullie wel voor jullie constante steun en begrip en de vele mooie momenten die we samen hebben beleefd. Ik zou het nooit zonder jullie hebben gered.)

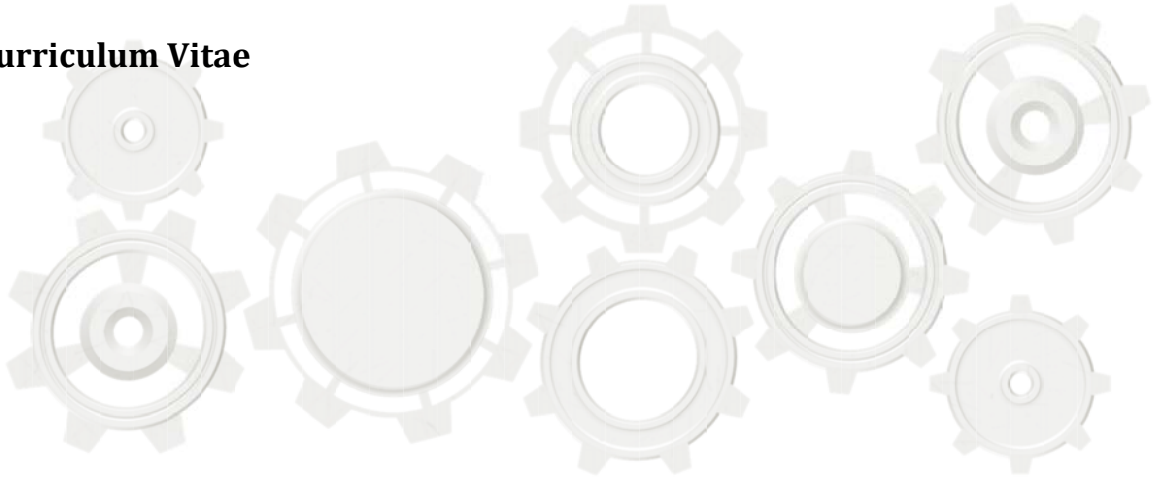
But that doesn't mean I did not miss my own parents like crazy. Without you I would never have even started a PhD. You always supported me in my plans and decision, which allowed me to be the person I am today. The daily chats and talks over skype gave me the feeling you were always around.

(Allerdings bedeutet das nicht, das ich meine Eltern immer sehr vermisset habe. Ohne Euch beiden hätte ich den Doktor wohl nie angefangen. Dank eurer ständigen Unterstützung und Ratschläge stehe ich heute hier. Auch die täglichen Gespräche über

Skype gaben mir das Gefühl, das ihr ständig in meiner Nähe seid. Vielen, vielen Dank. Ihr seit ein echtes Vorbild. Riesenknutscher 😊.)

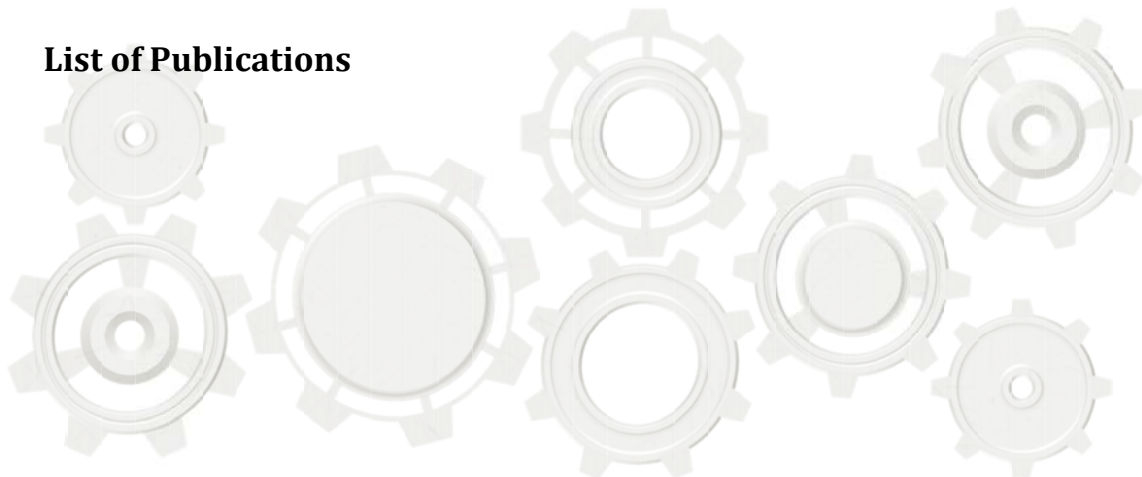
Last but not least, this book would have not been finished without you Alexander. You made me believe in myself again. When I thought I can't go any further you showed me what I am all capable of doing. I don't know how I can thank you for all the efforts. You are the best thing that ever entered my life. You made me laugh when I need it the most. I love you from the bottom of my heart. Let start the next adventure together.

Curriculum Vitae



Juliane Teapal was born on the 5th of February 1982 in Luckenwalde, Germany. After finishing High School at the Friedrichgymnasium in Luckenwalde she worked as an AuPair in Seattle, USA for a year. Back in Germany she did her Bachelor and Master at the Technical University of Applied Sciences Wildau with majoring in cell biology. During her study she worked as a student co-worker at the IBMT Fraunhofer, where she also did her Bachelor thesis investigating a new fluorescence labelling technology (SNAP-tag). Juliane did her Master thesis in two labs: the Lab of Jonas Tegenfeldt at Lund University, Sweden and of Albert van den Berg at Twente University, the Netherlands. Together with a PhD student she developed a technology to analyse movements of fluorescent DNA in nanoslits. Afterwards she worked for 6 months in the Group of Ludwig Gauckler at the Department of Material Sciences at the ETH Zurich, Switzerland to acquire knowledge in SEM and AFM microscopy. In 2008 she started as the first PhD Student of Marcel Janson in his lab of cell biology at the University of Wageningen, the Netherlands. In her research she investigated microtubule-based mechanism required for nuclear patterning. In her free time she enjoys sporting (race-biking, running and snowboarding), traveling and reading.

List of Publications



A microtubule-based mechanism for equidistant positioning of multiple nuclei

J.Teapal, L.J. Schuitmann, B. M. Mulder & M.E. Janson

Submitted

Diffusible crosslinkers generate directed forces in microtubule networks

Z.Lansky, M. Braun, A. Lüdecke, **J.Teapal**, M. Schlierf, P.R. ten Wolde, M.E. Janson, S. Diez

Submitted

Other related publications:

Schrödinger's capsules: a (micro) capsule that is open and closed, almost, at the same time

Baks, T., Boom, R., Devid, E., Dresselhuis, D., Falco, G., Folter, J. de, Leermakers, F.A.M., Li, J., Muntean, S.A., Poortinga, A., Robijn, G., Stoyanov, S., **Teapal, J.** & Voort Maarschalk, K. van der

Proceedings of the Physics with Industry 2010, 2010, pp. 67-85

Field-dependent DNA mobility in 20 nm high nanoslits

Salieb-Beugelaar, G. B.,* **Teapal, J.*** Van Nieuwkastele, J, Wijnperle, D, Tegenfeldt, J O., Lisdat, F, Van Den Berg, A, Eijkel, J C.T.

Nano Lett., 2008, 8 (7), pp 1785–1790

*Both authors contributed equally

Education Statement of the Graduate School

Experimental Plant Sciences



Issued to: Juliane Teapal

Date: 5 September 2014

Group: Cell Biology, Wageningen University & Research Centre

1) Start-up phase	<u>date</u>
<p>▶ First presentation of your project</p> <p>Analysis of Microtubule Associated Motors and Nonmotor Proteins in Fission Yeast</p>	Oct 24, 2008
<p>▶ Writing or rewriting a project proposal</p> <p>Regulation of polarity in microtubule arrays</p>	2008
▶ Writing a review or book chapter	
▶ MSc courses	
▶ Laboratory use of isotopes	
<i>Subtotal Start-up Phase</i>	<i>4.5 credits*</i>
2) Scientific Exposure	<u>date</u>
<p>▶ EPS PhD student days</p> <p>EPS PhD Student Day, Utrecht University</p> <p>EPS PhD Student Day, Wageningen University</p> <p>EPS Career Day (ExPectationS day)</p> <p>EPS Career Day (ExPectationS day)</p>	<p>Jun 01, 2010</p> <p>May 20, 2011</p> <p>Nov 19, 2010</p> <p>Nov 18, 2011</p>
<p>▶ EPS theme symposia</p> <p>EPS Theme 1 'Developmental Biology of Plants', Leiden University</p> <p>EPS Theme 1 'Developmental Biology of Plants', Wageningen University</p>	<p>Jan 30, 2009</p> <p>Jan 28, 2010</p>
<p>▶ NWO Lunteren days and other National Platforms</p> <p>FOM Introduction Day</p>	May, 2009

Dutch meeting on Molecular and cellular Biophysics/ Veldhoven	Oct 29-30, 2008
Dutch meeting on Molecular and cellular Biophysics/ Veldhoven	Oct 28-29, 2009
Dutch meeting on Molecular and cellular Biophysics/ Veldhoven	Oct 04-05, 2010
FOM-Meeting "Spatial design of biochemical regulation networks"	Mar 11, 2011
Dutch meeting on Molecular and cellular Biophysics/ Veldhoven	Oct 03-04, 2011
ALW meeting "Experimental Plant Sciences" Lunteren	Apr. 02-03, 2012
FOM-Meeting "Spatial design of biochemical regulation networks"	May 29, 2012
Dutch meeting on Molecular and cellular Biophysics/ Veldhoven	Oct 01-02, 2012
ALW meeting "Experimental Plant Sciences" Lunteren	Apr 22, 2013
FOM-Meeting "Spatial design of biochemical regulation networks"	May 30, 2013
▶ Seminars (series), workshops and symposia	
KNAW Biophysics Meeting/Amsterdam (every 2nd month/4 Talks)	2009-2013
1st Plant Sciences Seminar	Sep 2009
Invited seminar by Anna Akmanova	Sep 2008
Invited seminar by Remko Offeringa	Mar 2008
Invited seminar by Chris Hawes	Aug 2010
▶ Seminar plus	
▶ International symposia and congresses	
SEB cell symposium/Durham/UK	Aug 23-26, 2009
EU COST E50 Workshop 'Systems Biology for Plant Design' Wageningen/Netherlands	Jul 08-11, 2009
EMBO Conference : Microtubules-structure, regulation and Functions, EMBL Heidelberg	Jun 02-05,2010
EMBO Conference : Microtubules-structure, regulation and Functions, EMBL Heidelberg	May 23-26,2012
EMBO Meeting Amsterdam	Sep.21-24,2013
▶ Presentations	
Dutch meeting on Molecular and cellular Biophysics/ Veldhoven (Poster)	Oct 29-30, 2008
SEB/Durham/UK and Dutch meeting on Molecular and cellular Biophysics/ Veldhoven (Poster)	Aug 23-26, 2009

Education Statement

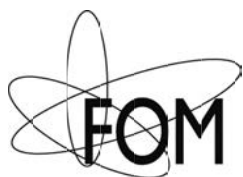
EMBO Conference : Microtubules-structure, regulation and Functions, EMBL Heidelberg (Oral)	Jun 02-05, 2010
Dutch meeting on Molecular and cellular Biophysics/ Veldhoven (Poster)	Oct 04-05, 2010
FOM-Meeting "Spatial design of biochemical regulation networks"(Oral)	Mar 11, 2011
Dutch meeting on Molecular and cellular Biophysics/ Veldhoven (Poster)	Oct 03-04, 2011
ALW meeting "Experimental Plant Sciences" Lunteren (Poster)	Apr. 02-03, 2012
EMBO Conference : Microtubules-structure, regulation and Functions, EMBL Heidelberg (Oral)	May 23-26,2012
FOM-Meeting "Spatial design of biochemical regulation networks"(Oral)	May 29, 2012
Dutch meeting on Molecular and cellular Biophysics/ Veldhoven (Oral)	Oct 01-02, 2012
FOM-Meeting "Spatial design of biochemical regulation networks"(Oral)	May 30, 2013
EMBO Meeting Amsterdam (Oral+Poster)	Sep.21-24,2013
▶ IAB interview	
Meeting with a member of the International Advisory Board	Feb 17, 2011
▶ Excursions	
<hr/> <i>Subtotal Scientific Exposure</i>	
	<i>27.7 credits*</i>
3) In-Depth Studies	<u><i>date</i></u>
▶ EPS courses or other PhD courses	
Gateway Technology Course	Nov 17-21, 2008
▶ Journal club	
Member of literature discussion group at Cell Biology	2008-2011
▶ Individual research training	
Physics in Industry, Lorentz Center, Leiden, NL	Oct 10-15, 2010
<hr/> <i>Subtotal In-Depth Studies</i>	
	<i>5.7 credits*</i>
4) Personal development	<u><i>date</i></u>
▶ Skill training courses	
PHD Day FOM (Writing skills, presentation skills)	2009
Dutch Language Course	2010

Education Statement

Business orientation week, Nyenrode Business University, The Netherlands	Apr 22-28, 2012
Scientific writing course, Wageningen University C1	Oct-Dec 2012
FOM Career Coaching (8 meetings, 1.5 h each)	Jul-May 2013
► Organisation of PhD students day, course or conference	
EU COST E50 Workshop 'Systems Biology for Plant Design' Wageningen/Netherlands	Jul 08-11, 2009
PhD Day Wageningen	May 20, 2011
EPS ExPectationS career day	Nov 18, 2011
Membership of Board, Committee or PhD council	
► Member of the EPS Council since November 2010	Nov 2010-Aug 2013
<hr/>	
<i>Subtotal Personal Development</i>	<i>9.6 credits*</i>
<hr/>	
TOTAL NUMBER OF CREDIT POINTS*	47.5

Herewith the Graduate School declares that the PhD candidate has complied with the educational requirements set by the Educational Committee of EPS which comprises of a minimum total of 30 ECTS credits

** A credit represents a normative study load of 28 hours of study.*



The work described in this thesis is part of the research program “Stichting voor Fundamenteel Onderzoek der Materie (FOM)”, which is financially supported by the “Nederlands Organisatie voor Wetenschappelijk Onderzoek (NWO)” under the project number FOM-W-03.

Financial support for the printing of this thesis was kindly provided by the Foundation for Fundamental Research on Matter (FOM) and the Laboratory of Cell Biology, Wageningen University.

